Astbury Centre for Structural Molecular Biology

UNIVERSITY OF LEEDS

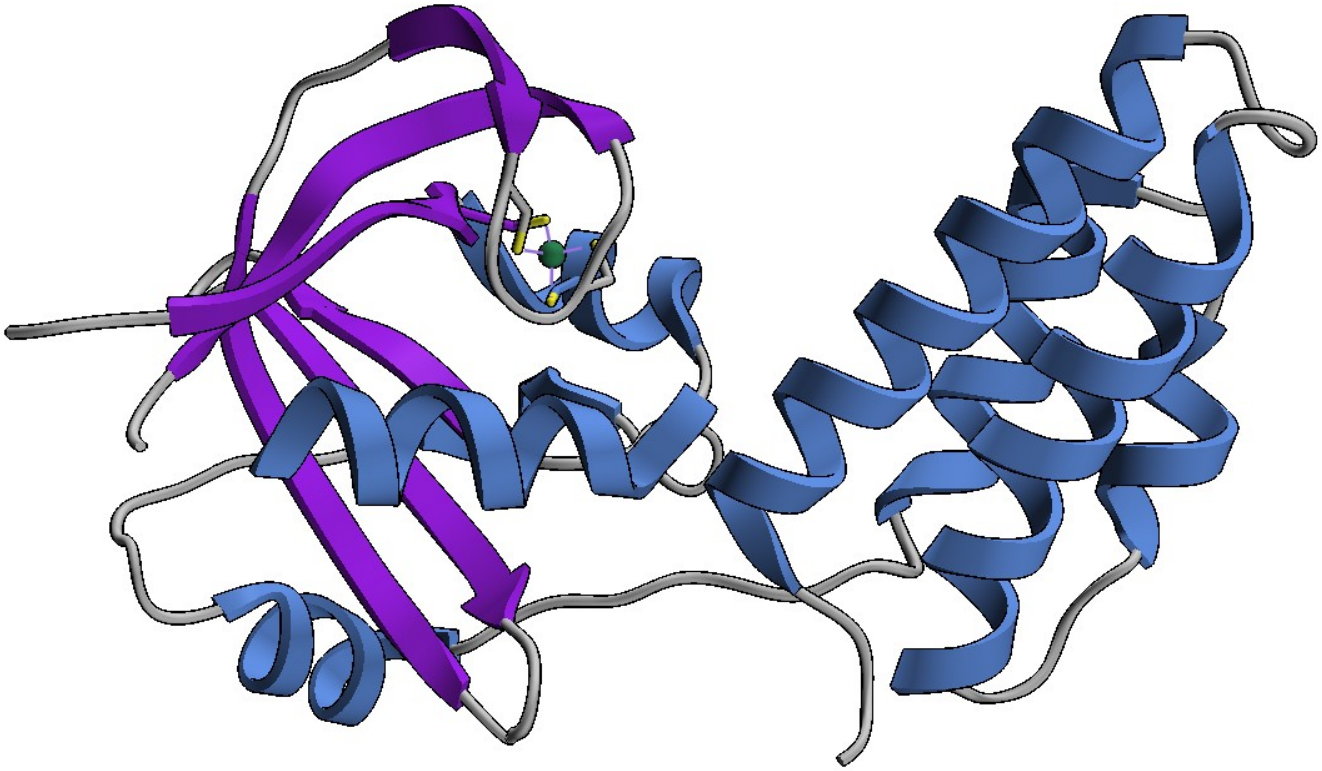

ASTBURY CENTRE

Annual Report 2012

Front cover illustration: the crystal structure of FusB. This two-domain metalloprotein, contains a four-cysteine zinc finger with a unique structural fold. The role that FusC plays in bacterial resistance to the antibiotic fusidic acid was elucidated by the O'Neill group and is described on page 43.

Acknowledgement

The Astbury Centre for Structural Molecular Biology thanks its many sponsors for support of the work and its members for writing these reports. The report is edited by David Brockwell.

This report is also available electronically via http://www.astbury.leeds.ac.uk

Mission Statement

The Astbury Centre for Structural Molecular Biology will promote interdisciplinary research of the highest standard on the structure and function of biological molecules, biomolecular assemblies and complexes using physico-chemical, molecular biological and computational approaches.

Introduction

2012 was a busy, eventful and successful year for the Astbury Centre, as this letter and the scientific reports that follow portray. Thank you to all Astbury members: the principal investigators, facility managers, technicians, students and postdocs for all of your efforts into generating this success. Without your enthusiasm, hard work, collegiality and excellent science that bring different disciplines together, this could not have happened. Thank you also to those that have funded our activities, including our members, Deans and Heads of School for supporting local events, and a wealth of funding bodies that includes MRC, BBSRC, EPSRC, EU, The Wellcome Trust, Leverhulme Trust, Royal Society, other Charities and Industry, for enabling us to prosecute our science in a well-funded and well-equipped environment.

This annual report provides summaries of some of the success stories from the Astbury Centre's research activities and outputs in 2012. In its pages you will find new and exciting research stories, which span fundamental research in the area of Structural Molecular Biology in its widest context. In addition, the exploitation and development of our fundamental research findings in biotechnology, bioengineering and medicine are described. The pages and co-authors of each report demonstrate the successes made possible by the interdisciplinary research within the Centre. They also highlight the breadth of activity in the Centre that spans studies of molecular interactions within cells, to the development of new physical and chemical methods for studying biological systems.

During 2012, the Centre continued in its quest of "Understanding Life in Molecular Detail" through an array of different activities, including seminars, publications, public lectures and other events. We continued to enjoy an excellent seminar series (organised by Arwen Pearson), hosting 14 lectures during 2012 with speakers from the UK, Germany, USA, Hong Kong, and The Netherlands. The Centre's Annual Research Retreat, held at the Thackray Medical Museum in Leeds in September, also provided an excellent opportunity for members to present and discuss their data in the form of seminars and posters. A hugely successful day was experienced by the 125 members who attended this event. Finally, by holding events focusing on research facilities (taster series, hands-on experience sessions and lectures) our facility managers provided opportunities for members to experience new research techniques, whilst a new series of "Research Theme" events enabled our principal investigators to meet to plan new activities in different areas, the first events in 2012 including "Imaging and Single Molecule Techniques", "Protein Modification Technologies" and "Biomembranes".

The Centre welcomed three new academic staff members in 2012 (James Duce (Alzheimer's Research UK Senior Research Fellow), Sergei Krivov (RCUK Research Fellow) and Simon Connell (Lecturer, School of Physics and Astronomy)) that bring, respectively, expertise in Alzheimer's disease, computational biology and biophysics, and AFM methodology. We were sorry to lose Narcis Fernandez-Fuentes, Steve Johnson and Paul Ko Ferrigno from the membership in 2012, although Paul Ko Ferrigno (now working for Avacta plc) will continue to play a role in the Centre as a visiting member. We were also delighted to welcome many new PhD students and postdoctoral members to the Centre this year. This takes our current numbers to 56 academic staff, 192 PhD students and 100 postdoctoral fellows.

Astbury Centre members continued to be successful in publishing their research. In total, members published 139 manuscripts in 2012, including papers in *Angewandte Chemie Int. Ed., Nature Communications and PNAS*. Highlights included – an understanding of the mechanism of bacterial resistance to fusidic acid (Edwards and O'Neill groups, front cover); the development of a sortase catalysed method for chemoselective N-terminal labelling of recombinant proteins (Turnbull and Webb groups); the production of biotemplated magnetic

nanoparticle arrays and quantum dots embedded in lipid nanotubules (Evans and Staniland groups) and the identification, by single molecule methods, of coat protein-mediated collapse of viral RNA during virus assembly (Stockley and Tuma groups). Astbury members also enjoyed success in raising grant income in 2012. Highlights included a large (£1.4M) Equipment Grant funded by the MRC (led by Michelle Peckham) for high resolution imaging equipment that brings new research capability to the Centre. Peter Olmsted, with colleagues in the Universities of Leeds, Imperial, Nottingham, Durham and Cambridge, were awarded a large (£4.8M) grant from the EPSRC for studies of membranes, while Adam Nelson was involved in leading a successful, large consortium bid to the EU (€196M) for a "European Lead Factory": the world's largest public-private partnership in health that involves 30 partners spanning universities, SMEs and Pharma which is due to commence in 2013. These, together with >£5.9M new income raised for project and programme grants, brings the Astbury portfolio to a £30M share in £50M worth of grants in 2012. These awards are testament to the success of our members and the Centre. Well done all!

2012 saw continuing success of the members of the Astbury Centre in terms of peer recognition. Our student and post-doc members again received several awards at a variety of international meetings, including best oral presentation (Scott Jackson, Peter Henderson's laboratory) and best posters (Jo Rushworth and Aneika Leney, from Nigel Hooper's and Alison Ashcroft and Sheena Radford's groups, respectively). Congratulations also to those who received honours: Andy Wilson for the 12th Bob Hay lectureship prize of the Royal Society of Chemistry and Robin Bon for the Thieme Chemistry Journal Award. Others also continued to develop our outreach activities: Bruce Turnbull inspiring local audiences (including "Café Scientifique", "The Humanist Society of West Yorkshire" and others) with his lecture entitled "Synthetic Biology – a Brave new world?", whilst student members gave presentations at the House of Commons (Tom Lanyon-Hogg (Alison Baker and Stuart Warriner's group); or won acclaim for their novel contribution in developing new games based on scientific research run by The Wellcome Trust (Thomas Forth (David Westhead's group).

The Astbury Society, currently led by the presidents Sasha Derrington and Megan Hughes, along with previous presidents Heather Cox and James Towey, played a magnificent role in Astbury activities hosting social events. In 2012 these included the now famous Christmas quiz and pizza night and new activities such as a Games Night, Film Night, Scavenger Hunt and the much-enjoyed cake bakes and coffee mornings. The society also hosted the barbeque and Sports Day at the sixth Annual Astbury Lecture which this year was given by Professor Roger Goody (Max Planck Institute, Dortmund, Germany). Photos of these events can be seen at www.astbury.leeds.ac.uk/about/society.php. Do take a look!

I hope that you enjoy reading this Annual Report, whether you are a member of the Centre, a visitor, a member of our Industrial Advisory Board, a funding agency that supports our activities or a passing reader with an interest in Structural Molecular Biology and the activities of our Centre. Finally, thanks to David Brockwell for preparing this report. It is with much excitement that we look forward to continuing our successes in 2013.

Sheena E. Radford
Director, Astbury Centre for Structural Molecular Biology,
Leeds, April 2013

Please note that this report (as well as those from previous years) is also available as a PDF document which can be downloaded from our website (www.astbury.leeds.ac.uk).

Contents

Contributions indexed by Astbury Centre Principal Investigator

Biomolecular mass spectrometry

James Ault, Helen Beeston, Paul Devine, Henry Fisher, Aneika Leney, George Preston, Caroline Pritchard, Charlotte Scarff, Dale Shepherd, Tom Watkinson, Lucy Woods, Lydia Young and Alison Ashcroft.

Introduction

The main focus of our research is the development and application of mass spectrometric techniques to investigate the tertiary and quaternary structures of biomolecules. We use non-covalent electrospray ionisation-mass spectrometry (ESI-MS) and tandem mass spectrometry (MS/MS) to determine the mass, conformational properties, stoichiometry, stability, and binding characteristics of proteins and protein complexes. We are also pioneers of ion mobility spectrometry-mass spectrometry (IMS-MS), which offers a unique opportunity to separate co-populated biomolecular entities on the basis of their physical shape and to measure their mass and cross-sectional area (Ω) in a single, rapid (≤ 2 mins) experiment.
Our major areas of research focus on protein folding, function and self-aggregation, protein-ligand interactions, biomolecular complex assembly, and oligonucleotide structure.

Results

Our recent method development work on membrane proteins has shown that ESI-MS and ESI-IMS-MS can be used to study these hydrophobic proteins in a native-like state. The procedure involves the use of amphipols (amphipathic polymers), which are a mild alternative to detergent micelles, to solubilise membrane proteins and to protect and preserve their structure from solution through to the gas phase. The bacterial β-barrel outer-membrane proteins PagP (20.2 kDa) and OmpT (33.5 kDa), whose interactions with amphipols had not been studied previously, were selected for this study (Figure 1).

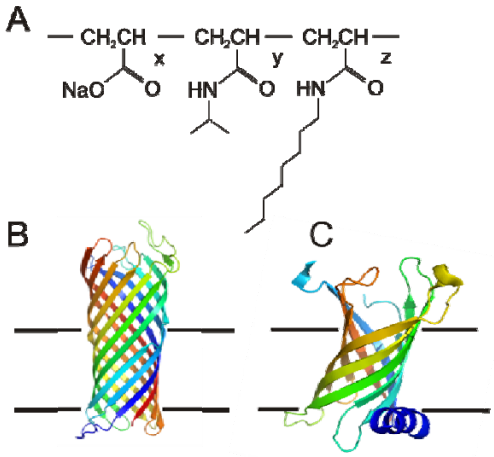

Figure 1: (A) Amphipol A8-35 (9-10 kDa; x = 29-34%, y = 25-28%, z = 39-44%). Crystal structures of the membrane proteins **(B)** OmpT (PDB:1I78) and **(C)** PagP (PDB:1THQ)

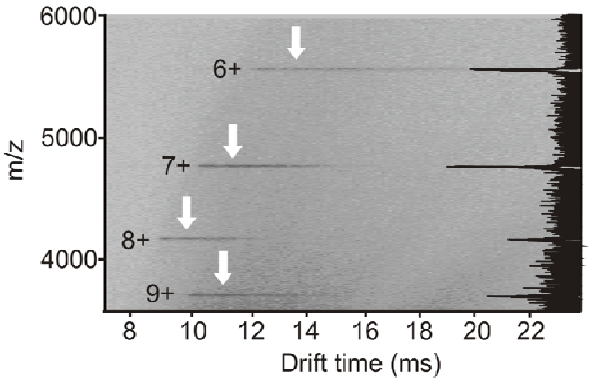

Figure 2: ESI-IMS-MS driftscope plot of the OmpT:amphipol complex. The charge states of the ions are labelled and highlighted with white arrows. The summed m/z spectrum for the complex is displayed on the right-hand side.

The PagP and OmpT membrane protein:amphipol complexes were analysed using ESI-IMS-MS. In these analyses, the proteins were separated from the amphipol in the gas phase, thus enabling measurement of the molecular mass of each protein, together with its cross-sectional area. Data for OmpT are shown in Figure 2. The cross-sectional area of OmpT was measured as 2705 $Å^2$ (ave. 6+, 7+ and 8+ ions), which is consistent with the cross-sectional area calculated from the crystal structure (1I78; 2718 $Å^2$).

Amphipols thus offer a simple method of trapping membrane proteins in detergent-free aqueous solutions and preserving them in a native-like conformation, from which ESI-MS analyses can be performed on μMolar amounts of material.

Publications

Arscott, S., Descatoire, C., Buchaillot, L. & Ashcroft, A. (2012) A snapshot of electrified nanodroplets undergoing coulomb fission. *Appl. Phys. Lett.* **100:** 074103.

Hodkinson, J., Radford, S. & Ashcroft, A. (2012) The role of conformational flexibility in beta(2)-microglobulin amyloid fibril formation at neutral pH. *Rapid Commun. Mass Spectrom.* **26:** 1783-1792.

Kang, L., Moriarty, G., Woods, L., Ashcroft, A., Radford, S. & Baum, J. (2012) N-terminal acetylation of alpha-synuclein induces increased transient helical propensity and decreased aggregation rates in the intrinsically disordered monomer. *Protein Sci.* **21:** 911-917.

Leney, A., McMorran, L., Radford, S. & Ashcroft, A. (2012) Amphipathic polymers enable the study of functional membrane proteins in the gas phase. *Anal. Chem.* **84:** 9841-9847.

Morrissey, B., Leney, A. , Toste Rego, A., Phan, G., Allen, W. , Verger, D., Waksman, G., Ashcroft, A. & Radford, S. (2012) The role of chaperone-subunit usher domain interactions in the mechanism of bacterial pilus biogenesis revealed by ESI-MS. *Mol. Cell Proteomics* **11:** M111.015289.

Ndlovu, H., Ashcroft, A., Radford, S. & Harris, S. (2012) Effect of sequence mutation on the mechanical response of amyloid fibrils probed by steered molecular dynamics simulation. *Biophys. J.* **102:**587-596.

Phillips, H., Chernikov, A., Fletcher, N., Ashcroft, A., Ault, J., Filby, M. & Wilson, A. (2012) The use of electrospray mass spectrometry to determine speciation in a dynamic combinatorial library for anion recognition. *Chem. Eur. J.* **18:** 13733-13742.

Preston, G., Radford, S., Ashcroft, A. & Wilson, A. (2012) Covalent cross-linking within supramolecular peptide structures. *Anal. Chem.* **84:** 6790-6797.

Funding

This work was funded by the BBSRC, the EPSRC, the Wellcome Trust, Waters UK Ltd., LGC, AZ, GSK, UCB and Medimmune. We thank the BMSS for student travel grants.

Collaborators

Leeds: S. Radford, N. Stonehouse, S. Harris, A. Wilson, P. Henderson and P. Stockley.
External: S. Arscott (CNRS, Lille, France), G. O'Connor (LGC, UK), M. Morris & K. Giles (Waters UK Ltd.).

Phase behaviour and transitions in complex biological systems

Piero Ricchiuto and Stefan Auer

Introduction

My research is focused on the application of theoretical computational tools developed in soft condensed matter physics to investigate the phase behaviour and transitions of complex systems of biomolecules. From a purely statistical mechanical point of view an ensemble of many peptides and proteins represents a new and important system which should bridge our understanding of colloidal systems, polymers, and proteins. The research highlights in the year 2012 were our Molecular Dynamics simulation of a model peptide system addressing the question of the importance of kinetics and thermodynamics in protein aggregation and the application of nucleation theory to describe the two-step nucleation of amyloid fibrils.

Protein aggregation: kinetics versus thermodynamics

In this study, we address the questions of how important are the kinetics in protein aggregation, and what are the intrinsic properties of proteins that cause this behavior. On the basis of our recent quantitative calculation of the equilibrium phase diagram of natively folded α-helical and β-sheet forming peptides, we perform molecular dynamics simulations to demonstrate how the aggregation mechanism and end product depend on the temperature, concentration, and starting point in the phase diagram. The results obtained show that there are severe differences between the thermodynamically predicted and the kinetically obtained aggregate structures. The observed differences help to rationalize the suggestion that monomeric proteins in their native functional structure can be metastable with respect to the amyloid state, and that the native fold is a special property that protects them from aggregation.

Two-step nucleation of amyloid fibrils: omnipresent or not?

Amyloid protein fibrils feature in various diseases and nanotechnological products. Currently, it is debated whether they nucleate in one step (i.e. directly from the protein solution) or in two steps (step one being the appearance of nonfibrillar oligomers in the solution and step two being the oligomer conversion into fibrils). In this work we employ nucleation theory to gain insight into the idiosyncrasy of two-step fibril nucleation (Figure 1) and to determine the conditions

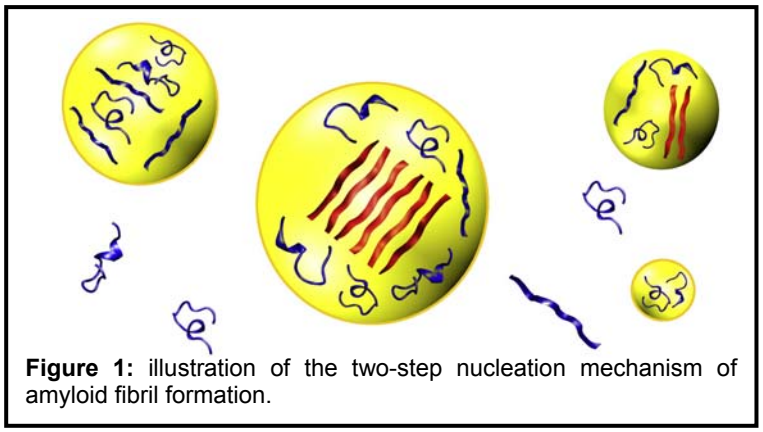

Figure 1: illustration of the two-step nucleation mechanism of amyloid fibril formation.

under which this process can take place. Presenting an expression for the rate of two-step fibril nucleation, we use it to qualitatively describe experimental data for two-step nucleated amyloid-β fibrils. Our analysis helps in understanding why, in some experiments, oligomers

rather than fibrils form and remain structurally unchanged and why, in others, the oligomers convert into fibrils.

Publications

Auer, S., Ricchiuto, P. & Kashchiev, D. (2012) Two-step nucleation of amyloid fibrils: omnipresent or not? *J. Mol. Biol.* **422:** 723-730.

Ricchiuto, P., Brukhno, A. & Auer, S. (2012) Protein aggregation: kinetics versus thermodynamics. *J. Phys. Chem. B* **116:** 5384-5390.

Funding

This work was supported by the EPSRC (EP/G026165/1).

Collaborators

External: D. Kashchiev (Sofia)

Interactions of nanoparticles and block copolymers with lipids in bilayer membranes

Shengwen Zhang, Andrew Nelson and Paul Beales

Introduction

Nanoparticles (NPs) and polymers are being developed for next generation medical therapies. These materials can be used to target the delivery of drugs to specific cells or tissues, or as highly sensitive image contrast agents in medical diagnostics. The engineering parameter space of these novel materials is vast and so it is essential to develop a fundamental understanding of the interactions between nanomaterials and biological systems to guide material optimisation for a given application. Cellular complexity dictates that minimal model systems are required to gain detailed understanding of interaction mechanisms. We focus our work on investigating the interactions of NPs with lipid bilayers, the structural matrix of the cell's plasma membrane and gateway to the cell's internal biochemistry.

Reconstituted lipid vesicles, whilst mimicking biomembranes, also have many technological applications including drug delivery, biosensors, food and cosmetics. Hybrid materials often have many functional advantages over unitary systems: we are therefore interested in exploring the structure and properties of hybrid lipid-polymer and lipid-NP composites.

Nanoparticle – membrane interactions

We have recently explored the NP size-dependence in the interaction between silica NPs and phospholipid bilayers in the form of giant vesicles (GUVs). Silica NPs are currently being developed as drug delivery vehicles due to their inherant ability to cross membranes and enter cells. We found the interaction mechanism is strongly size-dependent (Fig. 1). Small (18 nm) NPs adsorb on the membrane, condensing the lipids and rigidifying the bilayer. The resultant stress induced within the membrane is released through formation of a microscale pore.

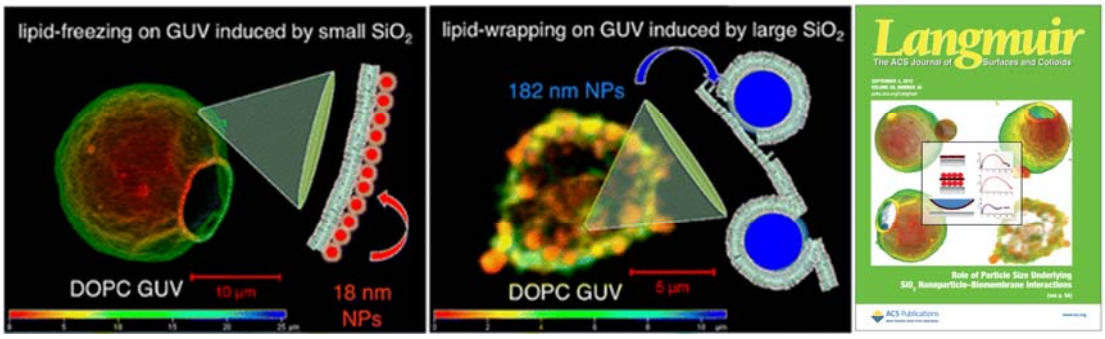

Figure 1: small (18 nm) NPs adsorb on the membrane and cause the lipids to condense. The resultant stress caused by "freezing" of the membrane is released by the formation of a microscale hole in the bilayer (*left*). Conversely, larger (182 nm) NPs are wrapped by the lipid bilayer causing membrane invaginations reminiscent of endocytosis (*centre*). This work featured on the cover of the September 4th 2012 edition of *Langmuir* (*right*).

Larger NPs (182 nm) are wrapped by the membrane and deplete lipid through a passive mechanism reminiscint of active endocytosis processes in cells. Fluorescence recovery after photobleaching (FRAP) studies demonstrate a reduced fluidity in the lipid bilayer of 1-2 orders of magnitude after interaction with 18 nm silica NPs but a slight increase in lipid mobility induced by the wrapping mechanism from larger NPs. A simplified theoretical model was used to explore the NP-membrane interaction in terms of the adsorption energy of the NP on the membrane and the bending mechanics of the lipid bilayer. This model predicts a cross-over in interaction mechanism for NPs in the size range ~30-40 nm, consistent with

our experimental findings. This suggests that the competition between these two energetic processes encompasses the key underlying physics in this NP-membrane interaction.

Hybrid lipid – diblock copolymer vesicles

We have demonstrated the ability to create hybrid bilayer membranes composed of phospholipids and amphiphilic diblock copolymers. These materials combine the inherent biocompatibility of liposomes with the robust mechanical strength of synthetic polymersomes. We anticipate that these versatile, composite materials will find many uses in biotechnology and nanomedicine. We have formed GUVs with well-mixed membranes composed of the block copolymer poly(butadiene-b-ethylene oxide) (PBd-PEO) and the common phospholipid POPC. The mechanical moduli and fluidity of these hybrid membranes vary with the relative composition of these two components, affording a broad range of tune-ability for vesicle properties.

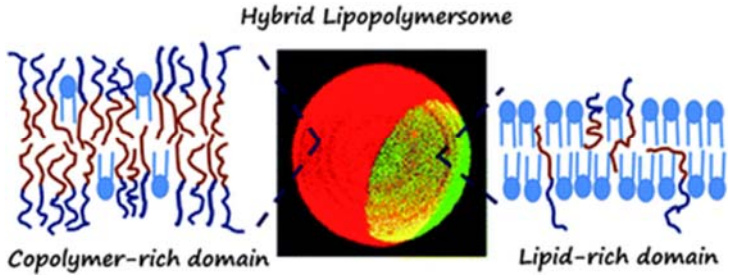

Figure 2: hybrid giant vesicles were formed from the diblock copolymer PBd-PEO and mixture of phospholipids and cholesterol. Well mixed membranes could be formed that, under appropriate conditions of temperature and composition, phase separate into coexisting lipid-rich and copolymer-rich domains.

Textured, hybrid vesicles can be created by phase separation of lipids into liquid-ordered or solid-like phases (Fig. 2). Domain morphology can be controlled via cooling rate and the nature of the particular phase formed by the lipids. Lipid-active membrane perturbants (e.g. cyclodextrin, phospholipases) can be used with these textured, hybrid vesicles to dissolve or otherwise remodel the lipid domains, or to initiate controlled release of the vesicle's encapsulated contents.

Publications

Nam, J., Vanderlick, T. & Beales, P. (2012) Formation and dissolution of phospholipid domains with varying textures in hybrid lipo-polymersomes. *Soft Matter* **8:** 7982-7988.

Zhang, S., Nelson, A. & Beales, P. (2012) Freezing or wrapping: the role of particle size in the mechanism of nanoparticle-biomembrane interaction. *Langmuir* **28:** 12831-12837.

Funding

This work was supported by the Biomedical & Health Research Centre at the University of Leeds, the Brian Mercer Award for Innovation (from the Royal Society), Yale University and the ENNSATOX programme (E.U. FP7 grant agreement no. NMP-229244).

Collaborators

External: T. K. Vanderlick, Yale University. J. Nam, Amore Pacific Corporation.

Improving on Nature: protein engineering and design

Sasha Derrington, Claire Windle, Laura Cross, Christopher Rowley, Anna Polyakova,
Chi Trinh, Adam Nelson, Arwen Pearson and Alan Berry

Introduction

We are using protein engineering and directed evolution in a wide range of projects to seek to create new enzymes with altered catalysis, to engineer new molecular machines, to create complex macromolecules, to interfere and engineer new orthogonal organelles and to screen vast libraries of directed evolution variants for non-natural catalytic function.

Modifying the activity of *N*-acetylneuraminic acid lyase using non- natural amino acids

N-Acetylneuraminic acid lyase (NAL) catalyses the reversible aldol condensation of *N*-acetyl-D-mannosamine and pyruvate to form *N*-acetylneuraminic acid, through a mechanism that involves the formation of a Schiff base with a lysine residue at position 165. This enzyme has previously been the focus of many traditional directed evolution experiments. Now by using a chemical mutagenesis strategy it has been possible to incorporate non-natural amino acids into the active site of NAL.

An in depth study of the enzyme K165 γ-thialysine has been carried out. The non-natural amino acid γ-thialysine was incorporated into the enzyme by inserting a cysteine residue at position 165 by site directed mutagenesis then subsequent reaction of the cysteine with 2,5-dibromohexan-1,6-diamide (diBr) to form dehydroalanine (dha). The dehydroalanine containing protein can then undergo a conjugate addition of a thiol, in this case aminoethanethiol, to create the non-natural amino acid (figure 1). This method of conversion has also been shown to work at many other positions within the protein and with a wide variety of thiols.

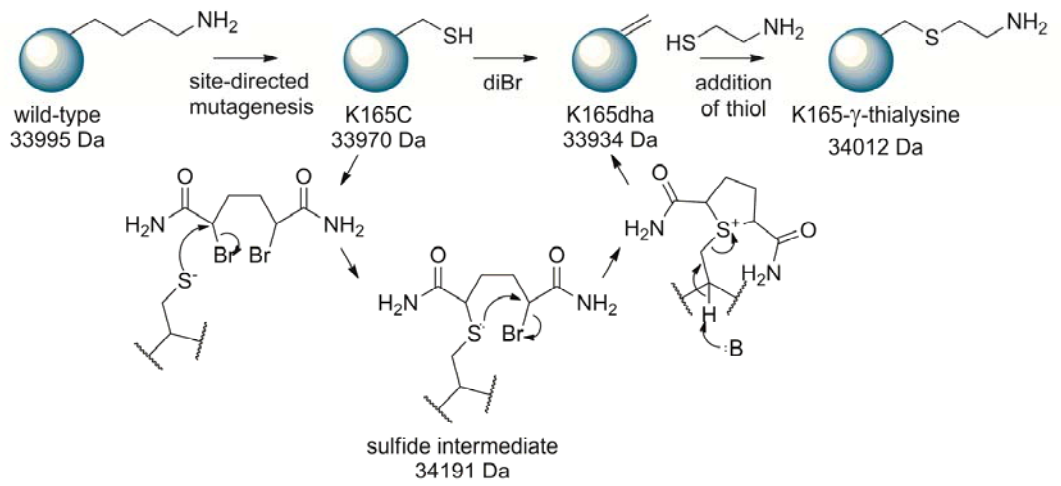

Figure 1: conversion of wild-type NAL into K165 γ-thialysine by chemical mutagenesis.

K165 γ-thialysine has been produced at a large enough scale for crystallographic and in-depth kinetic studies. The X-ray structure showed the K165 γ-thialysine active site to be practically identical to that of the wild-type, while kinetic analyses showed the activity of the enzyme to be much lower. Determination of the kinetic parameters for the reaction at a range of pH values showed the pH optima of K165 γ-thialysine NAL had been shifted from that of the wild-type. The inclusion of the sulphur in the γ-thialysine side chain at position 165 therefore unbalances the pKas in the active site of the enzyme, resulting in lower catalytic rates.

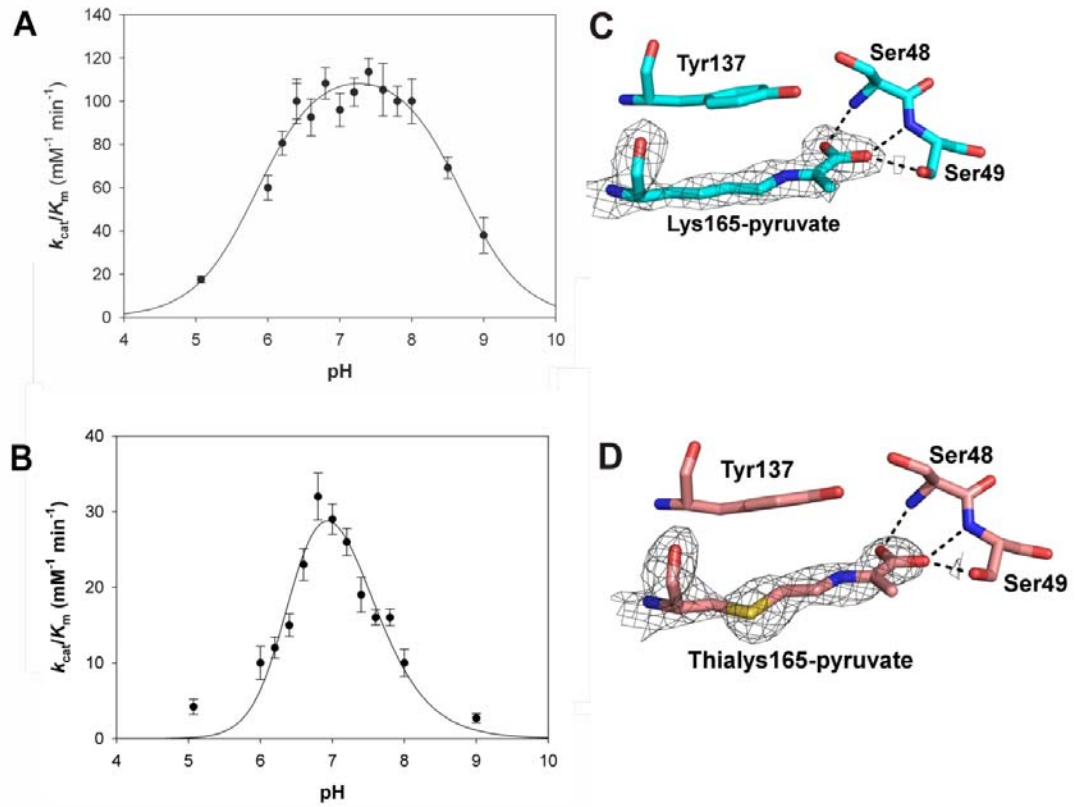

Figure 2: pH curves for **(a)** wild-type and **(b)** K165 γ-thialysine NAL. **(c)** and **(d)** the active site structures of the Schiff base complexes of wild-type and K165 γ-thialysine NAL.

Polyketide synthases and non-ribosomal peptide synthases.

Polyketide synthases (PKS) and non-ribosomal peptide synthases (NRPS) are large multi-modular proteins responsible for the formation of polyketides (PK) and non-ribosomal peptides (NRP), respectively. The compounds produced as secondary metabolites often have additional properties useful to us in everyday life. They are produced in an assembly-like fashion, adding small units together to form a larger compound. Our interests lie in the structure-function relationships of these enzymes that allow the selection of building blocks to make vastly different compounds. In the future we will edit this selection in a predictable manner.

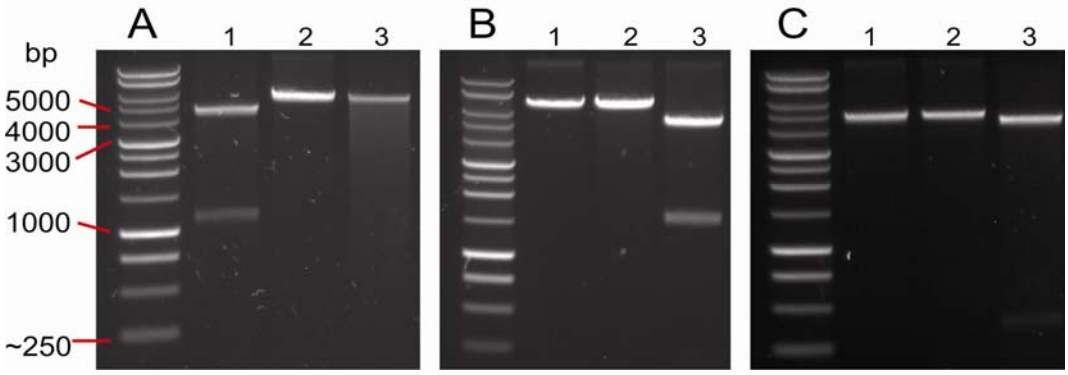

Figure 3: agarose gel showing successful cloning of *idm* genes which encode proteins responsible for starter unit biosynthesis. **(a)** *idmI* and pKK223-3 (~1.2kb) double (1) and single (2 & 3) restriction digests. **(b)** *idmJ* and pETDUET (~1.5kb) single (1 & 2) and double (3) restriction digests. **(c)** *idmK* and pKK223 3 (~300bp) single (1 & 2) and double (3) restriction digests.

Initial work has focussed on cloning and expression of proteins responsible for the formation of a starting unit of a PK/NRP. We intend to structurally characterise the proteins and any interactions formed, in preparation for attempting to engineer the natural substrate specificity.

Creating novel binding motifs for orthogonal receptors
This project looks at the interaction between the peroxisomal receptor PEX5 and the signal sequence PTS1 which allows targeting of proteins to the peroxisome. Mutated PTS1 sequences with be synthesised and screened against a library of PEX5 mutants with the aim to develop an orthogonal PEX5-PTS1 binding interaction.

mRNA display
A new project is using mRNA display methods to screen vast libraries of enzyme variants for novel activities.

Funding
Our work is funded by BBSRC, the Wellcome Trust and the Leverhulme Trust.

Collaborators
Leeds: P. Stockley, A. Baker, A. Cuming and S. Warriner.

Label-free electrochemical detection of enzymatic activity using microarrays

James Murray, Dominika Nowak, Steven Johnson and Robin Bon

Introduction

Recently, the immobilisation of peptide aptamers on gold electrode microarrays and the detection of their binding to proteins in cell lysates by label-free electrochemical spectroscopy have been demonstrated. We are currently investigating the use of this technology to construct substrate microarrays for the detection of activity and substrate specificity of enzymes responsible for post-translational modification of proteins. The concept is illustrated in Figure 1: Individual electrodes will be selectively functionalised with substrates via a self-assembled monolayer (SAM), and the conversion of the immobilised substrates will be detected by label-free electrochemical spectroscopy.

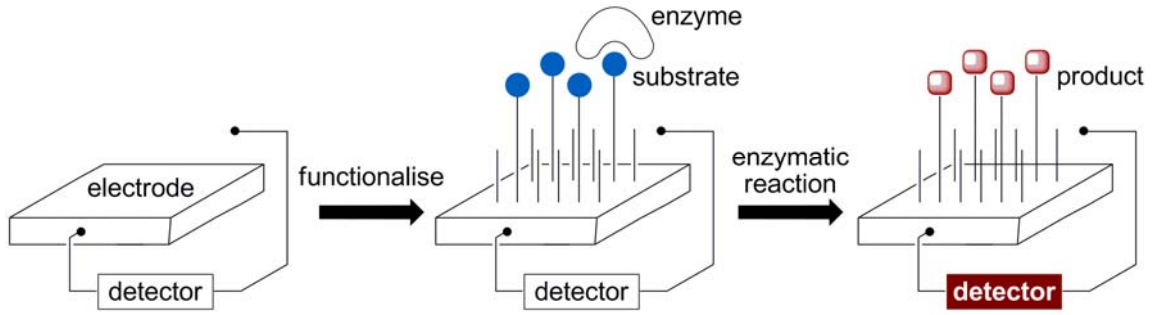

Figure 1: label-free electro-chemical detection of enzymatic activity. Substrates will be chemo-selectively immobilised on electrodes. Upon enzymatic processing, the change of their size and/or charge will be measured using label-free electrochemical spectroscopy.

Results

A collection of protease substrates labelled with an alkanethiol (for formation of SAMs) via a PEG linker (**1**) was synthesised using a combination of solution phase and solid phase methods (Figure 2). The synthesis protocols were used to prepare additional analogues of **1** incorporating a ferrocenyl group – a redox label – (**2**) and PEGylated peptides incorporating a fluorogenic aminocoumarin (**3**) for solution phase protease assays.

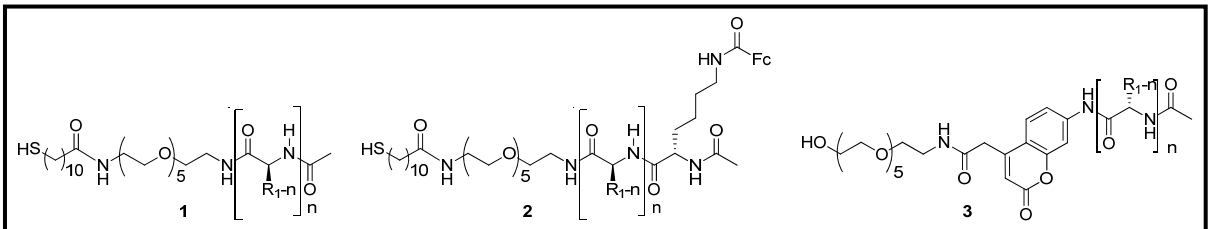

Figure 2: alkanethiol-labelled peptides **1** and **2** and PEGylated peptide **3**. Fc = ferrocenyl.

The efficiency of proteolysis of peptides **3** is currently being studied in solution. So far, Electrochemical Impedance Spectroscopy (EIS) and Cyclic Voltammetry (CV) have been used to characterise electrodes functionalised with peptides **1** and **2** and to evaluate the quality of the SAMs formed by these molecules. All electrochemical experiments were carried out in a bespoke three-electrode cell, including an Ag/AgCl reference electrode, a platinum wire counter electrode and a SAM-modified Au surface working electrode. Figure 3 shows a characteristic Bode plot (magnitude of impedance (log |Z|) and phase (Z) plotted as a function of frequency) for mixed SAMs assembled from different ratios of peptide **1a** and a

shorter dilutant. The magnitude of |Z| at 100 mHZ and the minimum phase angle of -88° are commensurate with the formation of a well-packed, insulating monolayer.

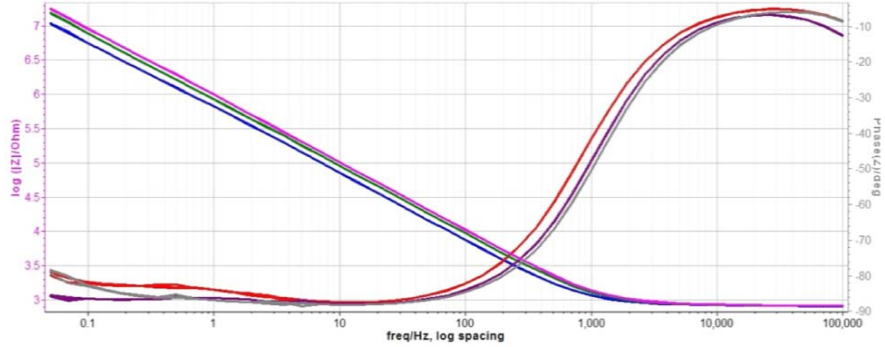

Figure 3: EIS (Bode plot) of a gold electrode modified with 0.5 mM mixed SAM (dilutant:peptide **1**). Red line – 9:1 ratio, purple line – 1:1 ratio and gray line – 1:9 ratio.

Figure 4 shows the redox process of $Fe(CN)_6^{3-/4-}$ using a SAM-modified electrode before and after SAM desorption. We observe significant suppression of redox activity following SAM assembly. This is observed for all SAMs investigated and independent of the ratio of the dilutant and peptide **1a** integrated within the SAM. These results are consistent with the formation of a well-packed, insulating molecular monolayer.

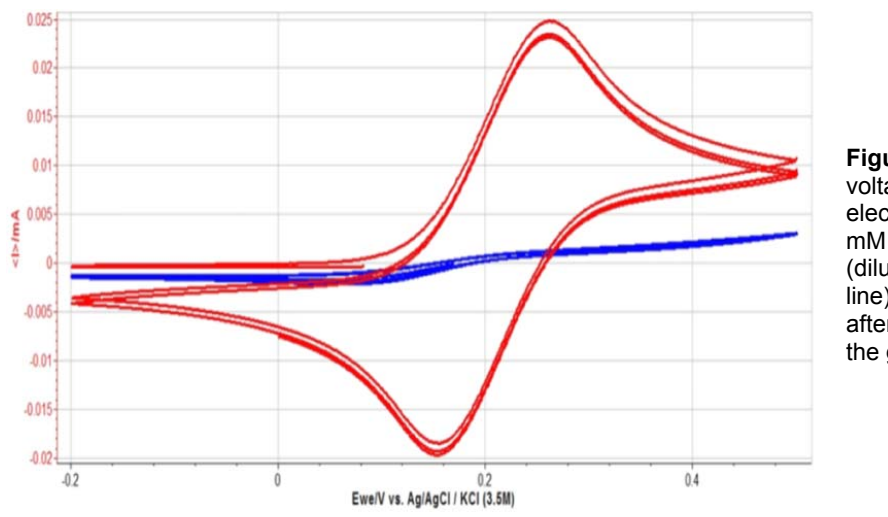

Figure 4: CV voltammograms of an electrode modified with 0.5 mM mixed SAM (dilutant:peptide **1** 1:1) (blue line) and a bare electrode after desorption of SAM from the gold surface (red line).

Unfortunately, peptide **2** proved unsuitable for CV measurements, most likely because of the instability of the ferrocenyl moiety during the measurements. Alternative redox labels are currently under investigation. We are also in the process of determining the suitability of peptides **1** as SAM-bound protease substrates using SPR.

Funding
We thank the Biomedical and Health Research Centre and EPSRC for funding.

Dissecting the folding mechanism of the outer membrane protein PagP

Gerard Huysmans, Lindsay McMorran, Robert Schiffrin, Steven Baldwin,
Sheena Radford and David Brockwell

Introduction

The *E.coli* outer membrane (OM) is densely packed with outer membrane proteins (OMPs) that carry out a diverse range of functions that include (non)specific transport of small and large ligands, proteolytic and synthetic reactions and cellular recognition and adhesion. However, despite their importance, understanding the biogenesis of OMPs and their folding and insertion into membranes is a formidable challenge (Figure 1). For soluble proteins, excellent progress towards answering how the information inherent in the amino acid sequence of a protein enables it to adopt a native, three-dimensional structure has been made by integrating experimental folding studies on small model proteins with computer simulations. By contrast, progress in understanding the folding mechanisms of membrane proteins has been much more limited, in part because of the complexity added to delineating the mechanisms of folding by the membrane environment in which the protein resides.

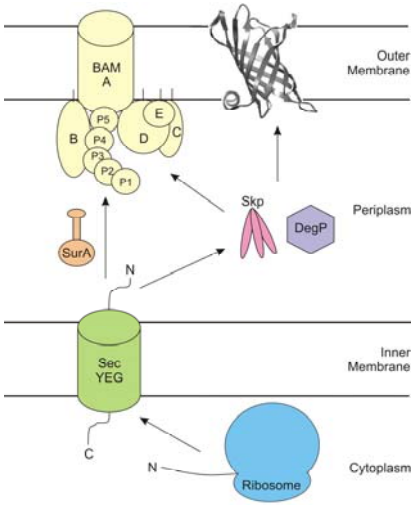

Figure 1: schematic of biogenesis of outer membrane proteins (OMPs) in *E. coli.* OMPs are synthesised on the ribosome before post-translational translocation across the inner membrane by the SecYEG translocon. Unfolded OMPs are then chaperoned across the periplasm to the β-barrel assembly (BAM) complex, which aids folding and insertion into the outer membrane. BAM complex proteins are labelled A-E, and the periplasmic polypeptide transport-associated (POTRA) domains of BamA are labelled P1-5.

Biological membranes comprise a complex two-dimensional fluid with a heterogeneous lipid composition that largely determines the physicochemical properties of the membrane. The organization of the lipid bilayer (a hydrophobic core flanked by often asymmetrical polar interfaces) poses significant spatial restrictions on the folding process, which are difficult to mimic *in vitro*. In addition, membrane curvature imposes stresses on the bilayer that may be alleviated or exacerbated by protein insertion and hence can also modulate the rate, or efficiency, of folding. In order to understand the native structures of membrane proteins, it is thus necessary to investigate how the lipid membrane contributes to, and/or limits, protein folding, stability and conformational dynamics.

Results

To address this question we have investigated the effects of lipid composition on the folding mechanism of the bacterial outer membrane protein PagP. Under a defined range of protein, lipid and denaturant concentrations we have previously shown that PagP displays single exponential folding kinetics, inserting into zwitterionic *di*$C_{12:0}$PC liposomes *via* a polarized transition state from a liposome-associated unfolded state. Using mutational analysis the C-terminal β-strands were found to be highly structured, while the N-terminal α-helix and β-

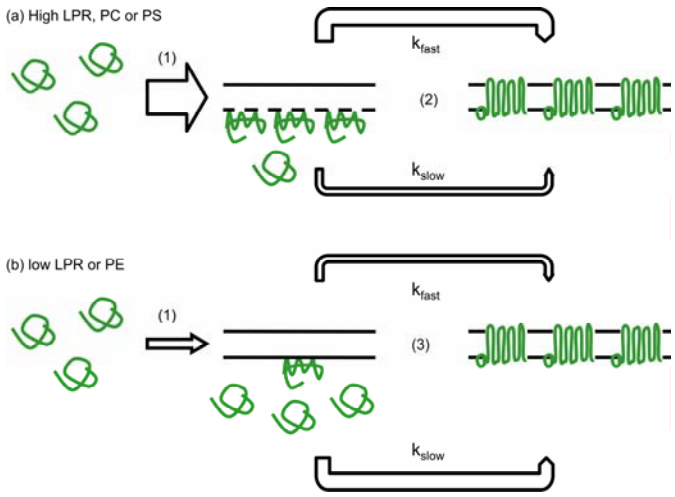

Figure 2: schematic representation of the folding mechanism of PagP. Folding is initiated by rapid adsorption to the membrane (1). The amplitude of this process is increased with increasing lipid-to-protein ratios (LPR) in (a) and decreased by decreasing LPR or by incorporation of *di*$C_{12:0}$PE in (b). Folding proceeds predominantly by a fast (2) or a slow folding route (3), modulated by the bilayer properties determined by the LPR and *di*$C_{12:0}$PE fraction in the liposome as indicated. The dotted line in (a) represents higher flexibility in the membrane compared to (b). Including *di*$C_{12:0}$PS in the liposome does not change the preferred pathway but does influence the rate of insertion. The thickness of the arrows indicates the amplitude of the phases.

strands remain largely disordered. By decreasing the denaturant concentration and the ratio of lipid to protein, PagP folds from a completely unfolded and membrane dissociated state, revealing additional kinetic refolding phases. Application of an interrupted folding assay definitively demonstrated that this complexity reflected the existence of parallel folding pathways (Figure 2). The kinetic partitioning between these pathways was found to be modulated by the elastic properties of the membrane. For example, folding into mixed *di*$C_{12:0}$PE:*di*$C_{12:0}$PC liposomes resulted in a decrease of PagP adsorption to the liposomes and a switch to a slower folding pathway. By contrast, inclusion of *di*$C_{12:0}$PS in *di*$C_{12:0}$PC liposomes only resulted in a decrease of the folding rate of the fast pathway. Our results were used to refine the kinetic folding mechanism of PagP and contribute to delineating the role of the membrane in membrane protein folding.

Current work

Our laboratory is also employing kinetic folding and spectroscopic techniques to look at refolding of PagP in low concentrations of urea, to allow investigation of how the chaperone proteins found in the periplasm of *E.coli* (Skp, SurA and the POTRA domains of BamA, Figure 1) can influence folding *in vitro*. By elucidating the mechanism of action of these proteins, which are essential for the correct trafficking, folding and insertion of OMPs *in vivo*, it is hoped to gain insights into the mechanisms of OMP folding in the cell.

Publications

Huysmans, G., Radford, S., Baldwin, S. & Brockwell, D. (2012) Malleability of the folding mechanism of the outer membrane protein pagp: Parallel pathways and the effect of membrane elasticity. *J. Mol. Biol.* **416:** 453-464.

Funding

We thank Nasir Khan for technical support and the Wellcome Trust and BBSRC for funding.

ATP-driven remodelling of the linker domain in the dynein motor

Anthony Roberts, Bara Malkova, Thomas Edwards, Peter Knight and Stan Burgess

Introduction

Dynein ATPases are the largest known cytoskeletal motor proteins in eukaryotic cells and perform critical functions: carrying cargo along microtubules in the cytoplasm and powering flagellar beating (Figure 1). Dyneins are members of the AAA+ superfamily of ring-shaped enzymes, but how they harness this architecture to produce movement is poorly understood. The work described in this report was focused on the fundamental mechanism that underlies movement and force production along microtubules. Dynein motors are also the largest of the three families of molecular motors- each motor domain being ~380 kDa in size, located within a ~520 kDa heavy chain that typically forms a much larger motor complex comprising between one and three heavy chains and numerous smaller polypeptide chains.

Results

We have used cryo-electron microscopy and single-particle image processing to determine (*ab initio*) three-dimensional maps of a native (full-length) flagellar dynein (from the single-celled alga *Chlamydomonas*) and an engineered cytoplasmic dynein motor domain (from the slime mold *Dictyostelium*) lacking the cargo-binding tail domain, in different nucleotide states. The structures show key sites of conformational change within the AAA+ ring and a large rearrangement of the "linker" domain, involving a hinge near its middle. Analysis of a mutant in which the linker "undocks" from the ring indicates that linker remodeling requires energy that is supplied by interactions with the AAA+ modules.

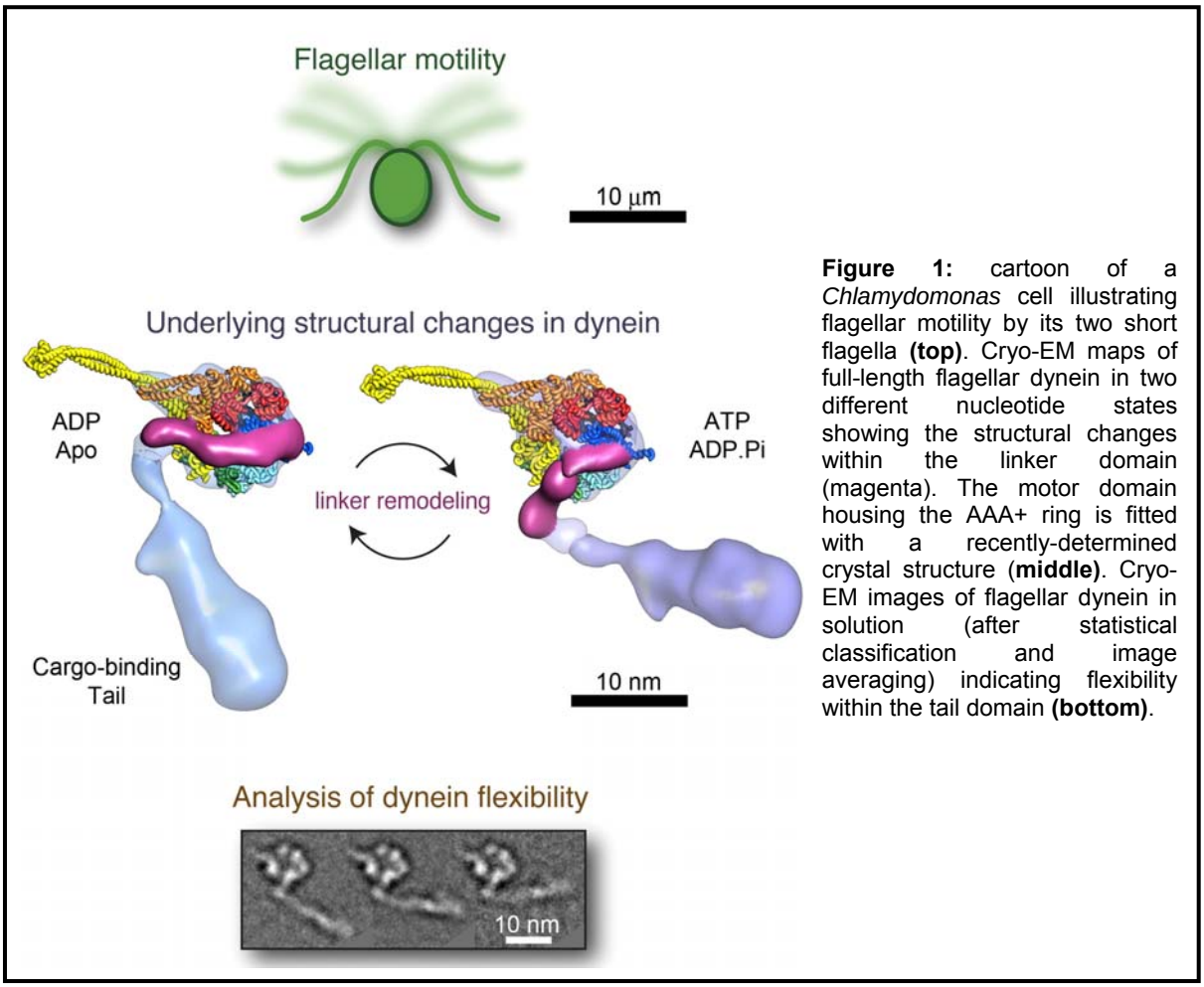

Figure 1: cartoon of a *Chlamydomonas* cell illustrating flagellar motility by its two short flagella **(top)**. Cryo-EM maps of full-length flagellar dynein in two different nucleotide states showing the structural changes within the linker domain (magenta). The motor domain housing the AAA+ ring is fitted with a recently-determined crystal structure (**middle)**. Cryo-EM images of flagellar dynein in solution (after statistical classification and image averaging) indicating flexibility within the tail domain **(bottom)**.

Remodelling of the linker is important for dynein because this domain connects directly to the cargo-binding tail domain. Analysis of individual cryo-EM images of full-length dynein shows that this tail domain is flexible in solution. Fitting our full-length dynein structures into lower resolution tomograms of whole flagella suggests how this mechanism could drive microtubule sliding that underlies the beating of cilia and flagella. The resulting configuration of dynein binding to microtubules also has implications for the mechanism of stepping by the dimeric cytoplasmic dynein that underlies cargo transport in many processes in eukaryotic cells essential for life.

Publications

Roberts, A., Malkova, B., Walker, M., Sakakibara, H., Numata, N., Kon, T., Ohkura, R., Edwards, T., Knight, P., Sutoh, K., Oiwa, K. & Burgess, S. (2012) ATP-driven remodeling of the linker domain in the dynein motor. *Structure* **20:** 1670-1680.

Funding

This work was supported by the BBSRC, the Wellcome Trust and the Human Frontiers Science Program Organization.

Collaborators

External: H. Sakakibara and K. Oiwa (Advanced ICT Research Institute, Kobe, Japan).
T. Kon and K. Sutoh (University of Tokyo, Japan).

Extreme biophysics: a single molecule approach to explore proteins from extreme environments

Megan Hughes, Toni Hoffmann, Katarzyna Tych, Danielle Walsh, Michael Wilson, David Brockwell and Lorna Dougan

Introduction

Life has adapted to a vast range of environmental conditions and it is now difficult to find any place on Earth devoid of life. Some conditions are extreme in the sense of being unfavourable to most eukaryotic life forms. The adaption of proteins played a key role in enabling extremophilic organisms to colonise such ecological niches (Figure 1). Understanding the physical properties of proteins from extremophilic organisms and their remarkable preservation capability is not only of fundamental interest, but also pivotal to our ability to rationally engineer biological materials for exploitation.

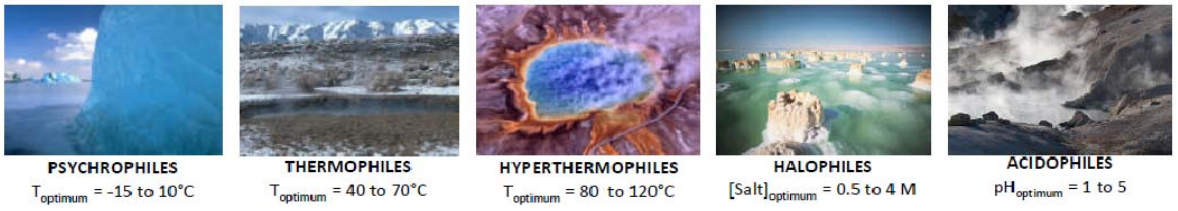

Figure 1: survival in the most adverse of environmental conditions requires extensive adaptations to enable life at the extremes of temperature, pressure or salinity. Extremophilic (extreme-loving) organisms have evolved unique features to enable them to function in these conditions (T_{opt}=optimum organism temperature).

Developing new tools to explore extremophile proteins

We are developing quantitative biophysical approaches to characterise the physical mechanisms of protein folding and stability in extreme environments. We have built a force spectroscopy instrument which we use to examine the conformational dynamics of single extremophilic proteins. This technique is used to apply a constant stretching force along a well-defined reaction coordinate, the end-to-end length of the protein, driving proteins to a fully extended unfolded state (Figure 2). By examining single molecules one at a time, the individual dynamics of protein subpopulations can be measured, revealing information which may be crucial for understanding and designing 'artificial' extremophilic proteins.

New insight gained from this approach

A single molecule approach provides a new perspective and reveals novel insight into the mechanisms of protein folding particularly with regard to how peptide chains fold in interplay with various environmental parameters. Moreover, this approach could aid in the design of extremophilic proteins which possess specific thermal or mechanical stability, binding specificity and conformational flexibility for exploitation in biotechnology and medicine. Our study will not only help to better understand life on Earth but also its prospects elsewhere.

Harnessing the power of extremophile organisms

Proteins with high stability are a prime target for biotechnology, for their prolonged life in storage and application and for their utility under extreme conditions. In addition to withstanding extreme temperatures, such proteins are resilient to organic solvents and proteolytic attack. While specific extremophilic proteins with particular capabilities have been sought, engineering stability into mesophilic proteins is an attractive alternative. The increased availability of complete genomes, coupled with the improved resolution of protein structures, has provided the potential to obtain stable proteins designed for individual

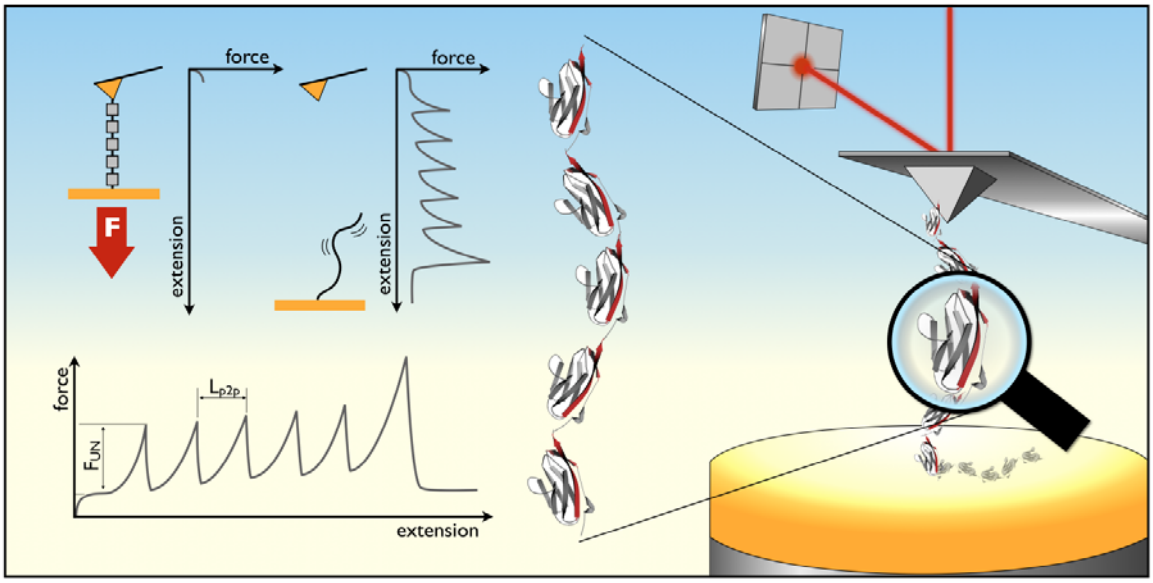

Figure 2: in single molecule force spectroscopy, the polyprotein chain is tethered between a substrate (e.g. gold) and the tip of a silicon nitride cantilever. Cysteine residues can be used to anchor one end of the protein by thiol-gold interactions while the opposite end of the polyprotein chain attaches non-specifically to the cantilever tip. The force acting on the protein displaces the cantilever with a known spring constant. That displacement is detected by the change of deflection of a laser focused on to the back of the cantilever tip.

potential applications. However, the advancement of extremophilic research relies on the continual development of enabling technology to examine and characterise the stability, flexibility and function of these proteins.

Publications

Hoffmann, T. & Dougan, L. (2012) Single molecule force spectroscopy using polyproteins. *Chem. Soc. Rev.* **41:** 4781-4796.

Funding

This work is being funded by the European Research Council, EPSRC and the BBSRC White Rose DTP in Mechanistic Biology.

Collaborators

External: L. Peck and M. Clark (British Antarctic Survey). A. Soper (Rutherford Appleton Laboratories).

Structural examination of biologically-relevant solutions using neutron diffraction

James Towey, Natasha Rhys and Lorna Dougan

Introduction

Over the past decade, significant advances have been made in the methods of neutron diffraction with isotopic substitution and in the development of more powerful computational tools. Neutron diffraction is an ideal probe for the structural study of liquids providing a full atomistic-level, structural examination of aqueous solutions.

Research theme 1: molecular mechanisms of cryoprotection

Glycerol–water liquid mixtures are intriguing hydrogen-bonded systems and essential in many fields, ranging from basic molecular research to widespread use in industrial and biomedical applications as cryo-protective solutions. Despite much research on these mixtures, the details of their microscopic structure are still not understood. One common notion is that glycerol acts to diminish the hydrogen bonding ability of water, a recurring hypothesis that remains untested by direct experimental approaches. We have characterised the structure of glycerol–water mixtures, across the concentration range, using a combination of neutron diffraction experiments and computational modelling. Contrary to previous expectations, we show that the hydrogen bonding ability of water is not diminished in the presence of glycerol. We show that glycerol–water hydrogen bonds effectively take the place of water–water hydrogen bonds, allowing water to maintain its full hydrogen bonding capacity regardless of the quantity of glycerol in the environment. We provide a quantitative measurement of all hydrogen bonding in the system and reveal a concentration range where a micro segregated, bi-percolating liquid mixture exists in coexistence with a considerable interface region (Figure 1). This work highlights the role of hydrogen bonding connectivity rather than water structuring/destructuring effects in these important cryo-protective systems.

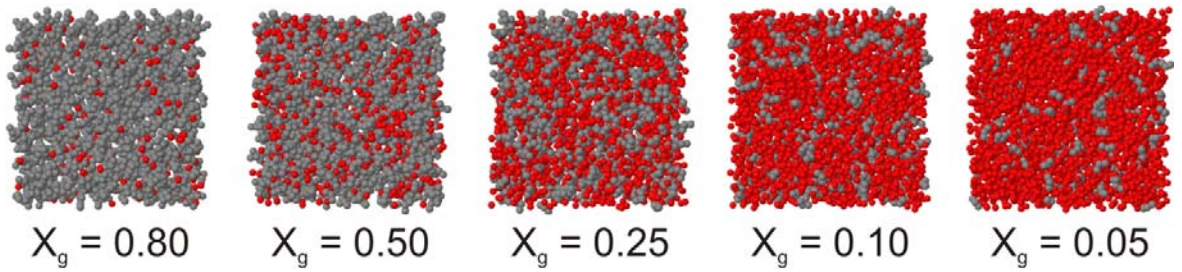

Figure 1: molecular scale segregation in glycerol-water solutions (x_g = mole fraction glycerol) is shown by clusters of glycerol (grey) and water (red) molecules. The snapshots show groups of water molecules and glycerol molecules hydrogen bonded together, forming clusters in the solution. To quantitatively assess this micro segregation, we completed a cluster analysis for glycerol and water across the concentration range.

Research theme 2: the role of hydrogen bonding in polyglutamine structure and association

Hydrogen bonding between glutamine residues has been identified as playing an important role in the intermolecular association and aggregation of proteins. To establish the molecular mechanisms of glutamine interactions, neutron diffraction coupled with hydrogen/deuterium isotopic substitution in combination with computational modelling has been used to investigate the structure and hydration of glutamine in aqueous solution. We find that the backbone of glutamine is able to coordinate more water molecules than the side chain, suggesting that charged groups on the glutamine molecule are more successful in attracting

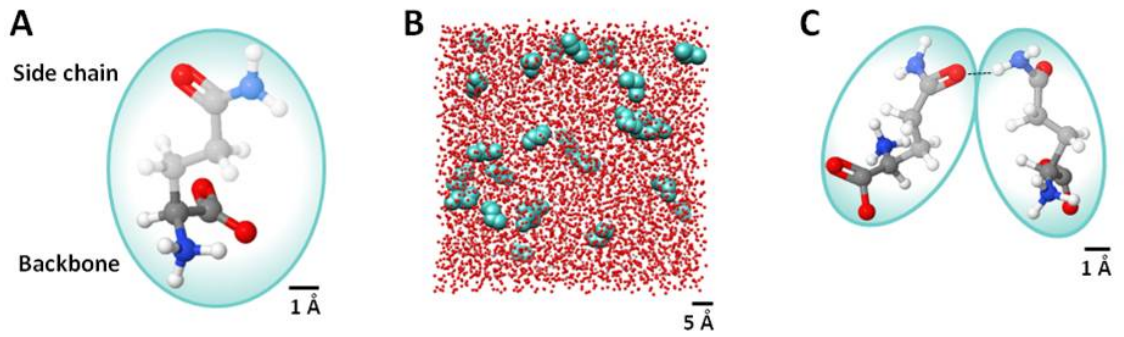

Figure 2: (a) the zwitterionic form of the glutamine molecule ($C_5H_{10}N_2O_3$). **(b)** Neutron diffraction experiments and computational modelling examine zwitterionic glutamine association in aqueous solution. The snapshot illustrates the association of glutamine molecules (blue) in a water solution (red) at 297 K. **(c)** Glutamine molecules associate into dimers through hydrogen bonds between the side chains.

water than the dipole in the side chain. In both the backbone and the side chain, we find that the carbonyl groups interact more readily with water molecules than the amine groups. We find that glutamine–glutamine interactions are present, despite their low concentration in this dilute solution. This is evidenced through the occurrence of dimers of glutamine molecules in the solution (Figure 2), demonstrating the effective propensity of this molecule to associate through backbone–backbone, backbone–side chain, and side chain–side chain hydrogen bond interactions. The formation of dimers of glutamine molecules in such a dilute solution may have implications in the aggregation of glutamine-rich proteins in neurological diseases where aggregation is prevalent.

Publications

Rhys, N., Soper, A. & Dougan, L. (2012) The hydrogen-bonding ability of the amino acid glutamine revealed by neutron diffraction experiments. *J. Phys. Chem. B* **116:** 13308-13319.

Towey, J. & Dougan, L. (2012) Structural examination of the impact of glycerol on water structure. *J. Phys. Chem. B* **116:** 1633-1641.

Towey, J., Soper, A. & Dougan, L. (2012) Molecular insight into the hydrogen bonding and micro-segregation of a cryoprotectant molecule. *J. Phys. Chem. B* **116:** 13898-13904.

Funding

This work is being funded by EPSRC (2010-EP/H020616/1).

Collaborators

External: A. Soper (Rutherford Appleton Laboratories, United Kingdom).

A novel relationship between β-amyloid precursor protein and tau in neuronal iron trafficking

Andrew Tsatsanis and James Duce

Introduction

The life essential element iron is required as a cofactor in metabolic processes throughout the body and specifically in tissues of high oxygen consumption, such as the central nervous system. Iron's ability to freely receive and donate electrons is critical (e.g. oxidative phosphorylation) and a deficiency in iron can lead to metabolic stress. However, the over presence of unbound iron is also detrimental as this may catalyze the production of toxic reactive oxygen species. Since too much or too little iron can compromise cell viability, cellular iron homeostasis is tightly regulated. This can be carried out through a number of ways, including our recently discovered ability for β-amyloid precursor protein (APP) to facilitate the movement of iron within extracellular fluid and maintain intracellular iron homeostasis. The iron homeostatic control of APP is partly through it's ability to bind to the iron exporter ferroportin (FPN) and with iron transporting proteins (e.g. members of the Transferrin family) that require Fe^{3+} loading. Efficiency of APP to assist in the efflux of intracellular iron through FPN requires it to be transported to the cell surface from within.

APP's iron homeostatic role is particularly evident within neurons and failure, either through reduced expression or disrupted localization on the cell surface, associates with age-related increases in brain iron and altered iron-related protein expression. Brain iron content is further increased in patients and animal models of neurodegenerative disorders such as Alzheimer's disease (AD) and Parkinson's disease (PD). This has created significant interest in the possibility that homeostatic disturbances in brain iron may contribute to a common underlying age-related pathogenesis of these diseases.

Results

We have identified a direct interaction with lactoferrin (LF) captured *in vitro* using sedimentation velocity and quenching of tryptophan fluorescence (Figure 1A&B), and *in vivo* using immunoprecipitation. We show this interaction is likely to cause the observed altered location of LF in hepatocytes (that correlates with iron changes) (Figure 1C-E) and decreased presence of LF in plasma from APP-deficient mice (not shown).

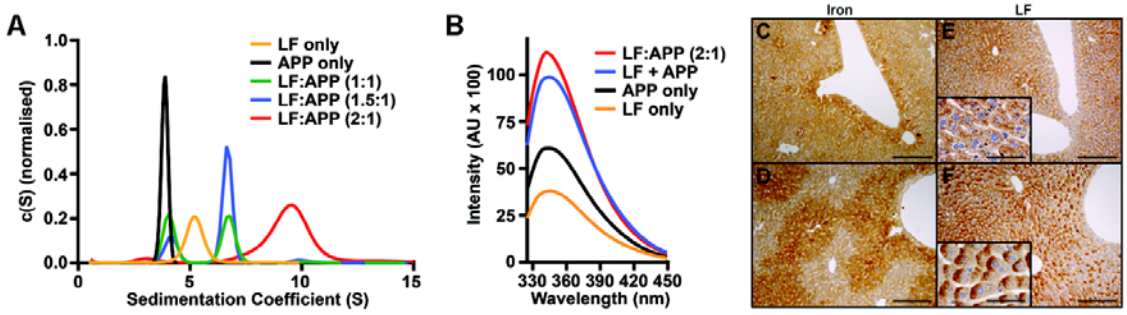

Figure 1: APP has a direct protein-protein interaction with Lactoferrin; a member of the transferrin family. (a) Sedimentation coefficient distributions of holo-Lactoferrin (LF) alone (orange) and APP in the absence (black) and presence of LF (green, blue & red). The c(S) distributions indicate two different complexes which form in a concentration-dependent manner. (**b**) Tryptophan fluorescence spectra (excitation wavelength of 295nm) for APP alone (black), holo-LF alone (orange) and a mixture of APP and holo-LF (red). The total expected intensity of the APP alone and holo-LF alone spectra was also calculated (blue). **(c & d)** Modified Perl's staining of liver detects a higher concentration of iron in $APP^{-/-}$ compared to WT mice. **(e & f)** LF was evenly distributed throughout WT mouse hepatocytes but pooled preferentially towards one side of the cell in $APP^{-/-}$ (see inset)**.**

In addition we have recently established a direct iron-related link between APP and another pathologically relevant protein called tau; whereby tau is required to transport APP to the cell surface, thus allowing it to interact with FPN and facilitate iron efflux. Upon tau's deletion within the mouse knockout model cell surface APP is decreased and intracellular iron accumulates (Figure 2), similar to when APP expression is disrupted (APP knockout mice) or in neurodegenerative diseases such as AD and PD. We are now currently investigating APP's ability to control iron homeostasis via its complex post-translational processing that is required for its correct localization within the cell. While the processing of APP, particularly within the brain, has been extensively studied due to its historic association with AD, it still lacks a conspicuous function until our recent discovery.

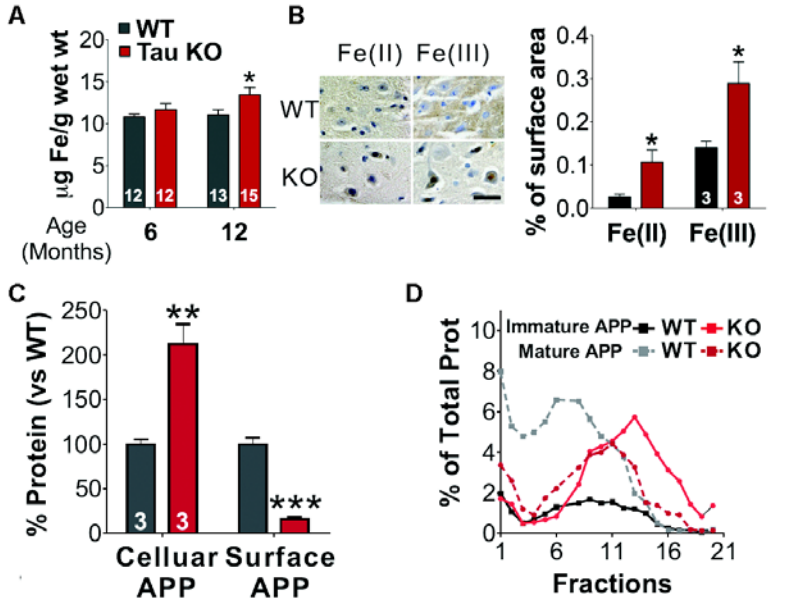

Figure 2: Tau deletion causes iron accumulation by preventing APP trafficking to the cell surface. (**a**) Substantia Nigra iron levels in tau KO mice compared to WT. **(b)** Fe^{2+} and Fe^{3+} histology (brown) and quantification in SN from aged WT and tau KO mice. **(c)** Densitometric quantification of cellular (total) APP and surface (biotinylated) APP in primary neuronal cultures of tau KO compared to WT mice. (**d**) Distribution of immature and mature forms of APP in an iodixanol step gradient of primary neuronal cultures from tau-KO compared to WT.

Publications

Gu, B., Duce, J., Valova, V., Wong, B., Bush, A., Petrou, S. & Wiley, J. (2012) P2X7 receptor-mediated scavenger activity of mononuclear phagocytes toward non-opsonized particles and apoptotic cells is inhibited by serum glycoproteins but remains active in cerebrospinal fluid. *J. Biol. Chem.* **287:**17318-30.

Lei, P., Ayton, S., Finkelstein, D., Spoerri, L., Ciccotosto, G., Wright, D., Wong, B., Adlard, P, Cherny, R., Lam, L., Roberts, B., Volitakis, I., Egan, G., McLean, C., Cappai, R., Duce, J. & Bush, A. (2012) Tau deficiency induces parkinsonism with dementia by impairing APP-mediated iron export. *Nat Med.* **18:**291-95.

Funding

This work was supported by a Senior Research Felloship from Alzhiemer's Research UK and NHMRC (Australia).

Collaborators

External: A. Bush and R. Cherny (University of Melbourne, Australia). R. Evans (Brunel University).

Structure, function and evolution of the Crimean Congo hemorrhagic fever nucleocapsid protein

Stephen Carter, Cheryl Walter, Rebecca Surtees, Antonio Ariza, John Barr and Thomas Edwards

Introduction

Recent research in our lab has focused on the Crimean-Congo hemorrhagic fever virus (CCHFV). CCHFV is a member of the *Bunyaviridae* family, and together with members of the *Arenaviridae* and *Orthomyxoviridae* families these viruses are known as segmented negative stranded RNA viruses (sNSV) by virtue of their multistranded genomes.

While these viruses are extremely diverse in their disease causing ability, they possess one common structural characteristic that is at the core of their respective life cycles; a ribonucleocapsid assembly (RNP). This is an association of the RNA genome with a virus-encoded nucleocapsid (N) protein, and its formation is essential for several fundamental aspects of the virus replication cycle including gene expression and virus assembly.

One aspect of our research is to try to understand how the structure of the CCHFV N RNP protein dictates and relates to its function. Towards this aim, we have solved the crystal structure of the CCHFV N protein to 2.1 Å. Our work describes the N protein structure, and the high degree of structural homology between the CCHFV N protein and the N protein from another sNSV member Lassa virus (LASV), which is an arenavirus. Furthermore the crystal structure of the CCHFV N protein guided site-directed mutagenesis of specific N protein residues, which delineate how N binds RNA and thus forms a competent RNP template for both RNA replication and mRNA transcription.

Results

The CCHFV N is composed of a globular core comprising 15 alpha helices (α1-8; α14-20) and a prominent additional structural element we termed the 'arm' comprising two long alpha helices (α9-10) extending away from the core, presenting an exposed loop at its apex, and supported by a small three helix bundle (α11-13; Figure 1A). Electrostatic surface potential suggests a possible RNA binding 'platform' adjacent to the arm. Additional results from CCHFV mini-replicon system show some of these residues are important in CCHFV-specific RNA synthesis.

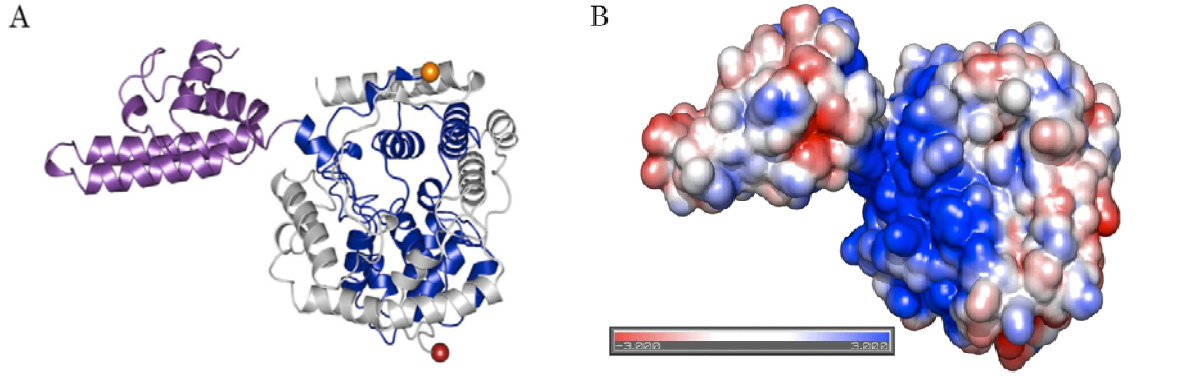

Figure 1: (a) Structure of CCHFV N monomer in ribbons representation. Helices are shown in silver for the N-terminal and dark blue for the C-terminal contribution to the globular domain, purple for the arm, which is in the middle of the primary sequence. **(b)** The electrostatic surface potential (generated with APBS). The scale bar shows the contour levels for the electrostatic potential at the solvent-exposed surface in kT/e.

Structural comparisons indicate that the CCHFV N globular domain exhibits a high degree of structural homology with the N-terminal domain of LASV N, a member of the *Arenaviridae*

family, whilst essentially structurally un-related to Rift Valley fever virus (RVFV), a member of the *Bunyaviridae* family. This data suggests the taxonony of two and three segmented RNA viruses may need re-examining.

The structural alignment provided additional clues about the RNA binding mechanism. The helix equivalent to LASV N α5 (yellow, Figure 2) is the helix in CCHFV N, α11, which precedes the long flexible loop at the base of the arm structure. This may represent a strong candidate for providing a similar RNA gating mechanism to that proposed for LASV N; RNA gating is mediated by a movement of α5 in the LASV N. Electrostatic surface of CCHFV N revealed an additional RNA binding 'pocket' equivalent to the LASV N RNA binding surface.

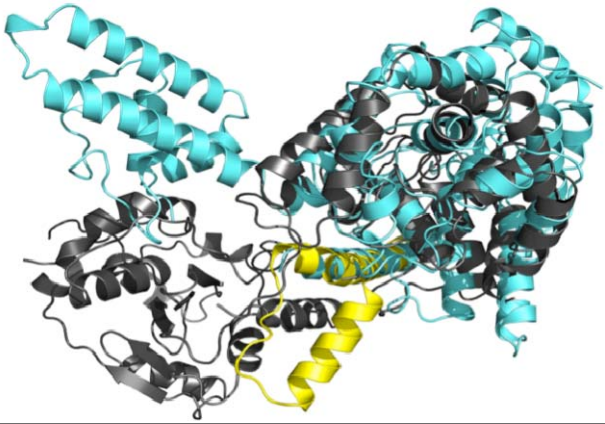

Figure 2: structural homology with LASV N. Structural alignment of CCHFV and LASV structures. The CCHFV N protein is shown in aquamarine, with most of the LASV N structure in grey. Highlighted in yellow are the LASV N elements that move upon RNA binding (α5, loop, α6). Note that there is no structural equivalent of the α6 RNA gate in CCHFV N.

Publications

Carter, S., Barr, J. & Edwards, T. (2012) Expression, purification and crystallization of the crimean-congo haemorrhagic fever virus nucleocapsid protein. *Acta Crystallogr. Sect. F Struct. Biol. Cryst. Commun.* **68:** 569-573.

Carter, S., Surtees, R., Walter, C., Ariza, A., Bergeron, E., Nichol, S., Hiscox, J., Edwards, T. & Barr, J. (2012) Structure, function, and evolution of the crimean-congo hemorrhagic fever virus nucleocapsid protein. *J. Virol.* **86:** 10914-10923.

Collaborators

External: Éric Bergeron and Stuart Nichol (Viral Special Pathogens Branch, CDC, Atlanta, USA).

De novo design and virtual high-throughput screening to identify novel inhibitors of membrane proteins

K. Simmons, A. Johnson and C. Fishwick

Introduction

Membrane proteins are intrinsically involved in both human and pathogen physiology, and are the target of 60% of all marketed drugs. During the past decade, advances in the studies of membrane proteins using x-ray crystallography, electron microscopy and NMR-based techniques led to the elucidation of over 250 unique membrane protein crystal structures. The aim of the European Drug Initiative for Channels and Transporter (EDICT) project is to use the structures of clinically significant membrane proteins for the development of lead molecules. One of the approaches used to achieve this is a virtual high-throughput screening (vHTS) technique initially developed for soluble proteins, another uses iterative rounds of ligand design based on newly available crystal structures to develop new ligands. The application of these methods to three targets as part of the EDICT project is discussed below.

Results

1. Identification of selective inhibitors of the potassium channel Kv1.1-1.2((3)) by high-throughput virtual screening

Two voltage-dependent potassium channels, Kv1.1 (KCNA1) and Kv1.2 (KCNA2), are found to co-localize at the juxtaparanodal region of axons throughout the nervous system and are known to co-assemble in heteromultimeric channels, most likely in the form of the concatemer Kv1.1-1.2((3)) . Loss of the myelin sheath, as is observed in multiple sclerosis, uncovers the juxtaparanodal region of nodes of Ranvier in myelinated axons leading to potassium conductance, resulting in loss of nerve conduction. The selective blocking of these Kv channels is therefore a promising approach to restore nerve conduction and function. The combined use of four popular virtual screening approaches (eHiTS, FlexX, Glide, and Autodock-Vina) led to the identification of several compounds as potential inhibitors of the Kv1.1-1.2((3)) channel. From 89 electrophysiologically evaluated compounds, 14 novel compounds were found to inhibit the current carried by Kv1.1-1.2((3)) channels by more than 80 % at 10 μM. Accordingly, the IC50 values calculated from concentration-response curve titrations ranged from 0.6 to 6 μM. Two of these compounds exhibited at least 30-fold higher potency in inhibition of Kv1.1-1.2((3)) than they showed in inhibition of a set of cardiac ion channels (hERG, Nav1.5, and Cav1.2), resulting in a profile of selectivity and cardiac safety.

2. A virtual high-throughput screening approach to the discovery of novel inhibitors of the bacterial leucine transporter, LeuT

A suitable protein for conducting a vHTS is LeuT, a bacterial homologue of the NSS family characterized by their ability to use the sodium gradient across the plasma membrane to drive the transport of its solute against its concentration gradient. From screening a library of commercially available molecules, 1000 compounds were selected for further evaluation and consensus scoring using the *de novo* design program SPROUT. These 1000 compounds were selected based on their predicted binding to the protein as predicted using the eHiTS scoring algorithm. From this set, 11 molecules were selected for purchase. These 11 compounds were chosen based upon their predicted binding affinity to the protein as determined using the eHiTS and SPROUT scoring functions and also their predicted binding pose. From an initial purchase set of 11 compounds, five compounds were found to exhibit activity against the protein when tested at 1 mM, a hit rate of 45%. The four most active compounds were tested for their dose-response inhibition of the [^{3}H]-leucine binding with their IC50 values being ~ 40 μM (Figure 1).

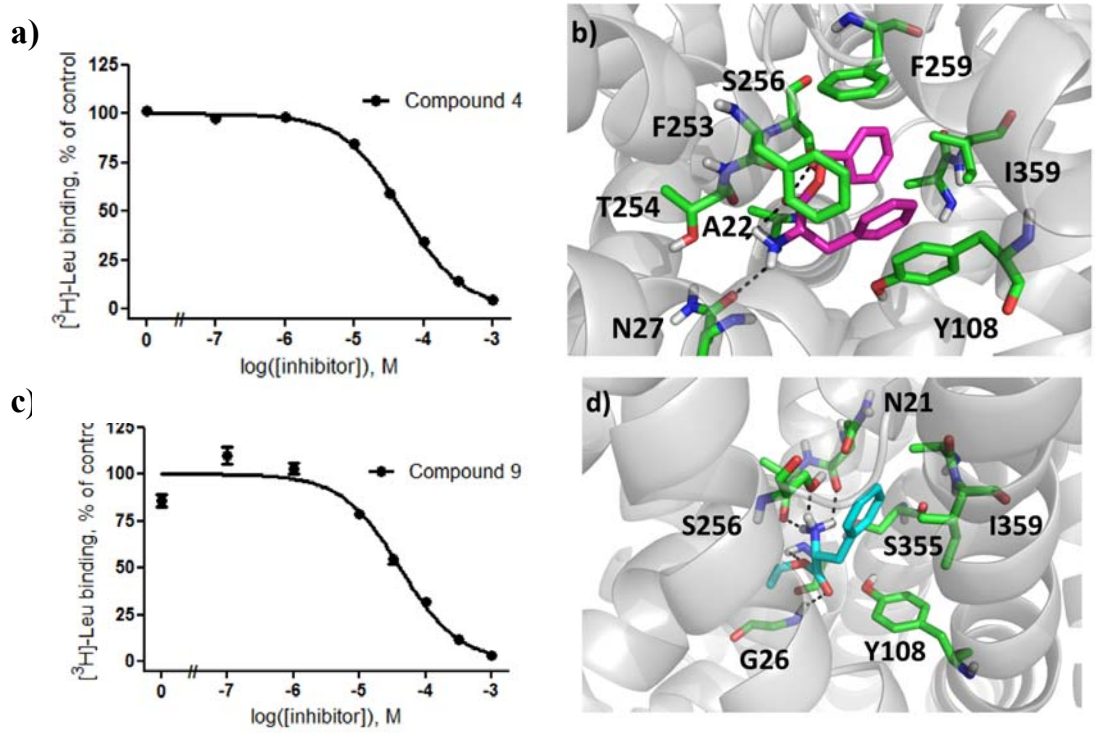

Figure 1: dose-response curves and binding pose of compounds 4 and 9. (a) Dose-response inhibition of [^{3}H]-leucine ([^{3}H]-Leu) binding to LeuT by compound 4. Normalized results are given as mean ± SEM on the basis of four independent experiments. **(b)** Compound 4 (magenta) docked into the crystal structure of the LeuT used for all vHTS (2Q72). The compound makes H-bonding interactions with Ala22, Asn27 and Ser256. **(c)** Dose-response inhibition of [^{3}H]-leucine ([^{3}H]-Leu) binding to LeuT by compound 9. Normalized results are given as mean ± SEM on the basis of four independent experiments. **(d)** Compound 9 (cyan) docked into the crystal structure of the LeuT used for all vHTS (2Q72). The compound makes H-bonding interactions with Asn21, Ala22, Gly24 and 26 and Ser256.

Probing the molecular mechanism of ligand binding by Mhp1

The hydantoin transporter Mhp1 is a sodium-coupled secondary active transport protein and a member of the growing 5-helix inverted repeat superfamily of transporters. The structure of Mhp1 was previously solved in three different conformations revealing the molecular basis of the alternating access mechanism but not the details of substrate binding. We have explored this through a combination of crystallography, ligand design, biochemical assays, molecular dynamics and site-directed mutagenesis. The crystal structure was solved in complex with L-5-indolylmethylhydantoin at 3.5 Å resolution. Using the structure, over 80 new ligands were designed, synthesised or procured and tested for binding to Mhp1 in competitive transport assays. From the deduced structure-activity relationships, roles were inferred for specific Mhp1 residues and tested by site-directed mutagenesis. Two of the new ligands were co-crystallised with Mhp1. Their positions in the protein confirm the poses predicted by docking but also reveal a novel conformational intermediate.

Publications

Wacker, S., Jurkowski, W., Simmons, K., Fishwick, C., Johnson, P., Madge, D., Lindahl, E., Rolland, J-F & de Groot, B. (2012) Identification of selective inhibitors of the potassium channel Kv1.1-1.2(3) by high-throughput virtual screening and automated patch clamp. *ChemMedChem* **7:** 1775-1783.

Funding

We thank the European Community's Seventh Framework Programme FP7/2007-2013 for support of this research under grant agreement n°HEALTH-F4-2007-201924, European Drug Initiative for Channels and Transporters (EDICT) Consortium.

Identification and optimisation of small molecule inhibitors of proteins for use as chemical probes or therapeutics

Ian Yule, Jeff Plante, Rachael Tennant, Jayakanth Kankanala, Rachel Trowbridge, Charlotte Revill, Joseph Thompson, Adam Nelson, Colin Fishwick and Richard Foster

Introduction

Our group is interested in the design, synthesis and optimisation of small molecules for therapeutic application or their use in the elucidation of biological function. By combining tools and techniques in medicinal chemistry, computer-aided drug design and chemical genetics we aim to identify and optimise targeted small molecules as key modulators of specific biological function to support both basic target validation of proteins implicated in disease and as potential starting points for future drug discovery.

The group has capabilities in a number of areas for which bioactive molecules may be identified, optimised and/or targeted, including:

Medicinal chemistry, probe synthesis and chemical genetics

- Bio-targeted small molecules
- Targeted imaging agents
- Small molecule microarrays

Computational-aided drug design

- Ligand- and structure-based design
- Virtual screening

High-throughput screening

- 30k member diverse lead-like small molecule library
- Fragment library
- Assay transfer/assay development

The activities are managed through the Medicinal Chemistry and Chemical Biology (MCCB) Technology Group as part of the Biomedical Health Research Centre (BHRC) at Leeds. Several new projects have been initiated during 2012.

Small molecule therapeutics

1. Development of a novel anticoagulant with minimal bleeding risk

We have identified potent, novel small molecule inhibitors of a key enzyme involved in regulation of the coagulation cascade with exceptional *in vivo* efficacy. The inhibitors have been identified by a number of parallel approaches incorporating virtual drug design, chemical synthesis and HTS of drug-like small molecule libraries and fragments. Presently, we are optimising the inhibitors for target potency, specificity and drug-like physicochemical properties using iterative rounds of medicinal chemistry development and screening using a panel of orthogonal bioassays.

2. Identification of novel inhibitors of TRP ion channel function as potential therapeutics

We have identified a series of novel inhibitors of a TRP ion channel implicated in cardioprotection. The compounds have been developed as agents to support detailed understanding of the role of the protein target and its relevance in disease as well for future development of small molecule-based therapeutics. These dual aims are being achieved through iterations of directed chemical synthesis aided by pharmacophore-based design and screening *via* a panel of orthogonal assays.

Diagnostics

Targeted contrast agents

We are designing and synthesising modular targeted high relaxivity MRI contrast agents for protein targeted cardiovascular disease monitoring and prevention.

Electrochemical microarrays
We are developing a small molecule electrochemical microarray for detection of protein-small molecule binding interactions. We are designing multiplexed small molecule microarrays to detect binding of proteins by electrochemical impedance. This approach constitutes a highly promising and flexible method towards the label-free detection of small molecule-protein interactions and has a number of potential therapeutic and translational applications, including micro- HTS and point-of-care diagnostics.

Funding
This work is funded by the MRC, EPSRC, Parkinson's UK, BBSRC, AICR, CRUK, BHF and BHRC.

Collaborators
Leeds: H. Philippou, R. Ariens and C. Fishwick (novel anti-coagulants), L.-H. Jiang, D. Beech, R. Sivaprasadarao (TRP channel inhibitors), R. Bon, S. Gilbert, S. Plein, A. Maqbool (targeted contrast agents), S. Johnson (Electrochemical microarrays).

Studies on hepatitis C virus replication and pathogenesis

Yutaka Amako, Michaela Conley, Bjorn-Patrick Mohl, Zsofia Igloi, Doug Ross, Joe Shaw, Hazel Stewart, Cheryl Walter, Carsten Zothner and Mark Harris

Introduction

Hepatitis C virus (HCV) infects 170 million individuals and is a major cause of chronic liver disease, including fibrosis, cirrhosis and hepatocellular carcinoma. The virus has a single stranded positive sense RNA genome of 9.5kb that contains a long open reading frame encoding a single polyprotein of 3000 amino acids which is cleaved into 10 individual polypeptides by a combination of host cell and virus specific proteases. We are interested in understanding the molecular mechanisms of viral genome replication and assembly, with a particular focus on the virus-host interactions that underpin these processes. The ultimate goal of this research is to identify new targets for the development of novel antivirals.

Results

A major focus of work is NS5A, a pleiotropic phosphoprotein with multiple roles in the virus lifecycle. We are investigating the role of NS5A in virus replication and assembly, as well as its interactions with cellular factors. For example, recently we have used a mass spectrometric approach to identify sites of phosphorylation within the protein and generated mutants of these phosphorylation sites to characterise the role of this post-translational modification in NS5A function. In collaboration with Grahame Hardie (Dundee) we are raising phosphospecific antibodies to these sites with the intention of probing the role of phosphorylation further. Other studies are investigating the interactions of NS5A with RNA, both *in vitro* and *in vivo*. Similar studies are ongoing with the viral capsid or Core protein with a view to dissecting the mechanism by which new virus particles are assembled.

We also use proteomic and imaging techniques to probe the multiprotein complex that replicates the viral genome (e.g. purifying nascent RNA from infected cells and identifying associated proteins by mass spectrometry, and genetically tagging the virus to enable either high resolution EM or fluorescent imaging). In collaboration with J. Mankouri we are utilising a recently installed confocal microscope with live cell imaging capability located within a category III containment facility – a unique resource within the UK for the study of HCV. This facility is currently being used to understand HCV induced autophagy.

In collaboration with Colin Fishwick (Leeds) we are applying structure-based drug design methodology to the NS2 protein, a key protease involved in the cleavage of the viral polyprotein. We have established a robust cell-based assay to identify small molecules with the ability to block NS2 mediated cleavage. We hope that these may form the basis for a novel future therapeutic approach.

Publications

Mohl, B.-P., Tedbury, P., Griffin, S. & Harris, M. (2012) Hepatitis c virus-induced autophagy is independent of the unfolded protein response. *J. Virol.* **86:** 10724-10732.

Funding

Doug Ross holds an Astra Zeneca CASE studentship. This work is funded by a Wellcome Trust (PhD studentship, project grant and Senior Investigator Award).

Collaborators

External: G. Hardie (University of Dundee), J. McLauchlan (MRC Virology Unit, Glasgow).
Leeds: J. Mankouri, S. Griffin, C. Peers and C. Fishwick

Disease-associated mutations abolish palmitoylation and membrane association of syntaxin 11 in natural killer cells

Andrew Hellewell, Ombretta Foresti, Nicola Topham and Eric Hewitt

Introduction

Natural killer (NK) cells are an important component of the innate arm of the immune system, killing infected and tumorigenic cells. NK cell recognition of target cells promotes the formation of an immunological synapse at the junction of the two cells. The polarised exocytosis of secretory lysosomes releases cytotoxic molecules at the immunological synapse. Perforin, a pore forming protein, facilitates the entry of granzymes into the target cell cytoplasm triggering apoptosis of the target cell. Subjects with Familial Haemophagocytic Lymphohistiocytosis (FHL), a rare familial disorder, display low NK cell cytotoxicity and a corresponding defect in secretory lysosome exocytosis. The SNARE protein syntaxin 11 is mutated in type 4 FHL (FHL-4). SNARE proteins mediate membrane fusion reactions, however the precise role of syntaxin 11 in secretory lysosome exocytosis is unknown. To better understand the function of this SNARE protein and why mutations in the protein result in FHL-4 we characterised the role of disease-associated mutations on the palmitoylation, membrane association and subcellular localisation of syntaxin 11.

Results

The C-terminal region of STX11 is necessary for palmitoylation and membrane association

SNARE proteins typically associate with membranes via a transmembrane domain; syntaxin 11, however, is an atypical SNARE in that it lacks a transmembrane domain. Instead syntaxin 11 is predicted to be palmitoylated at its cysteine rich C-terminus. We have demonstrated experimentally that syntaxin 11 is palmitoylated using the biotin switch assay (Figure 1A). This is an assay which switches palmitate groups on proteins for biotin such that they can then be pulled down from cell lysates on avidin beads. The FHL-4-associated mutant of syntaxin 11, Gln268X, which lacks the cysteine rich C-terminal region was not palmitoylated when expressed in the NK cell line YTS (Figure 1A). Moreover, syntaxin 11 Gln268X was not present in the membrane fraction of YTS NK cells (Figure 1B) and was instead in the cytosolic fraction. Thus the Gln268X mutation abolishes membrane palmitoylation and membrane association of syntaxin 11.

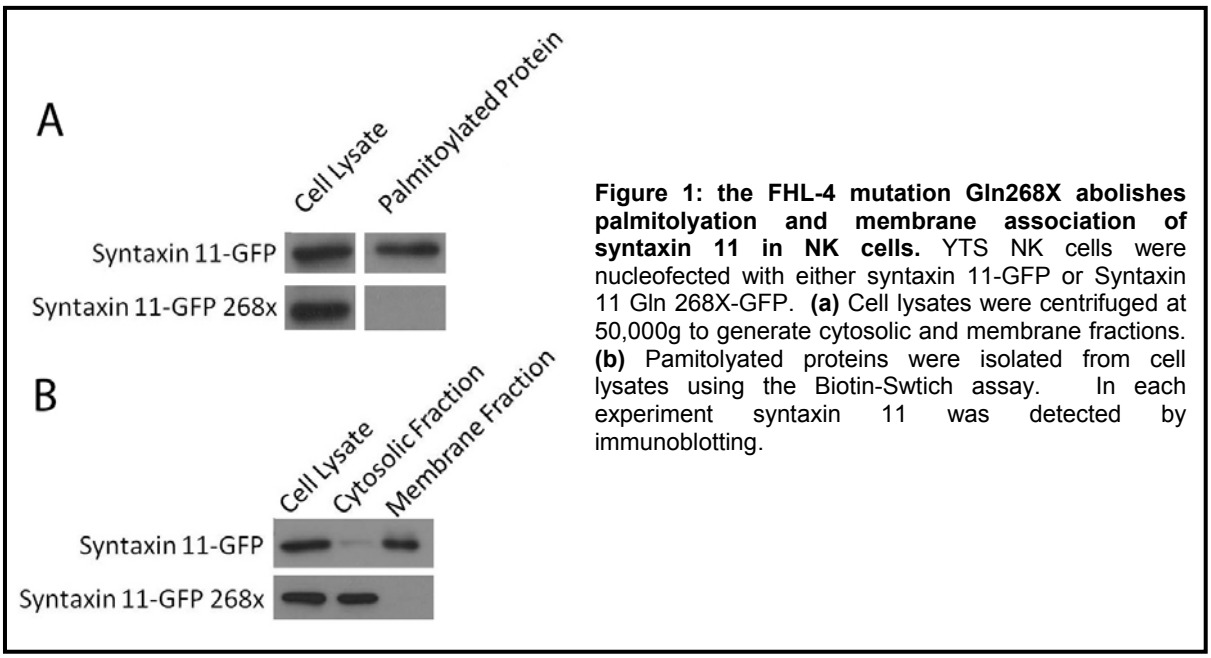

Figure 1: the FHL-4 mutation Gln268X abolishes palmitolyation and membrane association of syntaxin 11 in NK cells. YTS NK cells were nucleofected with either syntaxin 11-GFP or Syntaxin 11 Gln 268X-GFP. **(a)** Cell lysates were centrifuged at 50,000g to generate cytosolic and membrane fractions. **(b)** Pamitolyated proteins were isolated from cell lysates using the Biotin-Swtich assay. In each experiment syntaxin 11 was detected by immunoblotting.

Palmitoylation and membrane association are necessary for trafficking to the immunological synapse

During natural killer cell exocytosis, syntaxin 11 has been shown to traffic to the immunological synapse and to co-localise with secretory lysosomes. Using live-cell confocal microscopy we observed that in resting YTS cells, syntaxin 11 is localised to cytoplasmic puncta that are distinct from lysosomes (stained with Lysotracker), during conjugation with a target cell however, syntaxin 11 displays increased co-localisation with lysosomes at the immunological synapse. However, we found that syntaxin 11 Gln268X, exhibited a diffuse cytoplasmic localisation and did not traffic to the immunological synapse in activated YTS NK cells.

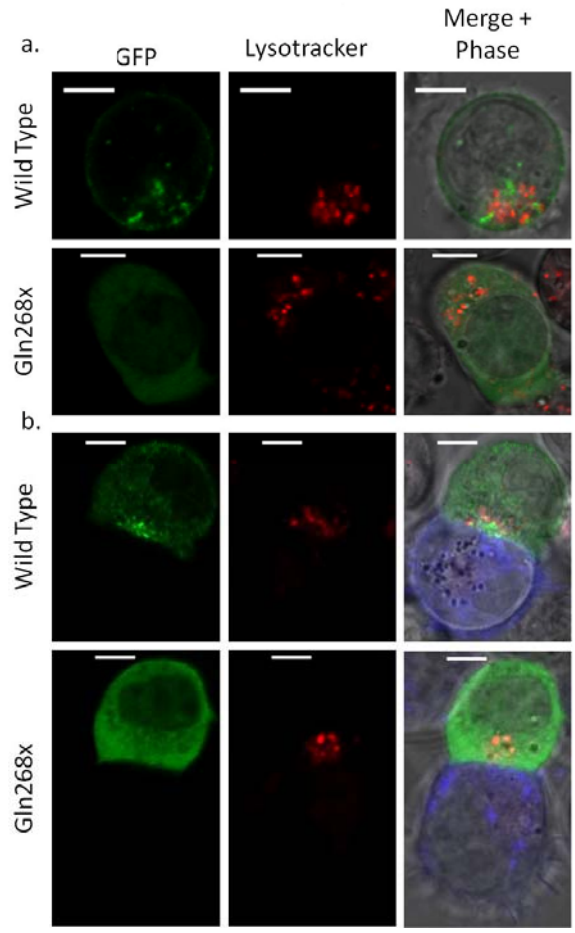

Figure 2: the FHL-4 mutation Gln268X prevents the recruitment of syntaxin 11 to the immunological synapse in activated NK cells. YTS NK cells were nucleofected with either syntaxin 11-GFP or Syntaxin 11 Gln 268X-GFP and incubated in the absence (A) or presence of the target cell line 721.221 (B) that had been labelled with Cell Trace (blue). Cells were stained with LysoTracker (red) to visualise secretory lysosomes and imaged by live cell confocal microscopy. Scale bar is 5 μm

Summary

Analysis of the FHL-4-associated mutant syntaxin 11 Gln268X reveals that palmitoylation is required for membrane association and recruitment of synatxin 11 to the immunological synapse in NK cells.

Funding

This work is supported by the Wellcome Trust.

Prion protein in zinc metabolism and action of amyloid-β oligomers in Alzheimer's disease

Rob Andrew, Heledd Griffiths, Kate Kellett, Nicole Watt, Isobel Whitehouse and Nigel Hooper

Introduction

The prion protein is probably best known for its role in the transmissible spongiform encephalopathies or prion diseases, such as Creutzfeldt-Jakob disease in humans and bovine spongiform encephalopathy in cattle. In these diseases the normal cellular form of the prion protein (PrP^{C}) undergoes a conformational conversion to the infectious form, PrP^{Sc}. However, understanding the physiological role(s) of PrP^{C} and whether loss of these contribute to disease are critical.

Alzheimer's disease (AD) is the commonest neurodegenerative disease of old age. Currently, there are no drugs available to halt or slow the progression of this devastating disease which is placing a huge burden on patients and carers. AD is characterised by the deposition in the brain of senile plaques that are composed of the amyloid-β peptide (Aβ). Through mechanisms that are poorly understood, Aβ oligomers, fibrils and/or aggregates are toxic to nerve cells.

Regulation of Aβ toxicity by the prion protein

PrP^{C} was recently identified as a high-affinity neuronal receptor for Aβ oligomers. We report that fibrillar Aβ oligomers recognised by the OC antibody, which have been shown to correlate with the onset and severity of AD, bind preferentially to cells and neurons expressing PrP^{C} (Figure 1). The binding of Aβ oligomers to cell surface PrP^{C}, as well as their downstream activation of Fyn kinase, was dependent on the integrity of cholesterol-rich lipid rafts. Fluorescence microscopy and co-localisation with sub-cellular markers revealed that the Aβ oligomers co-internalised with PrP^{C}, accumulated in endosomes and subsequently trafficked to lysosomes. The cell surface binding, internalisation and downstream toxicity of Aβ oligomers was dependent on the transmembrane low density lipoprotein receptor-related protein-1 (LRP1). The binding of Aβ oligomers to cell surface PrP^{C} impaired its ability to inhibit the activity of the β-secretase BACE1 which cleaves the amyloid precursor protein to produce Aβ. The green tea polyphenol (-)-epigallocatechin gallate (EGCG) and the red wine extract resveratrol both re-modelled the fibrillar conformation of Aβ oligomers. The resulting non-fibrillar oligomers displayed significantly reduced binding to PrP^{C}-expressing cells and were no longer cytotoxic. These data indicate that soluble, fibrillar Aβ oligomers bind to PrP^{C} in a conformation-dependent manner and require the integrity of lipid rafts and the transmembrane LRP1 for their cytotoxicity, thus revealing potential targets to alleviate the neurotoxic properties of Aβ oligomers in AD.

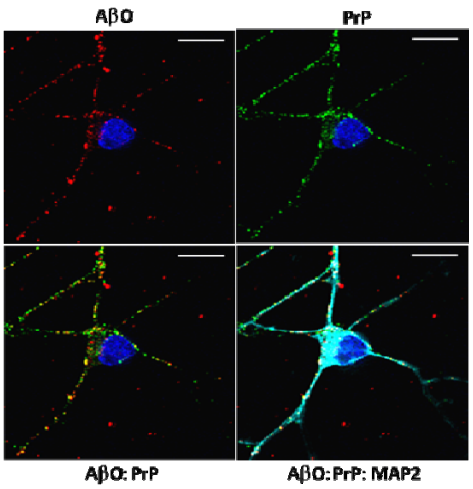

Figure 1: binding of Aβ oligomers (AβO) to rat primary hippocampal neurons expressing PrP^{C} (PrP).

The prion protein facilitates zinc uptake into neurons

Zinc is released into the synaptic cleft upon exocytotic stimuli, although the mechanism for its reuptake into neurons is unresolved. Using zinc specific fluorescent dyes we reported that PrP^{C} enhances the uptake of zinc into neuronal cells. This PrP^{C}-mediated zinc influx required

the octapeptide repeats and N-terminal polybasic region in PrP^C but not its endocytosis. Selective antagonists of α-amino-3-hydroxy-5-methyl-4-isoxazolepropionate (AMPA) receptors blocked the PrP^C-mediated zinc uptake and PrP^C co-immunoprecipitated with both GluA1 and GluA2 AMPA receptor subunits. Zinc-sensitive intracellular tyrosine phosphatase activity was decreased in cells expressing PrP^C and increased in the brains of PrP^C null mice, providing evidence of a physiological consequence of the process (Figure 2).

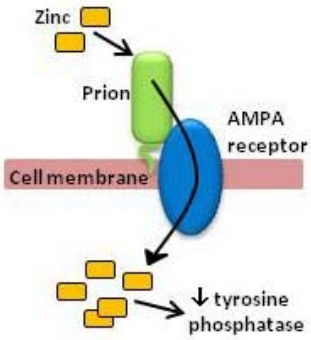

Figure 2: schematic for how PrP^C mediates zinc uptake into cells through AMPA receptors and affects intracellular tyrosine kinase activity.

This PrP^C-mediated zinc uptake was ablated in cells expressing familial prion disease-associated mutants of PrP^C and in prion-infected cells. These data suggest that alterations in PrP^C-mediated zinc uptake may contribute to neurodegeneration in prion and other neurodegenerative diseases.

Publications

Griffiths, H., Whitehouse, I. & Hooper, N. (2012) Regulation of amyloid-beta production by the prion protein. *Prion* **6:**1-6.

Lewis, V., Whitehouse, I., Baybutt, H., Manson, J., Collins, S. & Hooper, N. (2012) Cellular prion protein expression is not regulated by the Alzheimer's amyloid precursor protein intracellular domain. *PLoS ONE* **7:** e31754.

Vardy, E., Kellett, K., Cocklin, S. & Hooper, N. (2012) Alkaline phosphatase is increased in both brain and plasma in Alzheimer's disease. *Neurodegener. Dis.* **9:** 31-37.

Watt, N., Taylor, D., Kerrigan, T., Griffiths, H., Rushworth, J., Whitehouse, I. & Hooper, N. (2012) Prion protein facilitates uptake of zinc into neuronal cells. *Nat. Commun.* **3:** 1134-1134.

Funding

This work was funded by the MRC, Wellcome Trust, Alzheimer's Research UK and BBSRC.

Collaborators

Leeds: T. Turner, C. Fishwick, R. Foster, A. Nelson, C. Peers, D. Tomlinson.

The substrate of the quinol oxidase CymA is also a specific co-factor

Duncan McMillan and Lars Jeuken

Introduction

An overwhelming number of chemical reactions in nature are redox reactions. In biology, these reactions are catalysed by redox enzymes, many of which reside in the lipid membrane. Redox enzymes play a major role in almost all metabolic processes, including photosynthesis and biochemical processes such as the nitrogen cycle. By electrically connecting redox enzymes to electrodes, a powerful sensing platform is constructed that is able to characterise details of the catalytic mechanism of these enzymes.

Little is known about enzymatic quinone-quinol interconversions in the lipid membrane when compared to our knowledge of substrate transformations by globular enzymes. In 2012 we studied the enzyme mechanism of a relatively simple quinone converting enzyme, CymA, belonging to the NapC/NirT superfamily. In contrast to most other quinone oxidoreductases, members of this family are monotopic membrane proteins with one globular head domain, facing the periplasm in Gram-negative bacteria. CymA is found in the inner membrane of the γ-proteobacterium *Shewanella oneidensis* MR-1, which are bestowed with a remarkably diverse multicomponent and branched electron transport chain. CymA plays a central role in this multi-branched respiratory chain where it couples the oxidation of menaquinone-7 (MK-7) to a number of multi-heme cytochromes, terminal reductases and soluble extracellular electron carriers (Figure 1).

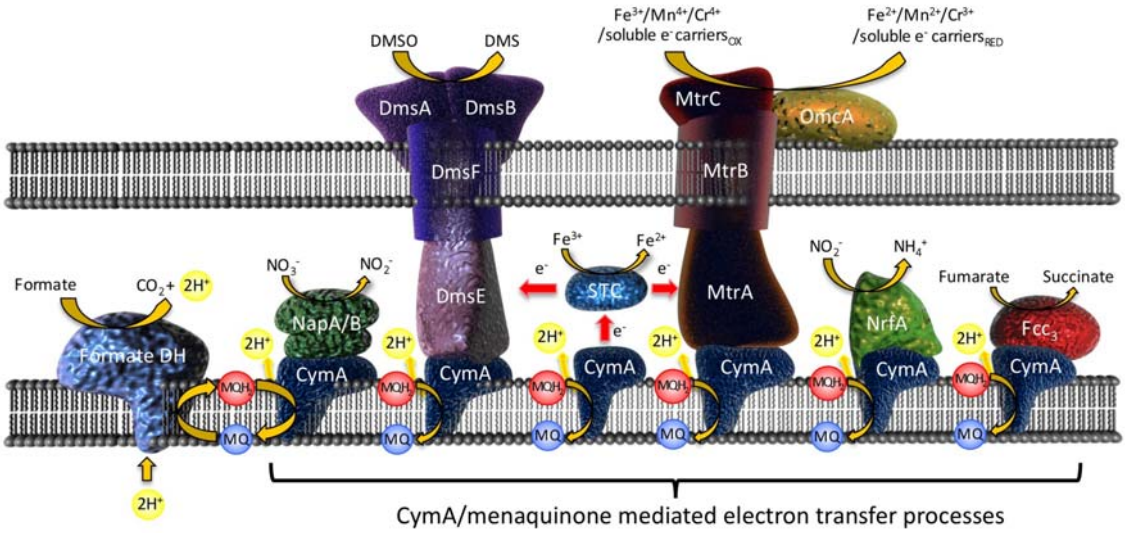

Figure 1: schematic of the role of CymA in Shewanella oneidensis MR-1 anaerobic respiration. Inner membrane-bound dehydrogenases pass electrons through the lipophilic menaquinone pool to CymA where they are passed to four functionally distinct periplasmic reductases. CymA also plays the key role in shuttling electrons to terminal electron acceptors outside the cell though either outer-membrane associated heme-proteins directly such as DmsE or MtrA or via STC as a periplasmic shuttle.

Membrane-modified electrodes

In order to study CymA with electrochemistry, CymA was adsorbed on a surface (the electrode) and the quinone substrate is supplied within vesicles immobilised onto the CymA (Figure 2). It was found that during purification of CymA, its substrate (menaquinone-7; MQ7) was co-purified, indicating that CymA has a high affinity of its substrate. After immobilisation of CymA on the surface, turn-over of the co-purified substrate was detected electrochemically. However, the hydrophobic substrate MQ-7 could be removed from the protein by rinsing the protein-modified electrode surface with a low concentration of

detergent (0.01% n-Dodecyl β-D-Maltopyranoside). To our surprise, the catalytic activity towards substrate homologues like menadione (commonly used to study the activity of quinone-converting enzymes like CymA) was lost upon removal of the MQ-7. Without removal MQ-7, menadione in solution could be catalytically converted by CymA, indicating that menadione could not displace MQ-7 from CymA even though menadione concentrations where many times higher than the co-purified MQ-7. Given the requirement for MQ-7 presence, it seems unlikely that menadione or other homologues access the quinone binding pocket directly during their 'catalytic' turn-over. We therefore suggest that menadione conversion is mediated via quinone-quinone interactions and that MQ-7 may also function as a tightly bound co-factor.

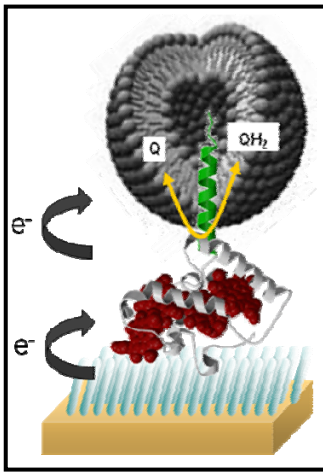

Figure 2: schematic showing a ribbon model of NrfH, a homologue of CymA, immobilised on a self-assembled monolayer modified template-stripped ultra-flat gold electrode with menaquinone-7 containing lipid vesicle. The SAM is shown as blue bars, the CymA polypeptide in white (globular head domain) or green (lipophilic tail domain) and the prosthetic heme groups in red.

Discussion

Several properties of lipophilic quinones and quinone oxidoreductases make this class of membrane enzymes unique in nature. Localisation of substrate and enzymes are restricted to the lipid membrane, where diffusion is an almost 2-dimensional property. Combined with the fact that quinones typically have concentrations of several pmol/cm^2 in the membrane, substrate-enzyme encounters will be much more frequent than typical encounters between globular enzymes and water-soluble substrates. We hypothesise that this has reduced the evolutionary pressure for a highly specific active site, which would only lower k_{off} rates and reduce the turn-over kinetics of the enzyme.

The traditional function of an enzyme is to lower the transition-state activation energy and thereby increasing the reaction rate. However, as has been noted before by others, this might not be required for quinone oxidation/reduction, which is an inherently fast reaction as long as a polar environment is provided to promote a rapid (de)protonation of the quinone. We hypothesize that the function of the quinone co-factors is to reduce the reactivity of the reaction intermediate, semiquinone, which are generally believed to be amenable to side-reactions, giving rise to damaging radical oxygen species.

Publications

Marritt, S., McMillan, D., Shi, L., Fredrickson, J., Zachara, J., Richardson, D., Jeuken, L. & Butt J. (2012) The roles of CymA in support of the respiratory flexibility of *Shewanella oneidensis* MR-1. *Biochem. Soc. Trans.* **40**: 2117-1221.

Marritt, S., Lowe, T., Bye, J., McMillan, D., Shi, L., Fredrickson, J., Zachara, J., Richardson, D., Cheesman, M., Jeuken, L. & Butt, J. (2012) A functional description of CymA, an electron-transfer hub supporting anaerobic respiratory flexibility in shewanella. *Biochem. J.* **444:** 465-474.

McMillan, D., Marritt, S., Butt, J. & Jeuken, L. (2012) Menaquinone-7 is a specific co-factor in the tetraheme quinol dehydrogenase CymA, *J. Biol. Chem.* **287**: 14215-14225.

Funding

This work is funded by the BBSRC and EPSRC.

Free energy landscape analysis of protein folding dynamics

Polina Banushkina and Sergei Krivov

Introduction

Understanding how proteins fold to their native state remains a problem of fundamental interest in biology, in spite of the fact that it has been studied for many years. While, the general principles of protein folding have been established, much controversy remains on fundamental topics such as: the nature of folding steps, the height of folding barriers and the value of the pre-exponential factor, the diversity of folding pathways, and the importance of residual structure in the denatured state. Moreover, now that misfolding has been shown to be the source of a range of diseases, a detailed understanding of what determines whether a polypeptide chain will fold to its native state or aggregate has become all the more important. In principle, this questions can be answered rigorously by determining the protein folding free energy landscape - the fundamental determinant of protein folding (and any other) reaction. However, in spite of their fundamental importance the quantitatively accurate free energy landscapes of proteins are yet to be determined.

State of the art experimental techniques lack the necessary spatial and temporal resolution for determination of such landscapes. Properties of the landscapes can be probed only indirectly. Simulation, in principle, can provide high spatial and temporal resolution, necessary for the determination of the quantitatively accurate free energy landscapes. Recently, due to advances in the hardware and simulation methodology realistic simulation of folding of small fast-folding proteins became computationally affordable. Notably, D.E. Shaw and co-workers reported realistic folding-unfolding simulations for a number of fast folding proteins with up to 100 residues in size. Which brings an exciting opportunity to perform detailed rigorous analysis of protein folding dynamics and to resolve the controversial issues by determining accurate free energy landscapes.

Quantitative analysis of protein dynamics in terms of the free energy landscapes is notoriously difficult. A poorly chosen reaction coordinate may hide the complexity of the free energy landscape and associated dynamics. Many approaches, though being based on solid physical intuition, often construct sub-optimal reaction coordinates. Recently we have developed a rigorous approach to construct optimal reaction coordinates and the high resolution free energy landscapes which provide accurate description of the dynamics.

Results

After the publication of the first realistic protein folding simulation, namely that of FIP35, by D.E. Shaw and co-workers we applied our rigorous methods to reanalyse the trajectory. It was found (see Figure 1) that the coordinate used by Shaw *et al.* is sub-optimal and the associated free energy landscape does not provide accurate description of the folding dynamics. In particular, we found that FIP35 is not a “barrier-less” folder but folds via a populated on-pathway intermediate separated by high free energy barriers; the high free energy barriers rather than landscape roughness are a major determinant of the rates for conformational transitions; and that the pre-exponential factor for folding kinetics $1/k_0$ is 10 ns rather than 1μs. While the latter value is generally accepted and is supported by a large body of indirect experimental evidences, the former is a first estimate obtained by a rigorous analysis in a direct manner.

The existence of the multiple approaches for reaction coordinate construction, naturally, poses the question of how different reaction coordinates can be compared. Which reaction coordinate provides better description of the dynamical process when different coordinates

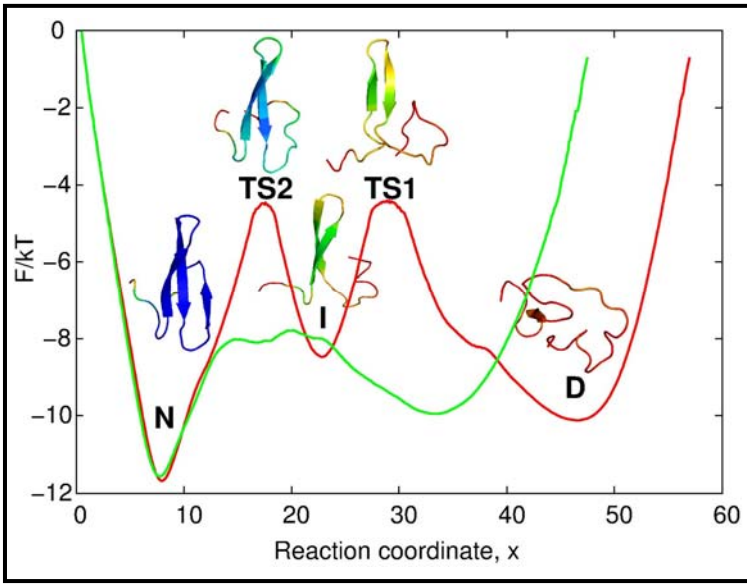

Figure 1: the free energy profiles of FIP35 protein determined by us (red) and by Shaw *et al* (green). Structures show the average conformations in configuration space region. Colors code the root mean square fluctuations of atomic positions around the average structure from 1.5 Å (blue) to 7 Å (red).

lead to different descriptions? A related question is whether one can establish that a putative optimal reaction coordinate is indeed the optimal one? We have developed a new fundamental criterion which is easy to apply. Reaction coordinate is optimal if its cut free energy profile, determined using length-weighted transitions, is constant, i.e., it is position and sampling interval independent. The observation leads to a number of interesting results. In particular, the equilibrium flux between two boundary states can be computed exactly as diffusion on a free energy profile associated with the coordinate for any equilibrium Markov process. It means that kinetics of protein folding on whatever complex free energy landscape can be computed as diffusion along the optimal reaction coordinate. The mean square displacement, for the trajectory projected onto the coordinate, grows linear with time. That for the same trajectory, projected onto a suboptimal coordinate, grows slower than linear with time, indicating sub-diffusion. The criterion showed that the coordinate used in the analysis of FIP35 is optimal, while that of Shaw is suboptimal.

Recently, the method was applied to (re)analyse simulation of all-helical protein HP35 (wild-type and mutant) to see whether the results found for all-beta FIP35 are transferable. In particular, the reaction coordinate and associate free energy landscape, determined with our method, provide quantitatively accurate description of the folding dynamics which is in good agreement with available experimental data. The pre-exponential factor is about $1/k_0 \sim 20$ns, in agreement with our previous estimate.

Funding
This work was supported in part by an RCUK fellowship and a BBSRC grant.

Studies of small DNA tumour viruses that cause disease in humans

Marietta Muller, Christopher Wasson, Emma Prescott, Hussein Abdul-Sada, Ashlea Rowley, Eric Blair, Adrian Whitehouse, Stephen Griffin, Richard Foster and Andrew Macdonald

Introduction

Members of the *Papovaviridae*, which includes the Papillomaviruses and Polyomaviruses, are the causative agents of a number of severe diseases in humans. Notable examples include cervical cancer, which is exclusively associated with infection with human papillomaviruses, and polyomavirus-associated nephropathy (PVAN) and progressive multifocal leukoencephalopathy (PML) caused by the BK and JC polyomaviruses, respectively. Current therapeutic strategies to treat these virus-associated maladies are lacking. We have established a multi-disciplinary research group to undertake a broad ranging analysis of these viruses in an effort to identify new targets for therapeutic intervention. These studies have revealed novel information about these viruses.

Results

Human papillomavirus: We have focussed our analysis on the least understood of the three transforming proteins encoded by this virus. The E5 protein is a small membrane protein expressed by all carcinogenic papillomaviruses. Little is understood of the role of E5 in the virus life cycle or its mechanisms of pathogenesis. We discovered that E5 functions as a virus-encoded ion channel or "viroporin" (Wetherill *et al*., 2012). We utilised *de novo* models of an E5 channel complex (Figure 1A) to identify small molecule inhibitors of E5 channel function and are currently using these models to reveal the functional determinants of E5 channel function *in vitro*. In addition we have established organotypic raft culture systems that mimic the natural three-dimensional nature of human skin (Figure 1B). These model systems allow us to grow HPV in the laboratory and provide an ideal opportunity to test our *in vitro* findings in a physiologically relevant system.

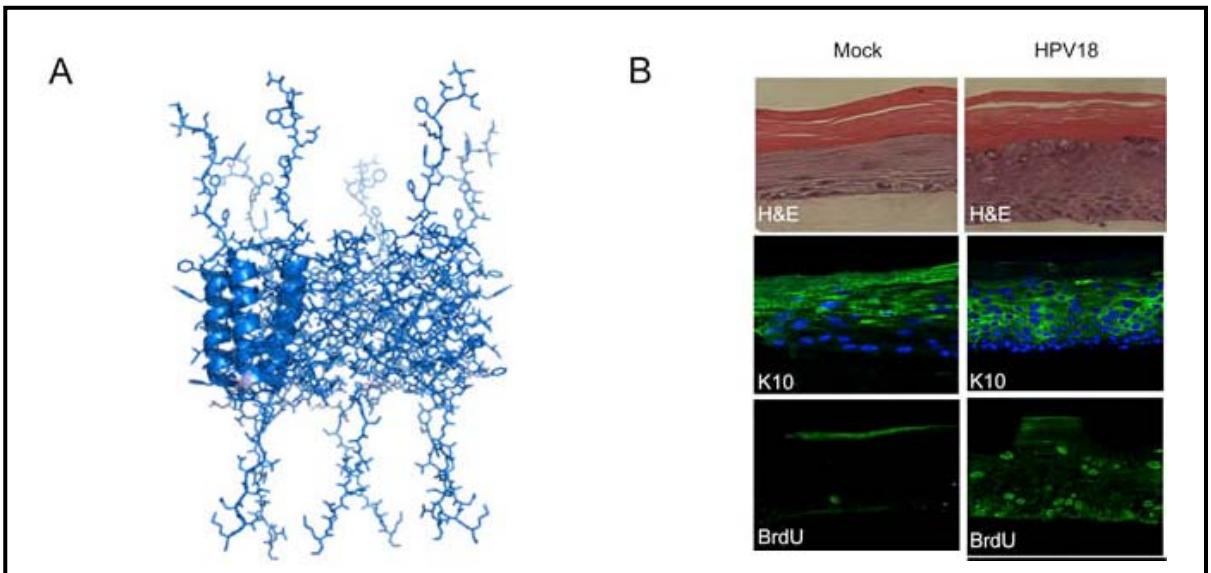

Figure 1: (a) *in silico* molecular modelling of an E5 channel complex (Wetherill et al., 2012). Molecular predictions, based on energy minimisation, suggest that the E5 channel is composed of a hexamer, with a hydrophilic region protruding from the membrane and a luminal pore lined with residues that mediate ion flow. **(b)** Immunohistochemistry of an organotypic raft culture section from control and HPV containing primary keratinocytes. Cells are stained with haematoxylin and eosin to show general morphology and keratin 10 as a marker of keratinocyte differentiation. BrdU staining highlights the increased host cell DNA replication occurring in cells containing HPV. Probing for a HPV late protein, E4 highlights a productive HPV life cycle in the raft culture model.

Human polyomaviruses: Our analysis currently covers three major polyomaviruses associated with disease in humans. These are the JC, BK and Merkel polyomaviruses. In collaboration with Prof. Adrian Whitehouse (UoL), we are dissecting the role of the Small T antigen of Merkel polyomavirus in transformation. Our studies have shown that this virus protein is an efficient and powerful inhibitor of the host innate immune response and is capable of preventing an inflammatory response. This may have profound implications for the persistent nature of virus infection and allow Merkel to persist in the host despite the presence of an immune response. In parallel studies we are beginning to understand more about the enigmatic agnoproteins that are encoded by BK and JC viruses. Our preliminary biochemical characterisation of these proteins suggests that they are ideal targets for antiviral therapeutics and work in 2013 will continue to target these proteins for study.

Publications

Wetherill, L., Holmes, K., Verow, M., Mueller, M., Howell, G., Harris, M., Fishwick, C., Stonehouse, N., Foster, R., Blair, G., Griffin, S. & Macdonald, A. (2012) High-risk human papillomavirus e5 oncoprotein displays channel-forming activity sensitive to small-molecule inhibitors. *J. Virol.* **86:** 5341-5351.

Wu, W., Macdonald, A., Hiscox, J. & Barr, J. (2012) Different NF-kappa B activation characteristics of human respiratory syncytial virus subgroups A and B. *Microb. Pathog.* **52:** 184-191.

Funding

This work was supported by Cancer Research UK, Yorkshire Cancer Research, Yorkshire Kidney Research Fund and the MRC.

Collaborators

External: S. Roberts (Birmingham), N. Coleman (Cambridge), S. Graham (Glasgow) and M. Imperiale (University of Michigan, USA).
Leeds: B. Turnbull (School of Chemistry), M. Webb (School of Chemistry), D. Tomlinson (Faculty of Biological Sciences) and M. McPherson (Faculty of Biological Sciences).

Flexibility within the rotor and stator structures of the vacuolar ATPase

Kostas Papachristos, Emanuele Paci, Michael Harrison, John Trinick and Stephen Muench

Introduction

The vacuolar H^+-ATPase (V-ATPase) is a large transmembrane ATP driven proton pump which is essential in eukaryotic cells. Proton pumping is achieved through the coupling of a 10 stroke proton pump (V_o) and 3 stroke ATP driven motor ((V_1)(Figure 1 A)). The remarkable efficiency of this molecular motor is hypothesised to be due in part to the intrinsic flexibility in the stator connections and central rotor axle which links the two motors.

Results

In collaboration with the group of Dr Paci molecular dynamic simulations have been carried out on the previously determined 3D reconstruction of the *Manduca sexta* V-ATPase. These simulations revealed two modes of flexing. The first is flexing of V_1 relative to V_o to a maximum angle of 20° in the longitudinal direction (Figure 1C). The second mode is a twisting of V_1 relative to V_o about the equatorial region. In order to see if this predicted flexing could be directly visualised, electron microscopy was used to capture a range of conformational states in both the Yeast and Manduca V-ATPase using negative staining and cryo-EM approaches. Single particle processing has revealed a range of conformations whereby the V_1 domain can be seen to flex relative to V_o to a maximum of 30° in agreement with the molecular dynamic simulations (Figure 1B). This has provided direct evidence of the flexibility within the V-ATPase and by implication the rotary ATPase family which has significant implications in understanding their high energetic efficiencies.

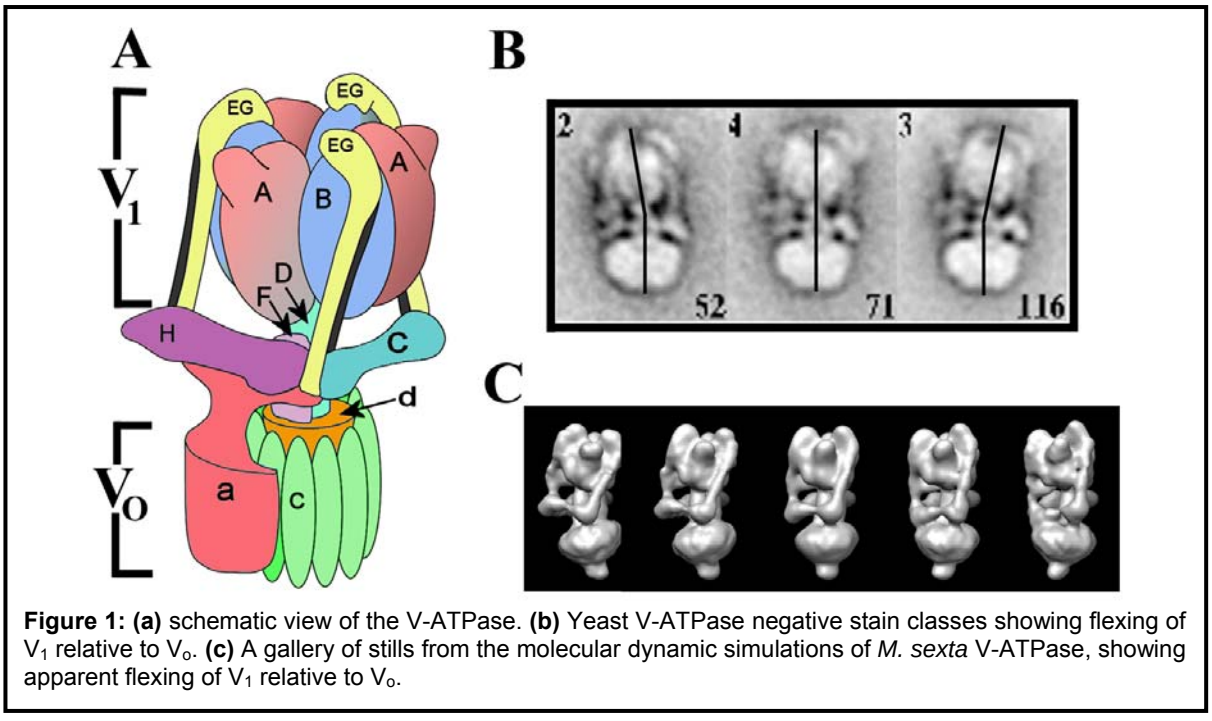

Figure 1: (a) schematic view of the V-ATPase. **(b)** Yeast V-ATPase negative stain classes showing flexing of V_1 relative to V_o. **(c)** A gallery of stills from the molecular dynamic simulations of *M. sexta* V-ATPase, showing apparent flexing of V_1 relative to V_o.

In addition to capturing the flexibility within the V-ATPase the group has also used single particle electron microscopy to study the structure of the isolated V_1 domain which is unable to turnover ATP. This structure has given us insights into the structural changes that bring about dissociation allowing us to propose a mechanism for V_1 dissociation. Moreover, the apparent rigidity of the stators within the isolated V_1 domain has implications for the elastic coupling model.

The mis-localisation of the V-ATPase plays a role in a number of disease states, such as Alzheimer's and cutis laxis disease. This localisation is thought to be driven through the glycosylation of several V-ATPase subunits, in particular the membrane bound *a* and *e* subunits. Electron microscopy and biochemical studies have shown that significant glycosylation of the V-ATPase is found at the base of V_o.

This work has been done in collaboration with Prof Wieczorek's group who provide us with *Manduca sexta* V-ATPase and some biochemical analysis. The yeast data was collected and processed by Chun Feng Song.

Publications

Fomovska, A., Huang, Q., El Bissati, K., Mui, E. , Witola, W., Cheng, G., Zhou, Y., Sommerville, C., Roberts, C., Bettis, S., Prigge, S., Afanador, G., Hickman, M., Lee, P., Leed, S., Auschwitz, J., Pieroni, M., Stec, J., Muench, S., Rice, D., Kozikowski, A. & McLeod, R. (2012) Novel n-benzoyl-2-hydroxybenzamide disrupts unique parasite secretory pathway. *Antimicrob. Agents. Chemother.* **56:** 2666-2682.

Funding

This work is funded by the MRC.

Development of tools and approaches to facilitate more systematic exploration of lead-like chemical space

Richard Doveston, Mark Dow, Daniel Foley, Thomas James, Steven Kane, John Li, Paul MacLellan, Paolo Tosatti, Stuart Warriner and Adam Nelson

Introduction

Chemists have explored chemical space (using synthesis and biosynthesis) in an uneven and unsystematic manner. An analysis of the scaffolds of the 25 million known cyclic small molecules (in 2008) revealed that one sixth of the compounds are based on just 30 (out of the 2.5 million) known molecular scaffolds! To address this historic uneven exploration, we have developed a vibrant research programme focusing on the identification and development of synthetic methods that have potential to facilitate more systematic exploration of chemical space

Extension to lead-like chemical space

A strongly developed theme within the Nelson group has been to develop diversity-oriented synthetic approaches that map onto the requirements of drug discovery programmes. This programme has been undertaken in collaboration with scientists from major pharmaceutical companies. Established diversity-oriented approaches have tended to focus on small molecules that lie well outside drug-like space. It is now generally accepted that attrition rates in drug discovery are strongly linked to molecular properties such including molecular weight and lipophilicity. Optimisation almost always leads to increases in both molecular weight and lipophilicity, so it is important to control the properties of initial lead molecules.

In collaboration with GSK, we have developed computational tools that allow the value of alternative synthetic approaches to be assessed. Thus, before any optimisation work is undertaken, we now routinely assess synthetic approaches for their potential to target under-explored regions of lead-like chemical space. We then focus on optimising those reactions that are likely to have the greatest value. We are thus continuing to develop a robust and growing toolkit of synthetic reactions that address the challenges raised in the nascent field of lead-oriented synthesis. This research programme is now feeding into the €196M European Lead Factory in which Leeds is a partner.

Summary

The development of general strategies that are able to deliver skeletally diverse compounds – but within the boundaries of lead-like chemical space – is demanding. Publications from this programme, and other programmes under active development in the group are listed below. Further details of research within the Nelson group may be found at www.asn.leeds.ac.uk.

Publications

Dow, M., Fisher, M., James, T., Marchetti, F. & Nelson, A. (2012) Towards the systematic exploration of chemical space. *Org. Biomol. Chem.* **10:** 17-28.

Joce, C., White, R., Stockley, P., Warriner, S., Turnbull, W. & Nelson, A. (2012) Design, synthesis and *in vitro* evaluation of novel bivalent s-adenosylmethionine analogues. *Bioorg. Med. Chem. Lett.* **22:** 278-284.

Kinnell, A., Harman, T., Bingham, M., Berry, A. & Nelson, A. (2012) Development of an organo- and enzyme-catalysed one-pot, sequential three-component reaction. *Tetrahedron* **68:** 7719-7722.

Timms, N., Daniels, A., Nelson, A. & Berry, A. Directed Evolution and (Semi-)Rational Design Strategies for the Creation of Synthetically-Useful, Stereoselective Biocatalysts. (2012) ed. Turner, N. J., in *Comprehensive Chirality*.

Tosatti, P., Nelson, A. & Marsden, S. (2012) Recent advances and applications of iridium-catalysed asymmetric allylic substitution. *Org. Biomol. Chem.* **10:** 3147-3163.

Funding
We thank EPSRC, BBSRC, the Wellcome Trust, the EU, Merck, GSK and AstraZeneca for support.

Collaborators
External: M. Bingham (Merck). We also acknowledge scientific collaborators from AstraZeneca and GSK who have also contributed strongly to this on-going programme.
Leeds: S. Marsden (School of Chemistry).

Structural and mechanistic insights into the FusB family of fusidic acid resistance proteins

Jennifer Tomlinson, Georgina Cox, Thomas Edwards, Gary Thompson, Arnout Kalverda, Steve Homans and Alex O'Neill

Introduction

A major focus in the O'Neill laboratory is on understanding the mechanisms by which bacteria resist the effects of the antibiotics that are used to treat the infections they cause. The antibiotic fusidic acid inhibits bacterial protein synthesis in the bacterial pathogen *Staphylococcus aureus* by blocking release of the translocase, elongation factor G (EF-G), from the ribosome. Resistance to fusidic acid is most commonly mediated by proteins of the FusB family, which bind to elongation factor G and protect it from the inhibitory effect of fusidic acid. The mechanism by which the FusB-type proteins interact with EF-G to mediate resistance to fusidic acid resistance is not fully understood, and recent efforts have therefore focused on gaining a detailed understanding of this protein-protein interaction (PPI).

Mapping of the binding interface between FusB and EF-G by mutagenesis

Previous studies using NMR chemical shift mapping have established that it is the C-terminal domain of FusB-type proteins that is responsible for mediating the interaction with EF-G. To more precisely delineate the EF-G binding site within this region, alanine-scanning mutagenesis was employed to systematically substitute conserved, surface exposed residues of FusB. Of 18 alanine substitution mutations generated, four resulted in FusB proteins that were no longer capable of binding to EF-G. The four residues identified lie in close proximity to each other in the three dimensional structure of the FusB protein, and reside within a region that matches previous *in silico* predictions for the EF-G-binding site on FusB.

Mapping the FusB binding site by NMR

We have previously shown that the C-terminal half of the EF-G protein (a protein fragment referred to here as EF-G_{C3}) contains the binding site for the FusB-type proteins. NMR backbone assignment of EF-G_{C3} has recently been undertaken in both the FusB-bound and free forms, and work is underway to use NMR chemical shift changes to identify the binding site for FusB on EF-G_{C3}. Preliminary docking studies show that the interaction site of FusB on EF-G is similar, but not identical to, that previously predicted *in silico*.

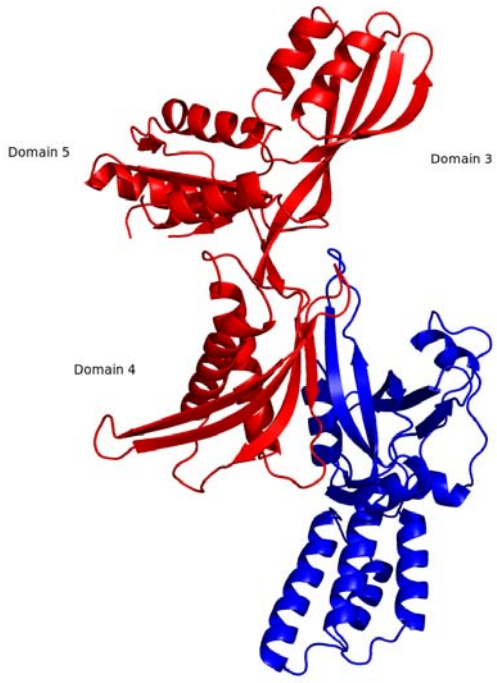

Figure 1: proposed model of the interaction between EF-G and FusB from initial docking of the crystal structures of the two proteins (PDB IDs 2XEX and 4ADN, respectively). Domains 3-5 of EF-G are shown in red, and FusB is shown in blue.

Our current model for the interaction between FusB and EF-G is shown in Figure 1; additional NMR and mutagenesis experiments are currently underway to further refine our model of this PPI, and thereby facilitate a better understanding of this unusual antibiotic resistance mechanism.

Publications

Cox, G., Thompson, G., Jenkins, H., Peske, F., Savelsbergh, A., Rodnina, M., Wintermeyer, W., Homans, S., Edwards, T. & O'Neill, A. Ribosome clearance by FusB-type proteins mediates resistance to the antibiotic fusidic acid. (2012) *Proc. Natl. Acad. Sci. U S A* **109:** 2102-7.

Funding

This work was funded by the BBSRC.

The cytoskeleton and molecular motors, from molecular mechanisms to super-resolution imaging

Kathryn White, Katarzyna Makowska, Marcin Wolny, Matthew Batchelor, Francine Parker Adriana Klyszejko, Kieran White, Christine Diggle, Dmitry Ushakov, Ruth Hughes and Michelle Peckham

Introduction

Actin is a small protein that polymerises into filaments, which comprise a major part of the cytoskeleton in cells. In skeletal and cardiac muscles, actin filaments are highly organised into muscle sarcomeres, about 2 microns long, arranged in series from one end of a muscle fibre to the other. The regular array of actin filaments surrounds thick filaments, which contain the motor protein myosin. The interaction of these two proteins in this highly ordered array results in the contraction of heart and skeletal muscle. The organisation of these cytoskeletal proteins is so precise that each thick filament has exactly 296 molecules of myosin in each thick filament. Building the almost crystalline structure of a muscle sarcomere is key to ensure that each sarcomere generates the same amount of force, and that the forces sum along the muscle to generate contraction.

In non-muscle cells, actin filaments and myosins play a key role in many functions such as cell-cell adhesion, cell-substrate adhesion, protrusion and retraction of the cell. The organisation of myosins and actin is much less well organised than in muscle, and much more dynamic, as the cytoskeleton can be constantly remodelled as the cell responds to its environment. Moreover, the array of myosins found in non-muscle cells is much more diverse, muscle myosins are absent, but there are about 20 different types of myosins in a single cell, which have a range of shapes, properties and functions. We still know very little about how they are specialised for their functions either in muscle, or in non-muscle cells.

Investigating mutations in skeletal actin that cause disease

About 30% of cases of the skeletal muscle disease Nemaline Myopathy are caused by mutations in the skeletal actin gene. This can be a severe disease, killing babies shortly after birth. We have investigated how some of these mutations cause disease by expressing these mutant actin isoforms in the flight muscle of *Drosophila* in collaboration with John Sparrow's group at the University of York. The flight muscle is remarkably similar to human muscle, and is a very useful tool to studying muscle structure and function.

We've discovered that the mutations investigated generate a similar phenotype in the flight muscle to that seen in humans, and interestingly, 3 severe mutations result in accumulation of actin in 'rods' in the nucleus as in humans (Figure 1). We think that export of actin out of the nucleus as a profilin-actin complex is disrupted by these three mutations.

Other new projects

The 39 genes that encode myosins in humans can be grouped into 12 different classes based on their sequence similarity. Class 2 is the major class with 13 genes, which includes all the cardiac, skeletal and smooth muscle myosins (10 genes) as well as 3 non-muscle myosin 2 isoforms. The remaining 26 genes are predominantly expressed in non-muscle cells. Three of these classes (6,7 and 10) encode myosins that contain a stable single alpha helix, that we've shown contributes to the movement of a myosin lever (Baboolal et al., 2009) and is found in many other proteins (Peckham & Knight, 2009). Using AFM and modelling (with Lorna Dougan and Emanuele Paci's groups) to extend the SAH domain is starting to show us how this domain behaves when it is stretched (BBSRC funded, Marcin Wolny and Matt Batchelor's work). Moreover, many of these myosins are implicated in disease, and we are currently investigating the roles of myosins in the development of metastasis in Prostate

Cancer (CRUK PhD studentship, and YCR funded; work of Katzaryna Makowska and Kathryn White), as well as how these myosins are regulated (Wellcome Trust funded, work of Adriana Klyszejko and Kieran White, in collaboration with Peter Knight and others).

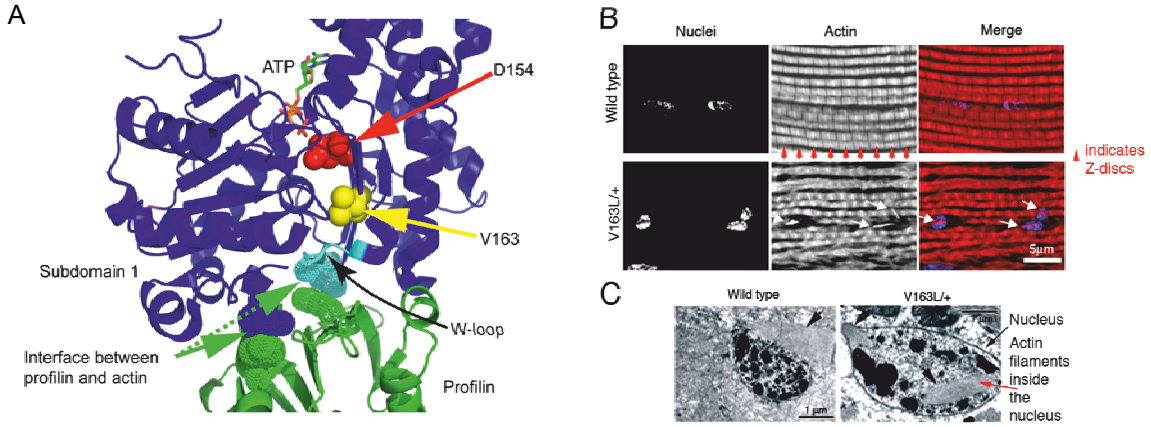

Figure 1: (a) 3 mutations in actin that result in 'nuclear rods'shown in the structure of profilin-actin complex. **(b)** All three mutations disrupt muscle structure and result in rods in Drosophila flight muscle (as shown here in a confocal image of an example for V163L heterozygotes). **(c)** Electron microscopy shows how the bundle of actin filaments inside the nucleus distorts and enlarges it.

In other new work, we have started to investigate the role of Tuba8 in brain, cardiac and skeletal muscle (Wellcome Trust funded, work of Christine Diggle, in collaboration with Eamonn Sheridan and others at LIMM), and the role of MEGF10 in muscle differentiation (MRC PhD studentship; work of Ruth Hughes, in collaboration with Colin Johnson at LIMM).

We have recently built a novel 'super-resolution' light microscope that can image within cells to a resolution ten times better (20nm) than a conventional microscope (work of Dmitry Ushakov, in collaboration with Hari Shroff at NIH (USA), and funded through a campaign donation and university funds). This type of microscopy is known as Photo-activated Light Microscopy (PALM). We have now obtained new funding to build a second kind of super-resolution microscope that uses structured illumination to increase resolution, with Prof. Towers in Engineering (Leeds) and in collaboration with Hari Shroff through the MRC/BBSRC/EPSRC Next Generation Optical Microscopy Initiative.

Funding
This work was funded by the YCR, CRUK, BBSRC, the Wellcome Trust and MRC.

β_2-microglobulin amyloid-lipid interactions

Sophia Goodchild, Tania Sheynis, Kevin Tipping, Andrew Hellewell, Rebecca Thompson, Eric Hewitt and Sheena Radford

Introduction

Amyloid fibril accumulation is the pathological hallmark of a number of devastating human diseases including type II diabetes mellitus, Alzheimer's disease and Parkinson's disease. Due to their prevalence, diversity and generally debilitating nature, amyloid diseases present one of the most important and costly challenges for modern medicine. Currently, one of the major stumbling blocks in stimulating the design of amyloid disease therapeutics is a lack of understanding of the mechanisms of cell death and tissue damage associated with amyloid disease pathologies.

While the molecular mechanism of amyloid disease is not yet well understood, interaction between amyloid proteins and cell membranes has been implicated in cytotoxicity. Hence, the membrane lipid composition and chemical environment in which amyloid-lipid interactions occur *in vivo* may play an important role in amyloid disease physiology. In this report we have investigated the interaction between β_2-microglobulin (β_2m), the precursor of amyloid fibrils formed in dialysis related amyloidosis, and lipid vesicles of differing anionic lipid composition at varying pH using a series of biophysical experiments including: tryptophan fluorescence quenching and a sucrose-gradient liposome flotation assay to measure β_2m-membrane interactions; and liposome leakage to measure membrane damage conferred by β_2m. Combined with visualization of membrane disruption by β_2m amyloid fibrils using cryo-electron tomography, these studies provide important insights into the molecular mechanism of amyloid-lipid interactions and the molecular basis of cytoxicity.

Results

β_2m monomer was expressed recombinantly and purified before being assembled into *long* straight fibrils by incubating quiescently at pH 2 for 48 h. *Long* β_2m fibrils were subsequently fragmented by agitation for 48 h to form *short* fibrils (Figure 1a). Despite different molecular architectures, upon addition of liposome vesicles a decrease in tryptophan

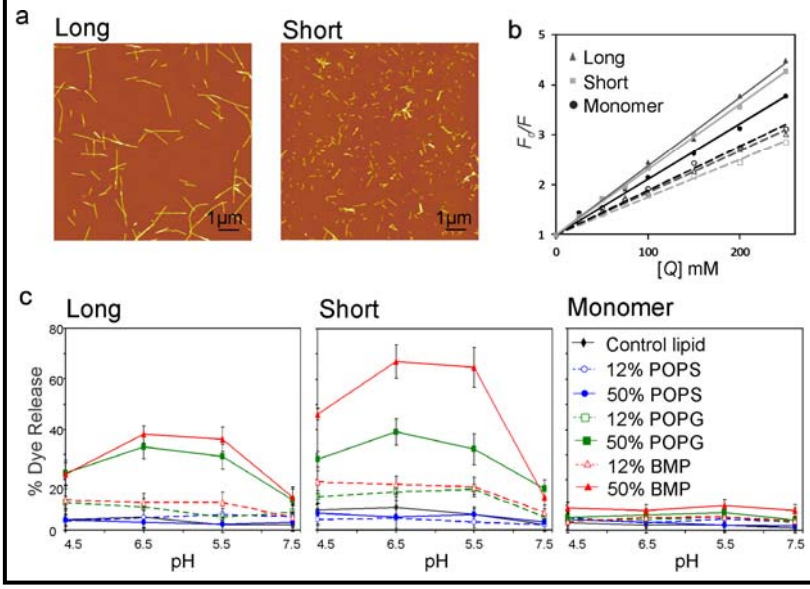

Figure 1: biophysical investigations of β_2m-lipid interactions. **(a)** AFM images of *short* (0.30 ± 0.01 μm) and *long* (1.30 ± 0.05 μm) β2m fibrils. **(b)** Stern-Volmer plots of Trp quenching by acrylamide for β_2m monomer, *short* and *long* fibrils in both the absence (*dashed line*) or presence of liposomes containing 12 % BMP (*solid line*), pH 4.5. **(c)** Relative CF dye release from LUVs containing 36 POPC: 20 POPE: 7 sphingomyleiln: 25 cholesterol (control) plus 12 or 50% POPS, POPG or BMP at pH 4.5-7.4. Errors: SD from n=3.

fluorescence quenching by aqueous acrylamide, corresponding to a decrease in tryptophan solvent accessibility, is seen for both β_2m monomer and fibrils (Figure 1b). This result indicates that both β_2m monomer and fibrils interact with the lipid bilayer. Indeed, physical

separation of membrane-associated β_2m, using a discontinuous 10:60:80% sucrose-gradient liposome-flotation centrifugation assay indicates that ~40-60% of β_2m protein associates with the lipid bilayer regardless of the β_2m species present. In addition, no significant correlation between β_2m membrane affinity and lipid composition or pH was observed (*data not shown*).

Previous studies have indicated that amyloid fibrils can cause membrane leakage. A carboxyflorescein (CF) dye release assay was used to investigate membrane damage resulting from interaction with β_2m. Briefly, β_2m was incubated with lipid vesicles loaded with 50 mM CF. The fluorescence of CF encapsulated in the lipid vesicle is self-quenched. The increase in CF fluorescence upon leakage from the liposomes was monitored and the extent of dye release was measured as the ratio of CF fluorescence due to dye release and CF fluorescence arising when the lipid vesicles were disintegrated by the addition Triton X-100 to 2%. Despite all species interacting with the liposomes, only β_2m fibrils, and not monomer, cause significant membrane damage (Figure 1c). Membrane damage conferred by fibrils primarily occurs at acidic pH, is inversely proportional to fibril length and requires an anionic lipid mix, but varies depending on the identity of anionic lipid component present (Figure 1c). Most strikingly, greatest membrane disruption was observed for lipids containing 50% bis(monoacylglycero)phosphate (BMP) liposomes at acidic pH (5.5-6.5), conditions likely to be encountered in the endocytotic pathway.

Membrane damage by specific interaction between β_2m fibrils and liposomes was also visualised using cryoelectron tomography. We demonstrate that *short* β_2m fibrils interact strongly with liposomes resulting in distortion of the normally spherical vesicles into pointed teardrop-like shapes with the fibril ends seen in proximity of the membrane disortions. Moreover, the tomograms indicated that the fibrils extract lipid from the membranes at these points of distortion by removal or blebbing of the outer membrane leaflet. Small (15-25 nm) vesicles, presumably formed from the extracted lipids are observed decorating the fibrils; a previously undescribed class of lipid-protein interactions in membrane remodelling (Figure 2).

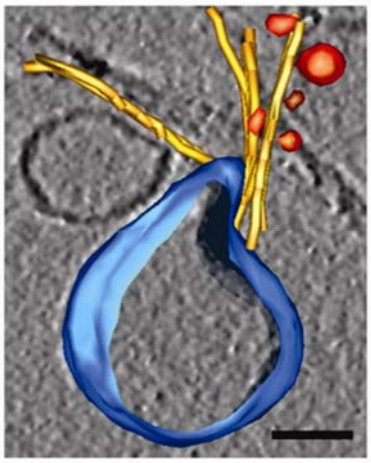

Figure 2: a rendered 3D model based on cryoelectron tomography of a distorted liposome (4 PC: 1 PG) (*blue*), surrounding fibrils (*yellow*) and adjacent small vesicles (*orange*). Scale bar: 50nm.

Together, these findings highlight a potential role of fibrils, and particularly fibril ends, in amyloid pathology, where specific disruption of vesicles of endosomic origin may potentially govern the physiology of β_2m amyloidosis.

Publications

Milanesi, L., Sheynis, T., Xue, W.-F., Orlova, E., Hellewell, A., Jelinek, R., Hewitt, E., Radford, S. & Saibil, H. (2012) Direct three-dimensional visualization of membrane disruption by amyloid fibrils. *Proc. Natl. Acad. Sci. U.S.A.* **109:** 20455-20460.

Funding

This work was supported by The Wellcome Trust, the European Union and the BBSRC.

Collaborators

External: H. Saibil (Birkbeck College, London), R. Jelinek (Ben-Guirion University of the Negev, Israel).

Using ion mobility mass spectrometry to probe amyloid systems

Lydia Young, Charlotte Scarff, Alessandro Sicorello, Tom Knapman, Lucy Woods, Hlengisizwe Ndlovu, George Preston, Sarah Harris, Andy Wilson, Alison Ashcroft and Sheena Radford

Introduction

More than twenty five proteins or peptides are associated with amyloid disease. The precise mechanisms by which these unrelated soluble protein or peptide monomers assemble into highly-ordered fibrillar deposits is unknown. Amylin (also known as islet amyloid polypeptide) is the amyloid peptide associated with type II diabetes. It is found *in vivo* as amyloid deposits in the pancreatic islets of sufferers and its self-aggregation is thought to be a pathogenic factor in the disease. Ataxin-3 is the protein associated with the neurodegenerative polyglutamine (polyQ) disease spinocerebellar ataxia type 3 (also known as Machado-Joseph disease). PolyQ diseases are a group of inherited neurodegenerative disorders caused by aggregation of specific proteins with expanded polyQ regions.

The work described in this report highlights two recent examples of how electrospray ionisation-ion mobility spectrometry-mass spectrometry (ESI-IMS-MS) can be used to probe amyloid systems that are otherwise difficult to study. ESI-IMS-MS represents a powerful technique for elucidating the structures of species within complex, heterogeneous samples. It enables separation and subsequent identification of individual components within complex mixtures, within a single experiment. In the study of amylin presented here, ESI-IMS-MS was used in parallel with molecular modelling to characterise the soluble oligomeric species of fibril-forming peptides. In the study of ataxin-3, ESI-IMS-MS was used with limited proteolysis, to provide insights into its structure and dynamics.

Results

For three of four peptides derived from the amyloidogenic core of amylin (Figure 1), oligomers >20-mer were detected using ESI-IMS-MS. This is the first time that oligomers of amylin fragments have been reported. For the non-fibril-forming peptide (GAIL), used as a control, no species larger than dimer were observed. An IMS calibration allowed collision

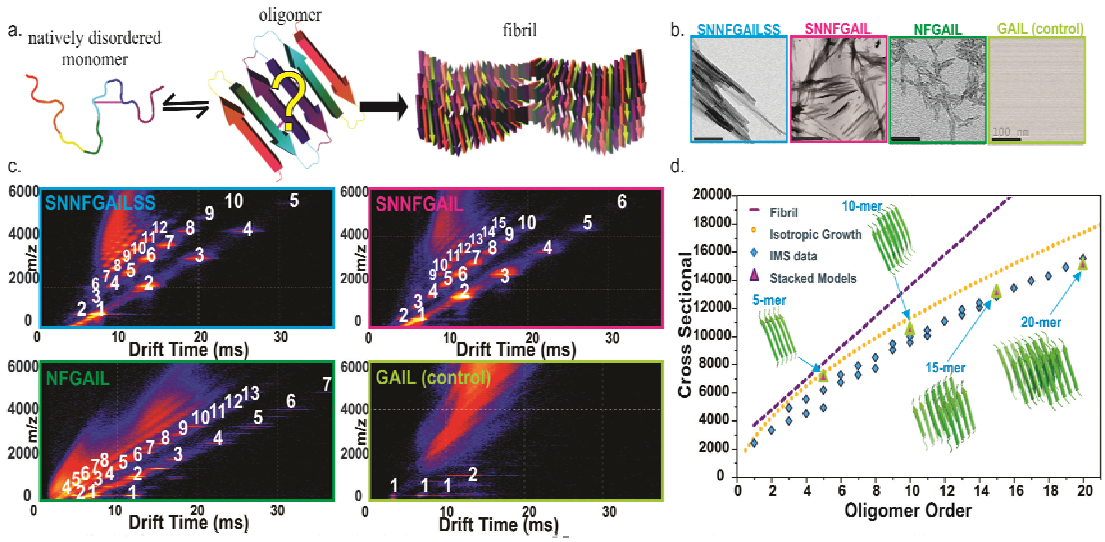

Figure 1: (a) hypothesis of amyloid progression, **(b)** EM images of peptide fibrils, scale bar is 100 nm. **(c)** ESI-IMS-MS data showing oligomers formed by peptides. **(d)** comparison with modeled structures.

cross-sections (CCS) of the oligomers to be estimated. These CCS were compared with molecular models to reveal a possible mechanism of amyloid fornation by the self-

assembling peptides. CCSs observed were comparable with single β-sheet models for the low-order oligomers, with higher-order oligomers fitting better with multiple β-sheet models. For ataxin-3 (Figure 2), ESI-IMS-MS revealed that the full-length protein populates a wider range of conformational states than the isolated Josephin domain (JD), most likely due to the flexibility of the C-terminal domain. ESI-MS spectra showed that the major products of JD and ataxin-3, after limited proteolysis, are mostly the same. These observations suggest that the C-terminal domain and the JD do not exhibit significant or long-lived interactions.

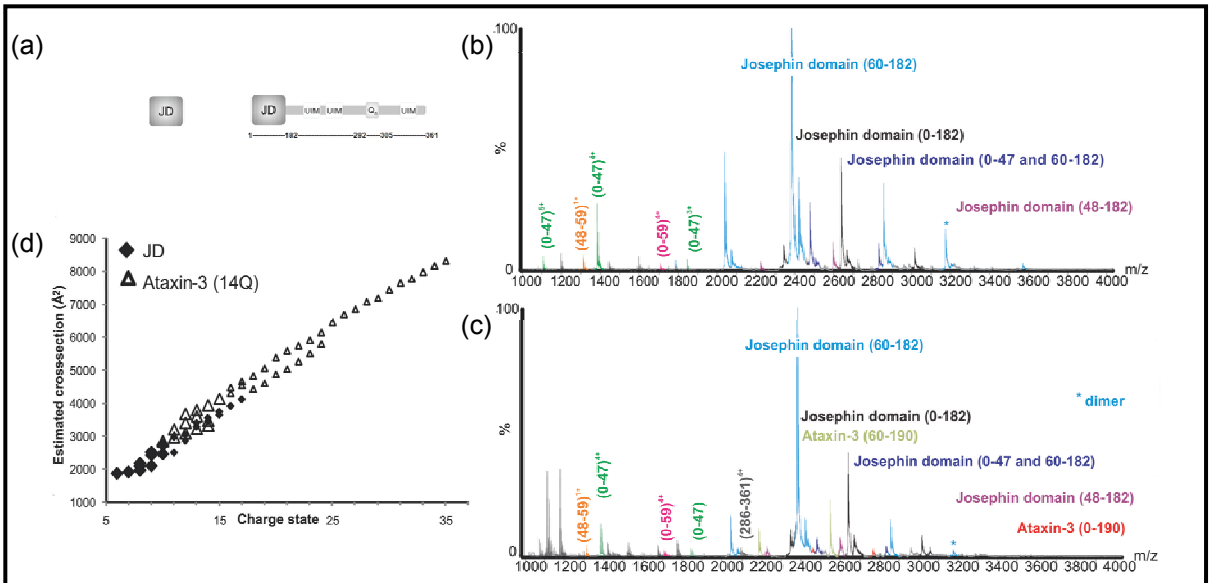

Figure 2: schematics of **(a)** the Josephin domain (JD, left) and ataxin-3 (right). ESI-MS spectra following limited proteolysis of **(b)** the JD, and **(c)** ataxin-3. **(d)** ESI-IMS-MS estimated CCS for JD and ataxin-3.

Publications

Hodkinson, J., Radford, S. & Ashcroft, A. (2012) The role of conformational flexibility in beta(2)-microglobulin amyloid fibril formation at neutral pH. *Rapid Commun. Mass Spectrom.* **26:** 1783-1792.

Kang, L., Moriarty, G., Woods, L., Ashcroft, A., Radford, S. & Baum, J. (2012) N-terminal acetylation of alpha-synuclein induces increased transient helical propensity and decreased aggregation rates in the intrinsically disordered monomer. *Protein Sci.* **21:** 911-917.

Ndlovu, H., Ashcroft, A., Radford, S. & Harris, S. (2012) Effect of sequence variation on the mechanical response of amyloid fibrils probed by steered molecular dynamics simulation. *Biophys. J.* **102:** 587-596.

Preston, G., Radford, S., Ashcroft, A. & Wilson, A. (2012) Covalent cross-linking within supramolecular peptide structures. *Anal. Chem.* **84:** 6790-6797.

Funding

This work was supported by the BBSRC, EPSRC, Micromass UK Ltd/Waters Corp. (Manchester, UK) and the Wellcome Trust.

Collaborators

S. Macedo Ribeiro (IBMC, Porto), J. Baum (Rutgers University, New Jersey).

Biomimetic production of precise nanomagnetic particles using magnetic bacteria and their biomineralisation proteins

Johanna Galloway, Masayoshi Tanaka, Jonathan Bramble, Andrea Rawlings, Stephen Baldwin, Stephen Evans and Sarah Staniland

Introduction

Scientific and economic interest in nanotechnology has grown in recent years. Within this the quest to produce tiny and highly tailored magnetic particles or nanomagnets is crucial. Nanomagnets have a range of practical uses such as: the development of 3D information storage systems providing high density data storage; medical applications such as site specific targeted therapies and image enhancers for diagnostic medicine.

However, as nanotechnology grows, so too does the need to develop precisely engineered nanomagnets. Different applications demand different shapes and sizes of particles and different magnetic properties. Producing nanomagnets with highly controlled; composition, size and shapes, in large enough amounts to be of use to these industries, have therefore become a key goal of researchers.

Magnetotactic bacteria are the simplest organisms that perform biomineralisation (Figure 1A). They take up iron ions from solution and produce nanoparticles of magnetite (Fe_3O_4) within lipid vesicles (called magnetosomes) with precise control, resulting in a strain specific uniform size and morphology. Interesting our recent TEM study has revealed how magnetic bacteria divide and what happens to the magnetosome chain within them during this process.

The aim of this group's research is to investigate, understand and then manipulate the biomineralisation process within these bacteria to enable the production of high-yields of customised nanomagnets for nanotechnological application using the genetic precision of nature.

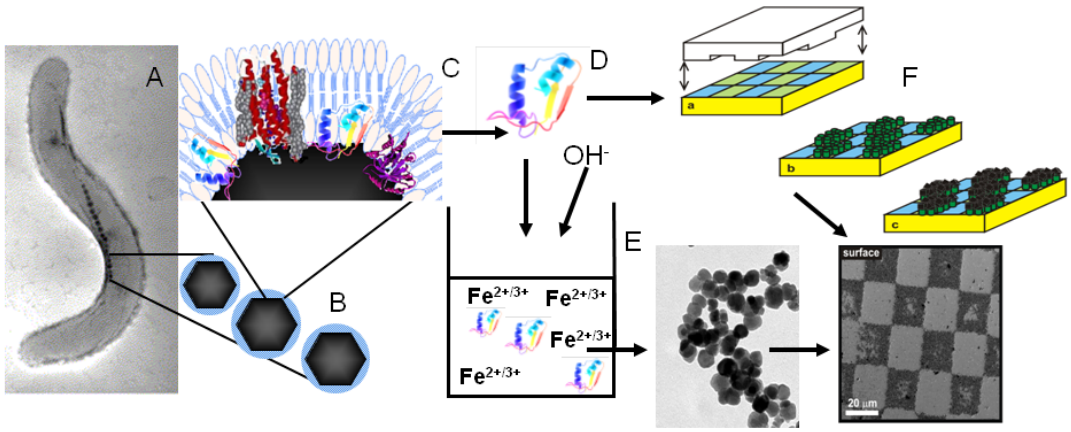

Figure 1: schematic of research activity. (a) a magnetotactic bacterium; **(b)** enlarged magnetosomes; **(c)** a close-up of the magnetosome membrane representing magnetosome membrane specific (Mms) proteins. **(d)** represents Mms6 with **(e)** depicting the *in vitro* precipitation. **(f)** Mms6 can be used to both control magnetic nanoparticle morphology and locate them in a pattern on a surface.

Results

The magnetic composition of magnetosomes as been successfully altered in vivo by doping the magnetosomes with cobalt resulting in magnetosomes with an increased magnetic coecivity compared to control magnetosomes. This was achieved with the addition of cobalt ions into the bacterial growth media which were taken up and incorporated into the

magnetite mineral in approximately 1% quantities. More recently we have increased the doping levels of cobalt to 3% and also achieved in vivo magnetosome doping with Mn (2.7 %) and Cu (15.6%). This has been achieved by a systematic study of growth and magnetosome over a range of concentrations of various transition metals to find the minimum inhibitory concentration for the microbes and the optimum doping levels. Additionally, we induced the production of independent nanoparticles of Te and Se within the cell. It must be noted that doping concentrations are restricted when magnetosomes are modified *in vivo* due to poisoning of the organism. We thus sought an *in vitro* route to offer more flexibility and higher-yields. Here, in collaboration with the lab of Prof. Matsunaga we build on their original method to develop a biomimetic route to more precise nanomagnets synthesized at room temperature using protein mediated precipitation of magnetic nanoparticles. The protein used was Mms6 (magnetosome membrane specific, 6 KDa) which was found to be unique to the magnetosome membrane and tightly bound to the crystal (Figure 1C & D). When this protein was expressed and purified and used *in vitro* it was found to control particle size and shape (Figure 1E).

Research is now being conducted in two parallel and complementary directions:
Firstly, the physical investigation of how Mms proteins interact with the forming mineral and control the magnetite's formation and morphology is being investigated (BBSRC funded). Several new proteins are being identified and expressed while their interaction with magnetite is being assessed using a range of spectroscopy, electron/force microscopy and neutron scattering techniques. Once key motifs, peptide and binding sites can be identified we could begin to design tailored additives for high-yield industrial nanomagnet production.

Secondly, we are developing a range of methods using the expressed Mms proteins *in vitro* for more advanced synthesis. We are enhancing this with the addition of membranes and vesicles to the systems (EPSRC funded). This is being furthered by experimenting with different proteins that affect the functionality of membranes. For example we are investigating novel metal ion transport proteins and vesicle deformation proteins which can be incorporation into vesicles along with Mms proteins to develop a range of novel, flexible biomimetic systems.

Finally, we have patterned a SAM surface with Mms6 and successfully mineralised morphologically controlled magnetic nanoparticles located in patterned on the surface (Figure 1F). Thus the protein has a dual purpose of controlling particle formation and locating the particles to the pattern. This is currently been advanced further to form customised nanomagnetic arrays. This is just one of many biomimetic systems we are developing to create several novel mineral/membrane assemblies, some tethered/free and attached to surfaces.

Publications
Galloway, J., Bramble, J., Rawlings, A., Burnell, G., Evans, S. & Staniland, S. (2012) Biotemplated magnetic nanoparticle arrays. *Small* **8:**204-208.

Galloway, J., Bramble, J., Rawlings, A., Burnell, G., Evans, S. & Staniland, S. (2012) Nanomagnetic arrays formed with the biomineralization protein mms6. *J. Nano Res.* **17:** 127-146.

Galloway, J. & Staniland, S. (2012) Protein and peptide biotemplated metal and metal oxide nanoparticles and their patterning onto surfaces. *J. Mater. Chem.* **22:** 12423-12434.

Rawlings, A., Bramble, J. & Staniland, S. (2012) Innovation through imitation: biomimetic, bioinspired and biokleptic research. *Soft Matter* **8:** 6675-6679.

Tanaka, M., Brown, R., Hondow, N., Arakaki, A., Matsunaga, T. & Staniland, S. (2012) Highest levels of Cu, Mn and Co doped into nanomagnetic magnetosomes through optimized biomineralisation. *J. Mater. Chem.* **22:** 11919-11921.

Tanaka, M., Critchley, K., Matsunaga, T., Evans, S. Staniland, S. (2012) Fabrication of lipid tubules with embedded quantum dots by membrane tubulation protein. *Small* **8:** 1590-1595.

Funding
This work has been funded by the EPSRC (Overseas Postdoctoral Life-science Interface Fellowship Scheme 2005-2008 EP/C53204X/1) while Masayoshi Tanaka is funded as a Royal Society Newton Fellow under the Newton international fellowship scheme. Research is being funded by the BBSRC (2010-1014 BB/H005412/1) and the EPSRC (2011-2015 EP/I032355/1).

Collaborators
External: B. Ward (University of Edinburgh, UK), A. Harrison (ILL, Grenoble, France), T. Matsunaga (Tokyo University of Agriculture and Technology, Tokyo, Japan), D. Cowan (University of the Western Cape, Cape Town, South Africa), A. Roychoudhury (University of Stellenbosch, Stellenbosch, South Africa), M. Edirisinghe and E. Stride (University College London, UK).
Leeds: C. Moisescu and L. Benning (School of Earth and Environment).

RNA aptamers as research tools and diagnostic reagents in amyloid disease

Simon White, Claire Sarell, Rachel Mahood, Amy Barker, David Bunka, Sheena Radford and Peter Stockley

Introduction

There are more than 30 known human disorders characterised by the self-assembly of proteins or peptides into amyloid fibrils and various oligomeric assemblies. The aggregation of the β_2-microglobulin (β_2m) protein (both full length and a truncated variant termed ΔN6) in the joints of patients undergoing long-term haemodialysis, leads to a debilitating, and ultimately fatal, disorder known as Dialysis Related Amyloidosis (DRA). Similarly, the amyloid-β (Aβ) peptide is considered the primary neurotoxic agent in Alzheimer's disease. The peptide accumulates into typical amyloid fibrils that are found deposited in the neuronal plaques associated with the disease. Aβ also forms a number of soluble, oligomeric species that are thought to play important roles in disease progression.

Nucleic acid aptamers are small structured polynucleotide sequences that can be isolated by automated *in vitro* selection from randomised oligonucleotide libraries (Figure 1). The chemical simplicity and adaptability of RNA aptamers make them a promising class of compounds for the diagnosis or therapy of human disease, including amyloidosis. Aptamers have advantages over antibodies as potential therapeutics and diagnostics as they are significantly smaller and are thus able to access epitopes hidden from antibodies. In addition, they do not carry the secondary functional signals of antibodies, such as complement fixation; do not elicit significant immune responses; can be stabilised against nuclease action by several non-toxic chemical modifications; are easily modified to include chromophores, fluorophores, radiolabels or reactive functional groups; and can be amplified *via* PCR. Several aptamer-based drugs are now approved for clinical use. Aptamers thus provide exciting new opportunities for exploitation in diagnosis and disease intervention.

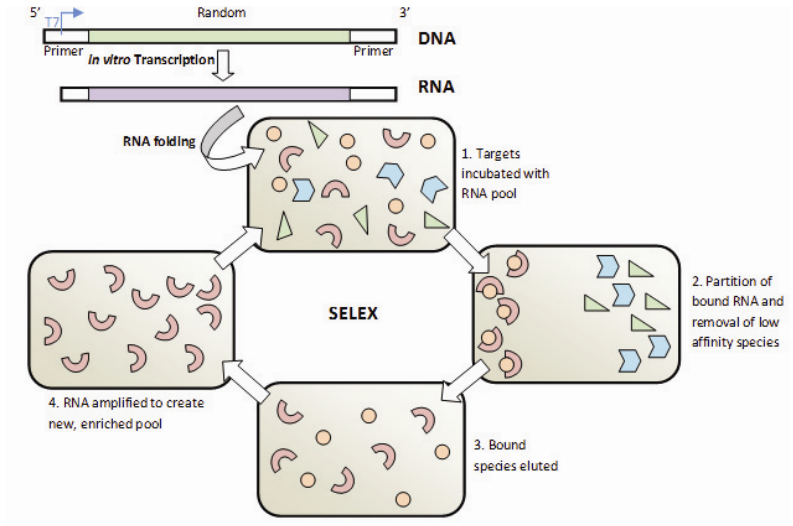

Figure 1: outline of SELEX. A degenerate library of RNA is incubated with the target that has been immobilised on streptavidin magnetic beads (Step 1). Binders are partitioned (Step 2) and non-binders removed by washing. Bound sequences are eluted by thermal denaturation or competition with free target (Step 3) and reverse transcribed and amplified (Step 4).

Searching for an anti- β_2m aptamer

Modified RNA aptamers were raised against monomeric β_2m (Figure 2A), monomeric ΔN6 and fibrils formed from these monomers that have three different morphologies, formed under different conditions. Two aptamers were isolated against monomeric β_2m: B6 and B9. The secondary structure of aptamer B6, as predicted by Mfold, is a 44 nucleotide long stem-loop interrupted by single-stranded bulges. This is the fragment of the full-length aptamer that encompasses the structural motif required for specific recognition of the target ligand and

was determined through enzymatic and chemical cleavage protection assays. The binding affinity of B6 was determined by Surface Plasmon Resonance and tryptophan fluorescence quenching (Figure 2 B): a dissociation constant of 100 nM was found, and B6 had no cross reactivity with monomeric ΔN6.

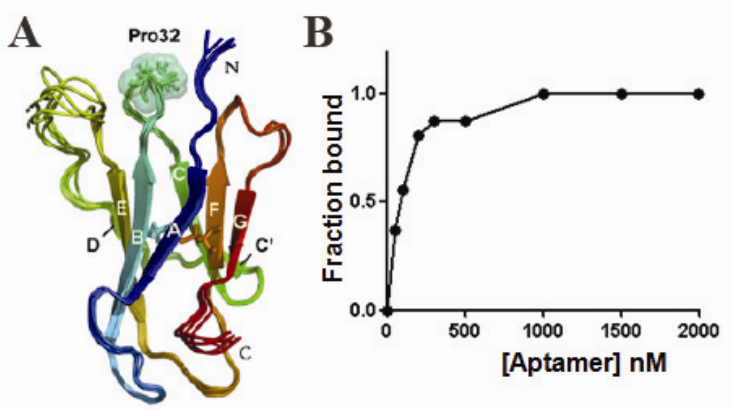

Figure 2: anti-monomeric β_2m aptamers B6 and B9. **(a)** The structure of monomeric β_2m and **(b)** fluorescence quenching experiment of B6 aptamer binding to β_2m monomer.

Work to raise aptamers against Aβ targets is ongoing, with aptamer sequences selected against fibrils with different morphology as well as monomeric Aβ. Aptamer binding affinities and epitopes will be determined as performed with β_2m aptamers. Aptamers will also be tested in a number of i*n vivo* assays, determining their potential as diagnostic probes or therapeutic agents.

Funding
This work was funded by the MRC and the BBSRC.

Collaborators
External: D. Walsh (Harvard Medical School).

Structure of a plasmid replication initiator protein: first example of the *Rep_Trans* family displays a novel fold

Stephen Carr, Simon Phillips and Chris Thomas

Introduction

Plasmids of the pT181 family are widespread among the staphylococci, typically carrying antibiotic resistance genes in a mobilisable context. As such they contribute the ongoing problem of "superbugs" such as MRSA. These plasmids replicate by a rolling circle mechanism, requiring the action of a plasmid-encoded replication initiator protein, Rep. Rep proteins have both DNA-binding and nicking/closing (or DNA-relaxing) activities, and also serve to recruit cellular replication components (such as the PcrA helicase) to the origin.

Similar Rep proteins are involved in virus replication and conjugative DNA transfer. All known examples require a conserved tyrosine residue for nicking/closing activity. Such relaxases can be broadly divided into two groups: those possessing a histidine-hydrophobic-histidine (HuH) amino acid motif, and those without (such as the pT181 family proteins). Sequence conservation among the latter is represented by the *Rep_trans* motif (pfam 02486). Structural data for examples of the HuH family is already available, but (despite over 20 years of effort) the structural characterisation of a *Rep_trans* example has until now remained elusive.

Results

Our studies of *Rep_trans* proteins have included RepSTK, encoded by plasmid pSTK1 which was isolated from the thermophile *Geobacillus stearothermophilus*. Previous work has identified that a 42 kDa N-terminally extended translation product is necessary for site-specific nicking and closing of DNA *in vitro*. Derived from this product, a 33 kDa C-terminally truncated form (RepSTK-b) retains both activity and stability at high temperature.

Crystals of RepSTK-b yielded diffraction data to 2.3 Å, phase information being obtained using heavy metal derivatives. Four monomers were present in the asymmetric unit, arranged as two dimers. Little variation was evident between monomers; the dimer represented by molecules a and c is presented in Figure 1.

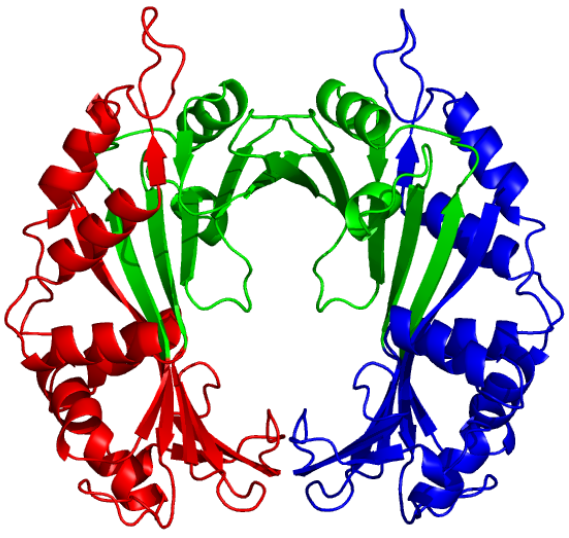

Figure 1: overall architecture of RepSTK-b, with *Rep_trans* motif in green.

Each monomer is crescent-shaped, with the dimer presenting a near-continuous antiparallel beta sheet lining a central hole roughly 20 Å diameter. The dimer interfaces are at the top and bottom in the orientation shown. Residues making up the active site are included within the span coloured in green in Figure 1, corresponding to the *Rep_trans* motif.

The side chains of conserved and active site residues project inward towards the centre of the structure, clustered around the essential nucleophilic tyrosine. The arrangement within one monomer is shown in Figure 2. HuH and *Rep_trans* motifs are fundamentally different: the active site of *Rep_trans* contains no histidine residues, nor does it utilise a nucleophilic

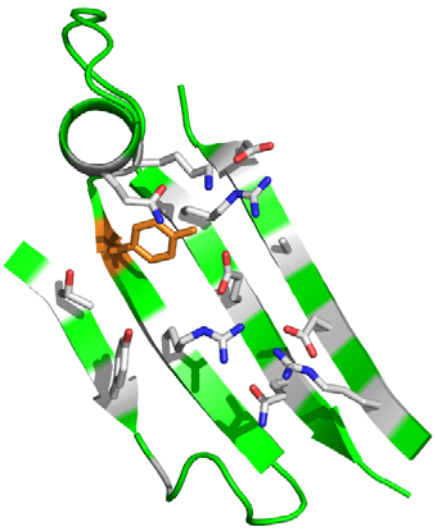

Figure 2: arrangement of active site residues surrounding the tyrosine nucleophile (shown in gold).

tyrosine approaching from a separate helical structure. We have also been unable to find any significant structural similarities to coordinates deposited within the PDB; we therefore believe the fold to be new.

The structure presents many useful clues regarding physical characteristics of Rep proteins and their likely mechanism of action. For example, the N-terminal extension to RepSTK required for isolation of a viable relaxase is an integral part of the beta sheet structure. Furthermore, the accommodation of a continuous DNA strand running through the central pore would account for the processivity conferred on PcrA helicases by such Rep proteins.

We are currently using these coordinates to solve diffraction data obtained from several staphylococcal Rep proteins of the pT181 family, and work is already well advanced on the structural determination of variants based on RepD, RepN and RepE.

Nucleic acid end labels for single molecule atomic force microscopy of DNA:RNA polymerase complexes

Oliver Chammas, Daniel Billingsley, William Bonass and Neil Thomson

Introduction

The visualisation of DNA-protein complexes by atomic force microscopy (AFM) provides insight into the interactions of proteins with the DNA on a single molecule basis. In the case of *E. Coli* RNA polymerase holoenzyme (RNAP) it is possible to investigate the interactions that occur on DNA templates containing multiple promoter elements. The outcomes of such interactions hold importance in the understanding of naturally occurring elements, such as nested genes.

In the study of DNA-protein complexes, however, AFM is typically not able to distinguish the polarity of the DNA. This limits the ability to study the interactions of more than one globular protein, particularly those similar in size, on the same individual DNA molecule. In studying more than one RNAP transcribing DNA molecules we need to know in which direction the molecules to infer outcomes of transcriptional interference events, which have implications for gene expression. To overcome this problem, the DNA molecules require a polarity label that can be morphologically identified in the AFM but does not significantly affect the system behaviour. Many labels for high resolution microscopy of DNA are protein based or consist of relatively large bulky materials, which can affect AFM sample preparation, as well as being morphologically indistinguishable from other proteins such as RNAP.

A new nucleic acid end-labelling approach

With this is mind, we developed a non-replicative PCR reaction to incorporate a single stranded DNA loop consisting of poly(A) sequence to one end of the DNA template. This loop was clearly distinguishable from the DNA template and RNAP by the AFM (see Figure 1). We also discovered that it had the added advantage for RNAP studies: it stalled an active transcribing RNAP at the end of the template without allowing it to release from the DNA. This enables us to investigate interactions and collision events between two or more RNAPs on single DNA molecules in aligned or convergent configurations.

The non-replicative nature of our initial method meant that recovery of labelled DNA and the efficiency of labelling was low. We have now further extended this approach and designed a new replicative PCR method for the addition of a single stranded DNA end loop label with high efficiency and yield. This method was used to incorporate homo-polynucleotide loops consisting of one of the four DNA bases (A, C, G or T) to the end of double-stranded DNA templates ~620 bp long.

The loop structure was observed with an occurrence greater than 70% for all four of the loop sequences that were incorporated. AFM also confirmed that the DNA recovered after the PCR reaction was the correct fragment through contour length measurements which showed an average length of 207.9±0.7 nm, which gave a base pair rise of 3.3nm, which is in the expected range for B-form DNA. Upon formation of open promoter complexes the loop was easily distinguishable from the RNAP by height and diameter as can be seen in Figure 1.

After transcription elongation approximately 90% of molecules had a RNAP molecule attached to the loop labelled end of the DNA template. This indicates that the loop structure was able to inhibit dissociation of the RNAP after transcription and so therefore inhibit re-association with the promoter.

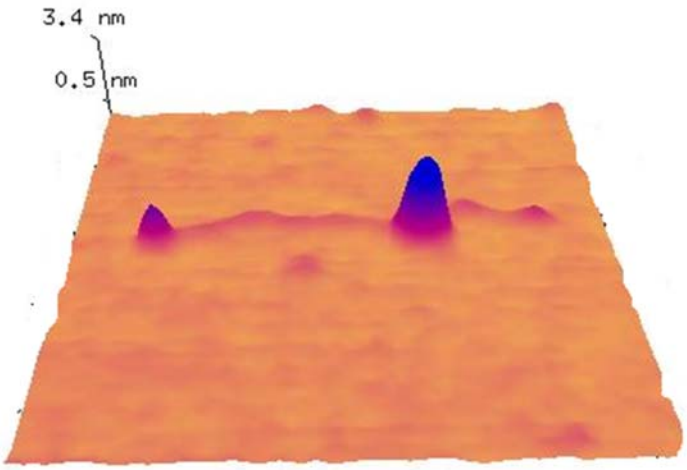

Figure 1: an *E. coli* RNA polymerase open promoter complex (middle) on a 620bp dsDNA template with a 20bp ssDNA end loop label on the left-hand side.

This nucleic acid loop labelling method is allowing us to use AFM to understand more about the fundamental interactions involved between polymerase during transcription. Moreover, it can be applied to the study of many DNA-protein interactions in the AFM, by acting as a fiducial marker.

Publications

Billingsley, D., Bonass, W., Crampton, N., Kirkham, J. & Thomson, N. (2012) Single-molecule studies of DNA transcription using atomic force microscopy. *Phys. Biol.* **9:** 021001.

Billingsley, D., Crampton, N., Kirkham, J., Thomson, N. & Bonass, W. (2012) Single-stranded loops as end-label polarity markers for double-stranded linear DNA templates in atomic force microscopy. *Nucleic Acids Res.* **40:** e99.

Funding

This work was funded by the EPSRC through Doctoral Training Centres.

Using artificial binding proteins to inhibit protein-protein interactions

Christian Tiede, David Hughes, Anna Tang, Adrian Whitehouse, Michael McPherson
and Darren Tomlinson

Introduction

Antibodies are the best-studied group of biological binding molecules to date. They are important in a wide variety of biological and medical applications, but as molecular biology reagents they are limited by their significant size, poor stability, production costs and batch-to-batch variation. To overcome these issues a number of alternative binding reagents (protein, RNA and DNA aptamers) have been developed. These can bind to epitopes on target proteins and so have potential as molecular biology tools, therapeutic agents and as diagnostic tools for detection and imaging of proteins in patient samples. The BioScreening Technology Group at Leeds was established to exploit a novel artificial binding protein (ABP) library. Our ABP is called an adhiron and is based on a constant small 91 amino acid scaffold protein that constrains two randomised nine amino acid loop regions for molecular recognition (Figure 1A). The scaffold protein is extremely stable with a T_m of 101°C and is the most stable ABP scaffold to date (Figure 1B), and maintains the beta structure following loop insertion (Figure 1C). We have developed a large naïve phage display library (>3×10^{10}) of adhirons that is of very high quality (86 % full length clones). The loop regions in the library contain an even distribution of each of the 19 amino acids excluding cysteines (Figure 1D).

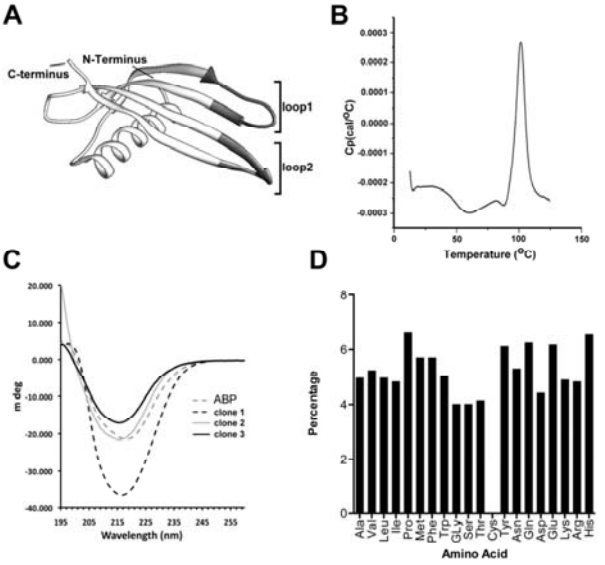

Figure 1: (a) The ABP is shown in white, the loop regions are shown in grey. **(b)** differential scanning calorimetry to measure melting temperature of scaffold protein. **(c)** circular dichroism examining structures of the ABP and three random clones. **(d)** amino acid composition of the loop regions showing an even distribution with little bias.

Developing specific reagents for inhibiting human SUMO2 interaction with RNF4

Small Ubiquitin-like Modifier (SUMO) regulates post-translational modifications involved in many aspects of cell function, including stress response, cell proliferation and apoptosis. To date the lack of suitable isoform specific reagents has limited understanding of the specific function of the isoforms. Recently, hSUMO1 specific binding reagents were identified but the same group failed to identify hSUMO2 specific binders. For the first time we have developed ABP reagents which differentiate between hSUMO1 and hSUMO2 isoforms (Figure 2A). To confirm this specificity we have developed assays that test ABPs ability to inhibit SUMO interactions in an isoform-specific manner. SUMO-targeted ubiquitin ligases (STUbL) are a unique class of E3 ubiquitin ligase enzymes that only recognise substrates modified with polymeric chains of hSUMO2. RNF4 is the only known cellular STUbL and contains two domains – one with SUMO Interacting Motifs (SIM) for binding SUMO and a RING domain responsible for its ubiquitination activity. *In vitro* recombinant RNF4 ubiquitinates polymers of hSUMO2 (poly-hSUMO$2_{2\text{-}8}$). ABPs specific for GFP (irrelevant control) and for hSUMO1 were unable to inhibit RNF4s ability to ubiquitinate poly-hSUMO$2_{2\text{-}8}$, whereas ABPs specific for hSUMO2 robustly inhibited this activity at less than 1 μM (Figure 2B).

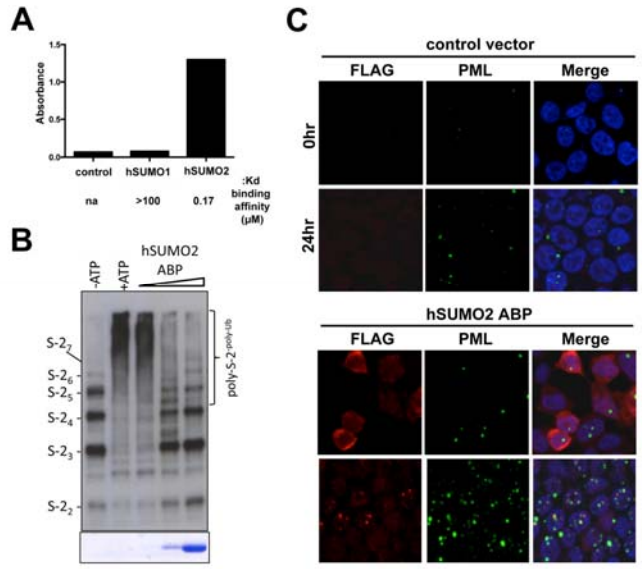

Figure 2: ABP targeting hSUMO2. **(a)** an ABP raised against hSUMO2 was tested to determine specificity for hSUMO1 and hSUMO2 by ELISA. The hSUMO2 ABP specifically bound to hSUMO2, which was reflected in the binding affinity. **(b)** blot showing the ability of the hSUMO2 ABP to inhibit RNF4's SUMO-targeted ubiquitin ligase activity. **(c)** a control vector or hSUMO2 binder was expressed in cells (red – anti-FLAG antibody) and cultured with arsenic to induce nuclear bodies, PML (green). RNF4 promotes degradation of PML. Blocking the interaction between hSUMO2 and RNF4 inhibits PML degradation.

To assess the hSUMO ABPs in a more physiological context, we expressed them in mammalian cell lines. A major role of cellular RNF4 is to maintain the levels of nuclear domain 10 (ND10) components such as promyelocytic leukaemia protein (PML). PML is SUMO-modified with both hSUMO-1 and hSUMO-2, but its modification with polymeric hSUMO-2 is critical for recruiting RNF4 in a SIM-dependent manner, leading to its ubiquitination and subsequent degradation by the 26S proteasome. Brief treatment of cells with arsenic trioxide (As_2O_3) induces the expression and SUMO modification of PML and when arsenic is removed PML levels return to normal in an RNF4-dependent manner. In cells expressing control or hSUMO1-ABPs, PML levels recover after removal of arsenic. By contrast in treated cell expressing hSUMO2 ABPs the levels of PML fail to return to normal (Figure 2C) demonstrating the specificity of the hSUMO2 ABPs.

Publications

di Martino, E., Tomlinson, D. & Knowles, M. (2012) A decade of FGF receptor research in bladder cancer: past, present, and future challenges. *Adv Urol.* **2012:**429213.

Tomlinson, D., Baxter, E., Loadman, P., Hull, M. & Knowles M. (2012) FGFR1-induced epithelial to mesenchymal transition through MAPK/PLCγ/COX-2-mediated mechanisms. *PloS One.* **7:**e38972.

Tomlinson, D., Knowles, M. & Speirs, V. (2012) Mechanisms of FGFR3 actions in endocrine resistant breast cancer. *Int J Cancer*. **130:**2857-66.

Funding

This work was supported by the Biomedical Health Research Centre and the Leeds CRUK Development Fund at the University of Leeds.

NMR studies of the large super-repeats in titin

Andras Czajlik, Arnout Kalverda, Gary Thompson, Chris Bartlett,
Larissa Tskovrebova, Steve Homans and John Trinick

Introduction

Titin is the largest protein yet found (chain weight ~3 MDa) and the third most abundant protein of muscle, after myosin and actin. Titin molecules are ~1 μm long and span between the Z- and M-lines in muscle sarcomeres. Most of the molecule consists of two classes of concatenated ~100 residue domains similar to I-set immunoglobulins and type III fibronectins. In the A-band titin is integral with the thick filament, where it is proposed to regulate exact assembly to the 294 myosin molecules present. In this region the Ig and Fn domains are arranged in 11 domain patterns, Ig-Fn-Fn-Fn-Ig-Fn-Fn-Fn-Ig-Fn-Fn, called large super-repeats, which are themselves repeated 11 times. Each super-repeat spans the 43 nm helical repeat of the thick filament. The entire 121 domain region is nearly half the ~300 domains making up titin. The size and stability of these Ig and Fn domains make them very suitable for structure studies by NMR, while it is the method of choice to gain insight in interdomain flexibility and the behavior of interdomain linker sequences.

Results

We have expressed in *E. coli* seven 2 and 3 domain overlapping constructs spanning one large super-repeat and we are studying the structure and flexibility of these. Figure 1 shows the ^{15}N–^{1}H HSQC-TROSY spectrum of the A67-A68 tandem illustrating the quality of the

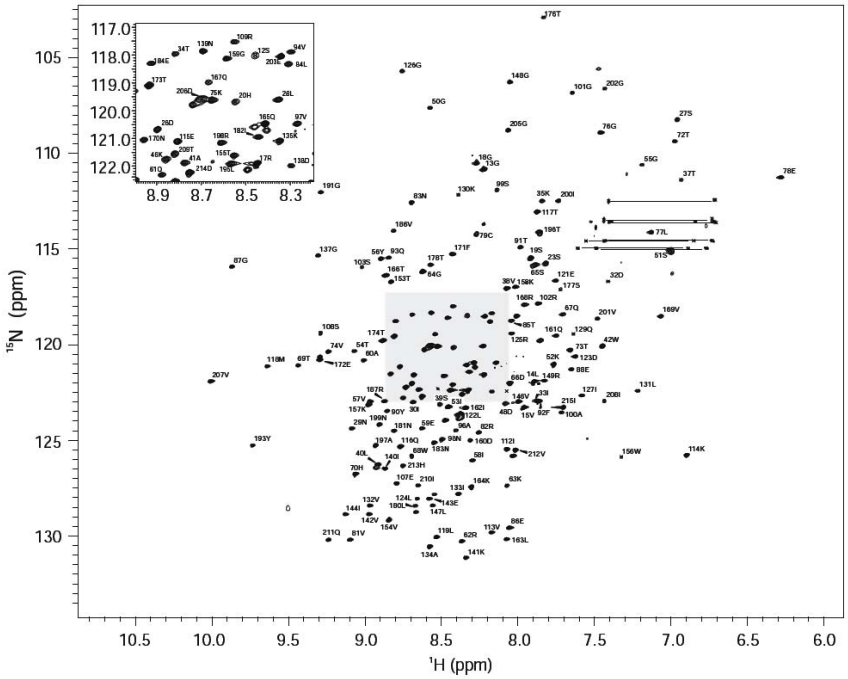

Figure 1: two-dimensional H–N HSQC-TROSY spectrum of the A67-A68 tandem at 750-MHz H frequency. Data were acquired at 293K using a uniformly ^{15}N, ^{13}C, ^{2}D labelled protein sample (~1 mM).

data and breadth of assignment. The spectrum show strong signals with uniform intensities, indicative of a well defined three-dimensional structure and appears to tumble as a single unit. The completeness of the assignments of A67-A68 tandem are 93.4% (170/182) for backbone ^{1}HN and ^{15}N, 94.9% (185/195) for $^{13}C\alpha$, 92.3% (167/ 181) for $^{13}C\beta$, and 86.7% (169/195) for $^{13}C0$ resonances. Most of the unassigned resonances were in loop regions. The chemical shift and TALOS data indicate the presence of fourteen β-strand regions from the

two domains. Determination of a high resolution NMR structure and a detailed description of the extent of inter-domain flexibility are in progress.

Publications

Czajlik, A., Thompson, G., Khan, G., Kalverda, A., Homans, S. & Trinick, J. (2012) H-1, N-15 and C-13 backbone chemical shift assignment of the titin A67-A68 domain tandem. *Biomol. NMR Assign.* **6:** 39-41.

Tskhovrebova, L. & Trinick, J. (2012) Making muscle elastic: the structural basis of myomesin stretching. *PLoS Biol.* **10:** e1001264-e1001264.

Tskhovrebova, L. & Trinick, J. (2012) Molecular rulers? *Curr. Biol.* **22:** R317-R318.

Funding

Supported by the British Heart Foundation and the EU MUZIC consortium.

Evidence that viral RNAs have evolved for efficient, two-stage packaging

Alexander Borodavka, Roman Tuma and Peter Stockley

Introduction

Positive-sense, single-stranded (ss)RNA viruses are ubiquitous pathogens affecting human health and causing losses of livestock and crops. Therapeutic interventions are currently limited while vaccination is practical for only a few human and animal viruses. Understanding all steps in viral lifecycles will lead to novel therapeutic strategies. Packaging of genomic RNA is the prerequisite step in production of infectious virions. Many icosahedral protein capsids spontaneously co-assemble around their genomes, resulting in relatively high packing densities. It has been proposed that this is accomplished by a gradual condensation of RNA, driven primarily by electrostatic neutralisation of the nucleic acid charge by positive charges on the coat protein. However, the proposed mechanism cannot account for the observed specificity of packaging, i.e. discrimination between viral and the abundant non-viral RNA within cells. Here we took advantage of two model systems, bacteriophage MS2 and a plant virus, Satellite Tobacco Necrosis virus (STNV), for which *in vitro* assembly assays have been developed. The two viral coat protein architectures are distinct, the STNV CP having a positively charged N-terminal extension on a canonical jelly-roll globular domain, which is essential for assembly, whilst the MS2 CP dimer exhibits an RNA binding cleft. These differences allow us to identify conserved and distinct features of their assembly mechanisms and provide the basis for generalization.

Results

Single molecule fluorescence correlation spectroscopy (FCS) allowed us to selectively monitor coat protein (CP) or viral RNA components during assembly *in vitro* at low concentrations (<1 μM). This permitted detection of early, transient RNA:CP complexes. FCS is also excellent tool for hydrodynamic sizing of large RNA molecules. The viral, protein-free RNAs exist as an ensemble of differing conformers, most of which are larger than the capsids into which they must eventually fit. Remarkably, instead of gradual RNA condensation, which would be expected on the basis of the charge neutralisation mechanism, addition of CPs to their cognate RNAs results in a rapid collapse (<1 min, Fig. 1A & B) in their solution conformations. Collapse depends on protein-protein interactions and multiple specific RNA-CP interactions, since it does not occur on non-viral RNA or with the non-cognate viral RNA (Fig 1A & B). The collapsed state is smaller than the capsid and appears to consist of complexes with sub-stoichiometric amounts of coat proteins correctly organized to form a partial capsid shell of the correct size. The full complement of CPs are recruited in a second slower stage of assembly (Fig. 1C). Given that this two-stage assembly has been demonstrated for

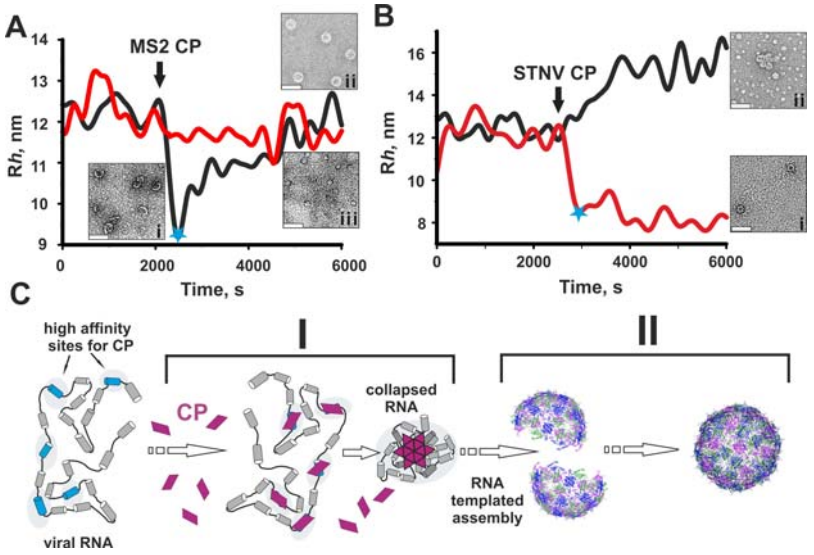

Figure 1: hydrodynamic radius (Rh) changes of viral RNAs (MS2-black, STNV-red) during assembly with MS2 coat **(a)** or STNV coat **(b)**. The initial collapse is indicated by blue star. **(c)** A two-stage mechanism of ssRNA virus assembly: Stage I-coat protein mediated rapid RNA collapse; Stage II-RNA-templated completion of capsids.

two unrelated viruses it may constitute a mechanism conserved among a large class of viral pathogens and provides a potential target for therapeutic intervention.

Publications

Borodavka, A., Tuma, R. & Stockley, P. (2012) Evidence that viral RNAs have evolved for efficient, two-stage packaging. *Proc. Natl. Acad. Sci. U.S.A.* **109:** 15769-15774.

Funding

This work was supported by Wellcome Trust.

Protein modification reagents and binding studies on bacterial toxins

Thomas Branson, Martin Fascione, Edward Hayes, Pintu Mandal, James Ross, Daniel Williamson, Michael Webb and Bruce Turnbull

Introduction

Sortase A (SrtA) catalyses the reversible attachment of virulence factors to the cell walls of Gram positive bacteria via C-terminal modification of proteins at an LPXTG recognition sequence. The enzyme has been widely exploited for introducing labels at the C-terminus of recombinant proteins, but the reversibility of the reaction necessitates the use of large excesses of the labelling reagents and the method has rarely been used for N-terminal labelling of proteins.

Results

We have developed new reagents for efficiently labelling any protein that has at least one unhindered glycine residue at its N-terminus (Figure 1). By using depsipeptide substrates (i.e., containing an ester bond) the trans-peptidase reaction becomes effectively irreversible and allows quantitative labelling of proteins with only a small excess of the labelling reagent.

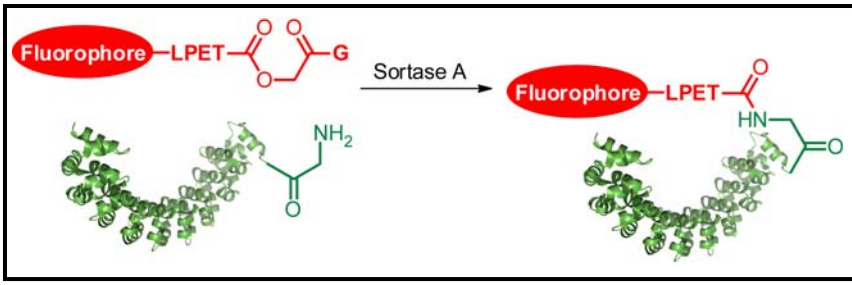

Figure 1: schematic depiction of labelling a protein using a fluorescent depsipeptide substrate for the Sortase A enzyme.

In other studies we have continued to investigate the carbohydrate-binding specificity of the cholera toxin. It has long been known that patients with blood group O are more severely affected by El Tor cholera than those in blood groups A or B. Krengel and co-workers discovered a secondary carbohydrate binding site for blood group oligosaccharides in the closely related *E. coli* heat-labile toxin (Figure 2) which led to the hypothesis that blood group A and B oligosaccharides that are shed from the surface of cells could help prevent the toxin from reaching its primary ligand in the cell membrane.

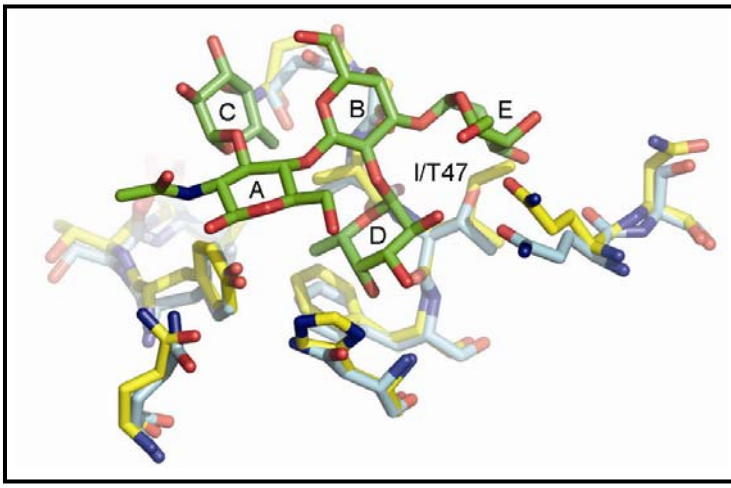

Figure 2: overlay of structure of *E. coli* heat-labile toxin (light blue; 2O2L.pdb) and a model of El Tor CTB (yellow) constructed using the structure of classical biotype CTB (3CHB.pdb). The blood group B Lewis-y oligosaccharide is shown in green. Galactose E, which is absent in the equivalent blood group O oligosaccharide, sits in close proximity to residue 47 in the protein which is either an isoleucine or threonine residue.

We have chemically synthesised blood group O and blood group B oligosaccharides of the Lewis-y series and used isothermal titration calorimetry and saturation-transfer difference NMR spectroscopy to show that both carbohydrates are ligands for the *E. coli* version of the

toxin, but only the blood group O oligosaccharide can bind to the toxin responsible for El Tor cholera. The difference in specificity appears to arise from a single mutation at residue 47 in the binding site (Figure 2) in which a threonine residue allows blood group B binding, whereas an isoleucine residue does not. This result suggests that surface mutations on the protein could be used to engineer cell/tissue selectivity into the protein, e.g., for targeting tumours that overexpress certain oligosaccharides on their surface.

Publications

Mandal, P., Branson, T., Hayes, E., Ross, J., Gavin, J., Daranas, A. & Turnbull, W. (2012) Towards a structural basis for the relationship between blood group and the severity of el tor cholera. *Angew. Chem. Int. Ed. Engl.* **51:** 5143-5146.

Turnbull, W. & Stalford, S. (2012) Methylthioxylose - a jewel in the mycobacterial crown? *Org. Biomol. Chem.* **10:** 5698-5706.

Turnbull, W. (2012) Biophysical studies on the interactions of bacterial toxins, in "Glyco-bioinformatics", Eds. M. G. Hicks and C. Kettner, Beilstein Institute, Frankfurt, pp 55-68.

Williamson, D., Fascione, M., Webb, M. & Turnbull, W. (2012) Efficient N-terminal labeling of proteins by use of sortase. *Angew. Chem. Int. Ed. Engl.* **51:** 9377-9380.

Funding

This work is funded by the Royal Society, EPSRC, Newton International Fellowships, AstraZeneca and the University of Leeds.

Collaborators

External: A. Daranas and J. Gavín (University of La Laguna, Tenerife).

Chemical and biochemical approaches to protein regulation and modification

Heather Cox, James Gowdy, Jeffrey Hollins, Katherine Horner, Darren Machin, Tom McAllister, Diana Monteiro, Philip Morrison, James Ross, Daniel Williamson, Briony Yorke, Daniel O'Sullivan, Michael Rugen, Christopher Bartlett, Samuel Ness, Henry Farrer, Matthew Thorley, Arwen Pearson, Alison Ashcroft, Bruce Turnbull and Michael Webb

A new protein for pantothenate biosynthesis in the Enterobactericeae

The pathway to pantothenate in bacteria has long been thought to have been fully characterised. The extant pathway consists of four enzymes: a hydroxymethyl transferase and a reductase which generate d-pantoate, a decarboxylase to produce β-alanine and an ATP-dependent synthetase to join these fragments. We have now reported the discovery and preliminary characterisation of an essential fifth protein limited to a small subset of enteric Gram-negative bacteria. This protein, PanZ, is required for the activation of the pyruvoyl-dependent aspartate α-decarboxylase (ADC) from the zymogenic form in which it is expressed.

PanZ is a putative Acetyl-CoA dependent acetyl transferase. We have analysed the interaction of a constitutively inactive form of ADC with PanZ using isothermal titration calorimetry and mass spectrometry. These experiments (Figure 1) demonstrated that the proteins interact with nanomolar affinity in a 4:4 complex. We are now using a combination of NMR, X-ray crystallography and small angle X-ray scattering to determine the structure of this complex and how interaction of the two proteins leads to formation of active ADC. In related work, we are using the same set of techniques to investigate the function of other proteins which putatively interact with other components of the pathway.

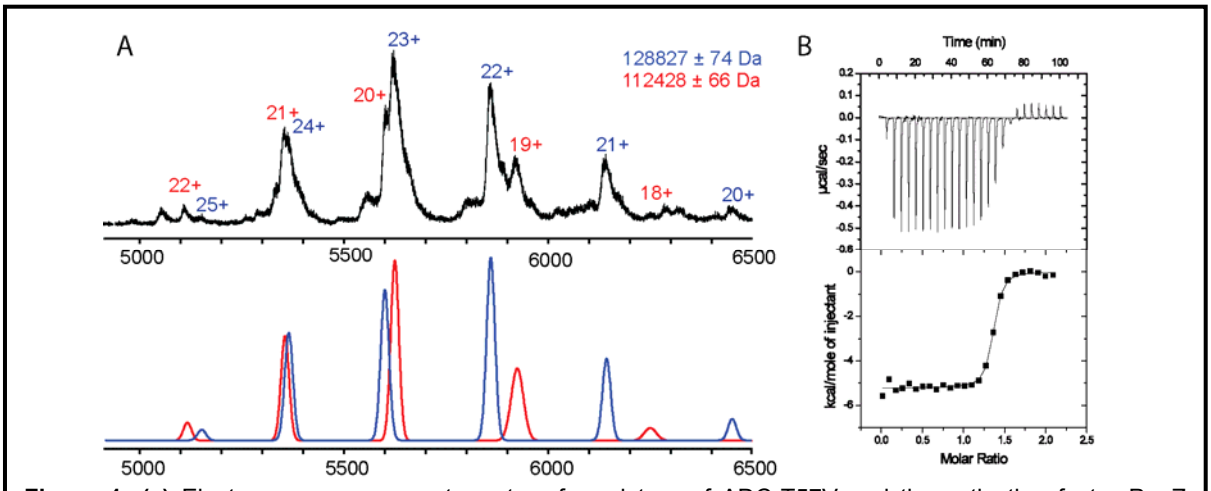

Figure 1: (a) Electrospray mass spectrometry of a mixture of ADC-T57V and the activating factor PanZ reveals a mixture of 4:4:4 and 4:3:3 complexes of ADC, PanZ and coenzyme A (simulation below). **(b)** Isothermal titration calorimetry analysis then demonstrated that coenzyme A (bound to PanZ) is required for the interaction. In the absence of saturating CoA, superstoichiometric quantities of panZ are required to saturate ADC-T57V in titrations.

Development of stable analogues of phosphohistidine

A major continuing interest in our group is the development of stable analogues of phosphohistidine. We propose to use these probes to understand the role of phosphohistidine in the mechanism of an unusual ADP-dependent kinase which we are currently investigating. In addition we are investigating the use of our analogues as haptens for antibody production (with Claire Eyers, Manchester). We have recently reported our optimised synthetic strategy to generate our class of triazole analogues, using P(III) chemistry to produce a key alkynyl phosphonate intermediate as shown below (Figure 2).

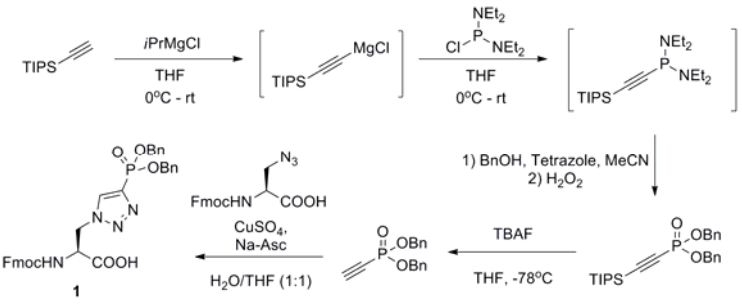

Figure 2: strategy used for the production of the stable phosphonate analogue of phosphohistidine 1 using P(III) chemistry to generate a precursor fully-compatible with the Fmoc-strategy for solid phase peptide synthesis.

Other work

We are working with Dr Ben Murray (School of Earth and Environment) to investigate how biological materials affect the atmosphere via the nucleation of ice in tropospheric clouds. We also collaborate with Bruce Turnbull to develop methodology to apply the transpeptidase sortase A from *Staphylococcus aureus* in the modification of expressed proteins.

Publications

McAllister, T. & Webb, M. (2012) Triazole phosphohistidine analogues compatible with the fmoc-strategy. *Org. Biomol. Chem.* **10:** 4043-4049.

Monteiro, D., Rugen, M., Shepherd, D., Nozaki, S., Niki, H. & Webb, M. (2012) Formation of a heterooctameric complex between aspartate alpha-decarboxylase and its cognate activating factor, PanZ, is CoA-dependent. *Biochem. Biophys. Res. Commun.* **426:** 350-355.

Murray, B., O'Sullivan, D., Atkinson, J. & Webb, M. (2012) Ice nucleation by particles immersed in supercooled cloud droplets. *Chem. Soc. Rev.* **41:** 6519-6554.

Nozaki, S., Webb, M. & Niki, H. (2012) An activator for pyruvoyl-dependent L-aspartate alpha-decarboxylase is conserved in a small group of the gamma-proteobacteria including *Escherichia coli*. *MicrobiologyOpen* **1:**298-310.

Saha, K., Webb, M., Rigby, S., Leech, H., Warren, M. & Smith, A. (2012) Characterisation of the evolutionarily conserved iron sulphur cluster of sirohydrochlorin ferrochelatase from *Arabidopsis thaliana. Biochem. J.* **444:**227-237.

Webb, M., Lobley, C., Soliman, F., Kilkenny, M., Smith, A., Blundell, T. & Abell, C. (2012) Structure of *Escherichia coli* aspartate alpha-decarboxylase Asn72Ala: probing the role of Asn72 in pyruvoyl cofactor formation. *Acta Crystallogr. Sect. F Struct. Biol. Cryst. Commun.* **68:** 414-417.

Williamson, D., Fascione, M., Webb, M. & Turnbull, W. (2012) Efficient N-terminal labeling of proteins by use of sortase. *Angew. Chem. Int. Ed. Engl.* **51:** 9377-9380.

Funding

This work was funded by the Wellcome Trust, BBSRC, NERC and EPSRC.

Collaborators

External: J. Hibberd (University of Cambridge), C. Eyers (University of Manchester), A. Smith (University of Cambridge), N. Hironori (National Institute for Genetics, Japan), E. Snell (Hauptmann-Woodward Institute, Buffalo, USA).

Identification of the ribonucleoprotein complex required for efficient viral RNA processing in oncogenic herpesviruses

Brian Jackson, Sophie Schumann, Belinda Basquero and Adrian Whitehouse

Introduction

Post-transcriptional events which regulate mRNA biogenesis are central to the regulation of gene expression. As a consequence, cells have evolved a 'gene-expression production line' that encompasses the routing of a nascent transcript through multimeric mRNA–protein complexes that mediate its splicing, polyadenylation, nuclear export and translation. Of these events it has become clear that splicing is particularly important for mRNA nuclear export, as recruitment of multiprotein complexes required for mRNA export are bound to mRNA in a splicing dependent manner. Two multiple protein complexes, namely, hTREX and the EJC bind at separate locations on spliced mRNA. hTREX, which comprises Aly, UAP56 and the multiprotein ThoI complex, is recruited exclusively to the 5' end of the first exon, providing 5'-polarity and therefore directionality observed in mRNA export.

However, in contrast to the majority of mammalian genes, analysis of herpesvirus genomes has highlighted that most lytically expressed viral genes lack introns. Herpesviruses replicate in the nucleus of the host mammalian cell, and therefore require their intronless mRNAs to be exported out of the nucleus to allow viral mRNA translation in the cytoplasm. This therefore leads to an intriguing question concerning the mechanism by which the viral intronless mRNAs are exported out of the nucleus in the absence of splicing. To circumvent this problem, and to facilitate viral mRNA export, γ-2 herpes viruses encode the ORF 57 protein. ORF 57 interacts with Aly, binds viral RNA, shuttles between the nucleus and the cytoplasm and promotes the nuclear export of viral mRNA.

Results

We are currently investigating how an intronless viral mRNP is assembled in KSHV and what role ORF57 plays in that process. We have shown that ORF57 interacts with hTREX and is essential for the recruitment of hTREX onto intronless viral mRNA transcripts. Importantly, ORF57 does not recruit the EJC to intronless viral transcripts. Moreover, we are currently determining how ORF 57 recognises the viral mRNA and allows recruitment of hTREX. This is the first system that has distinguished between hTREX and EJC *in vivo* and demonstrates that recruitment of hTREX alone to mRNA transcripts is sufficient for their nuclear export. Therefore, we believe this viral system is an exciting model to further study mRNA export mechanisms. We propose a model for herpesvirus mRNA export, whereby ORF57 mimics splicing in order to recruit the mRNA export machinery to intronless viral mRNAs.

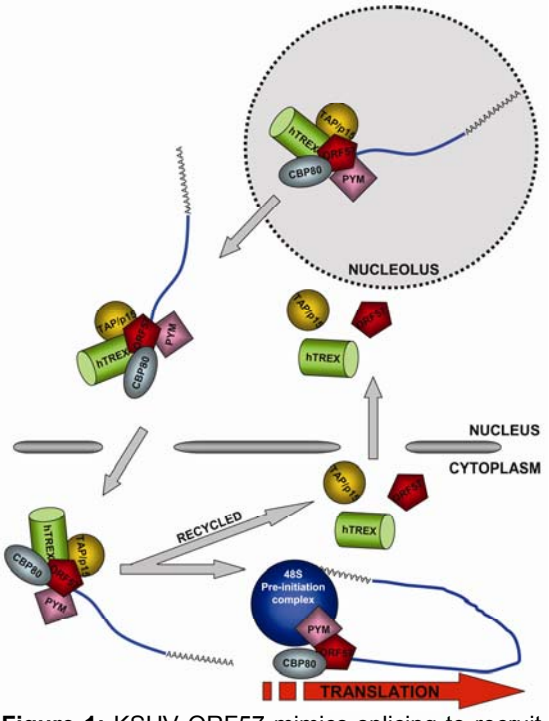

Figure 1: KSHV ORF57 mimics splicing to recruit the necessary nuclear export factors onto viral intronless transcripts and also mimics an EJC to enhance their translation.

We are now determining the structure of the interaction interface at atomic-resolution

between ORF57 homologues and the hTREX proteins, such as Aly, In collaboration with Dr Alexander Golovanov (University of Manchester) and Professr Stuart Wilson (University of Sheffield). This will provide a detailed comparison of the binding interfaces between ORF57 homologues and Aly using solution-state NMR. The regions of HSV ICP27 and HVS ORF57 involved in binding by Aly have been mapped as residues 104-112 and 103-120, respectively. We have identified the pattern of residues critical for Aly recognition, common to both ICP27 and ORF57. The importance of the key amino acid residues within these binding sites was confirmed by site-directed mutagenesis. The functional significance of the ORF57-REF/Aly interaction was also probed using an *ex vivo* cytoplasmic viral mRNA accumulation assay and this revealed that mutants that reduce the protein-protein interaction dramatically decrease the ability of ORF57 to mediate the nuclear export of intronless viral mRNA. Together these data precisely map amino acid residues responsible for the direct interactions between viral adaptors and cellular REF/Aly and provide the first molecular details of how herpes viruses access the cellular mRNA export pathway. Future work will utilise these identified binding interfaces as possible new drug targets, to be used in the future for anti-viral drug design efforts, for the prevention or treatment of KSHV-related malignancies using rational-based drug design approaches.

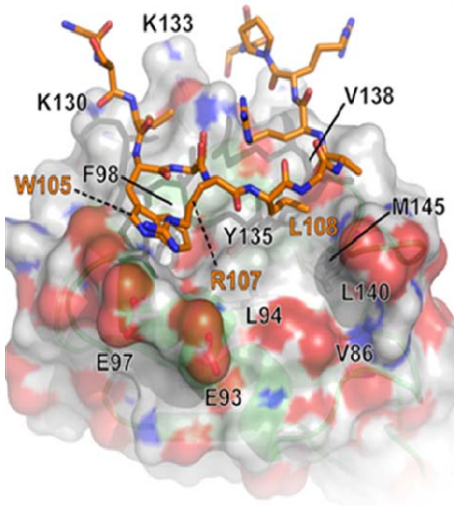

Figure 2: ORF57 homologue (HSV ICP27) recognizes and specifically binds to the surface of the RRM domain of cellular export factor REF/Aly

Publications

Dyson, O., Walker, L., Whitehouse, A., Cook, P. & Akula, S. (2012) Resveratrol inhibits KSHV reactivation by lowering the levels of cellular EGR-1. *PLoS ONE* **7:** e33364.

Jackson, B., Noerenberg, M. & Whitehouse, A. (2012) The Kaposi's sarcoma-associated herpesvirus ORF57 protein and its multiple roles in mRNA biogenesis. *Front. Microbiol.* **3:** 59-59.

Munday, D., Surtees, R., Emmott, E., Dove, B., Digard, P., Barr, J., Whitehouse, A., Matthews, D. & Hiscox, J. (2012) Using SILAC and quantitative proteomics to investigate the interactions between viral and host proteomes. *Proteomics* **12:** 666-672.

Turrell, S., Filby, M., Whitehouse, A. & Wilson, A. (2012) Cellular uptake of highly-functionalized ruthenium(ii) tris-bipyridine protein-surface mimetics. *Bioorg. Med. Chem. Lett.* **22:** 985-988.

Turrell, S., Macnab, S., Rose, A., Melcher, A. & Whitehouse, A. (2012) A herpesvirus saimiri-based vector expressing trail induces cell death in human carcinoma cell lines and multicellular spheroid cultures. *Int. J. Oncol.* **40:** 2081-2089.

Funding

This project is funded by the BBSRC, YCR, BSF and Wellcome Trust.

Exploring protein-protein interaction inhibitors and peptide nanostructures

Valeria Azzarito, Anna Barnard, Alice Bartlett, George Burslem, Hannah Kyle, Kerya Long, Natasha Murphy, Panchami Prabhakaran, George Preston, Silvia Rodriguez-Marin, David Yeo, Alison Ashcroft, Thomas Edwards, Sheena Radford, Adam Nelson, Stuart Warriner and Andrew Wilson

Introduction

This report summarises our group's investigations in the area of chemical biology principally based around two key peptide secondary structure motifs; α-helices and β-sheets. The α-helix is the most abundant secondary structural feature found in proteins and, as such, plays an important role in a significant number of protein-protein interactions (PPIs), many of which are implicated in disease development and progression. Proteomimetics can act as inhibitors of PPIs by matching the special orientation of key binding residues on the native α-helix.

β-sheet peptide nanostructures posses unique physical properties due to their complex internal architecture. Examples include amyloid fibrils which have been identified as key players in the etiology of numerous debilitating and terminal diseases. Covalent cross-linking has been proposed as an effective method for extracting structural information from such supramolecular peptide structures.

α-Helix mimetics as PPI inhibitors

Aromatic oligoamides based on three different scaffolds; 2-*O*-alkylated, 3-*O*-alkylated and *N*-alkylated (Figure 1a), reported from our group act as effective inhibitors of the oncogenic p53-*h*DM2 interaction. The more recently designed 2-*O*-alykated trimers were compared to the original 3-*O*-alkylated regioisomers. Initial molecular modelling studies on the two scaffolds indicated a significant difference in backbone curvature (Figure 1d.) which was confirmed by both solution and solid-state conformational studies. This difference in curvature arises due to the different internal hydrogen bonding patterns within the trimers where the 2-*O*-alkylated compounds are able to form 6-membered hydrogen bonding rings whereas the 3-*O*-alkylated compounds are forced to twist in order to adopt a 5-membered hydrogen bonding ring. In addition, an automated microwave synthetic methodology has been optimised for the *N*-alkylated scaffold, whilst molecular dynamics simulations on protein-bound oligoamides have been performed. In other developments, we have shown that mass spectrometry can be

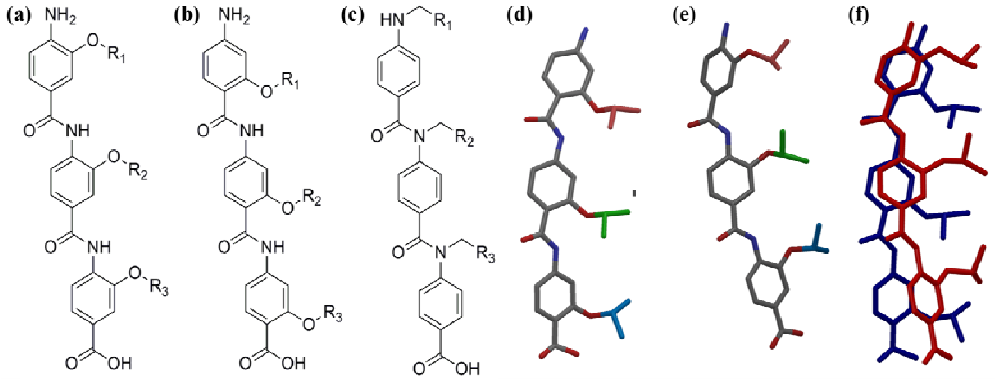

Figure 1: structures of **(a)** 3-*O*-alykylated helix mimetic scaffold; **(b)** 2-*O*-alkylated scaffold and **(c)** *N*-alkylated scaffold. Modes of **(d)** a 2-*O*-alkylated scaffold where $R_1 = R_2 = R_3$ = iPr and **(e)** a 3-*O*-alkylated scaffold where $R_1 = R_2 = R_3$ = iPr. **(f)** Overlay of both model structures demonstrating the difference in backbone curvature.

used to speciate dynamic combinatorial libraries based on iron (II) tris bipyridyl chelates**.**

Covalent cross-linking within peptide nanostuctures

Covalent cross-linking between the strands of a β-sheet using 3-aryl-3-(trifluoromethyl)diazirine (TFMD) to generate a highly reactive and non-selective carbene in combination with mass sepctrometry (MS) and tandem mass spectrometry (MS/MS) has been found to be a very effective method for the analysis of secondary structure in amyloid fibrils (Figure 2). Peptide $A\beta_{16\text{-}22}$ (Ac-KLVFFAE-NH_2) is known to form distinct morphologies at different pHs; at neutral pH it assembles into filaments and at pH 2.0 into nanotubes. Two TFMD modified peptides were synthesised with the cross-linker substituted for either F19 or F20 ($A\beta_{16\text{-}22}$-F19* and $A\beta_{16\text{-}22}$-F20*, respectively). It was therefore envisaged that the change in sequence or a change in pH would after supramolecular structure and lead to formation of distinctive cross-links. The resulting MS fragmentation patterns were only dependent on cross-linker position and not on the assembly pH. It is likely therefore that the filament and nanotube structures contain the same β-sheet unit with pH-dependent higher order packing.

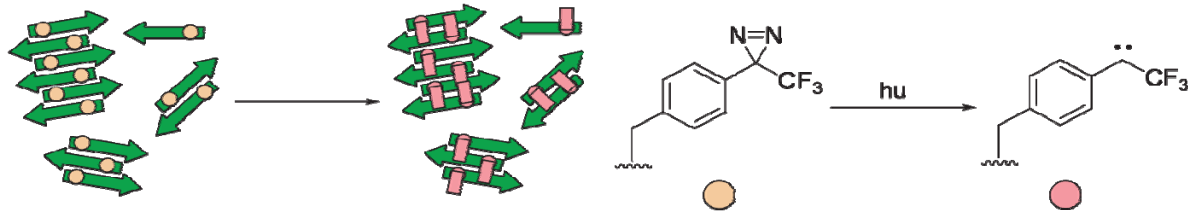

Figure 2: cartoon representation of the cross-linking strategy along with the structure of the 3-aryl-3-(trifluoromethyl)diazirine cross-linker and its corresponding reactive carbene.

Publications

Azzarito, V., Prabhakaran, P., Bartlett, A., Murphy, N., Hardie, M. J., Kilner, C., Edwards, T., Warriner, S. & Wilson, A. (2012) 2-o-alkylated para-benzamide alpha-helix mimetics: The role of scaffold curvature. *Org. Biomol. Chem.* **10:** 6469-6472.

Fuller, J., Jackson, R., Edwards, T., Wilson, A. & Shirts, M. (2012) Modeling of arylamide helix mimetics in the p53 peptide binding site of hdm2 suggests parallel and anti-parallel conformations are both stable. *PLoS ONE* **7:** e43253.

Phillips, H., Chernikov, A., Fletcher, N., Ashcroft, A., Ault, J., Filby, M. & Wilson, A. (2012) The use of electrospray mass spectrometry to determine speciation in a dynamic combinatorial library for anion recognition. *Chem. Eur. J.* **18:** 13733-13742.

Preston, G., Radford, S., Ashcroft, A. & Wilson, A. (2012) Covalent cross-linking within supramolecular peptide structures. *Anal. Chem.* **84:** 6790-6797.

Funding

We gratefully acknowledge EPSRC, the University of Leeds, The Wellcome Trust, Yorkshire Cancer Research and The European Research Council for financial support of this research.

Collaborators

External: M. Shirts (Virginia) and N. Fletcher (Belfast).

Functional nanoparticle-bioconjugates for biosensing and biocatalysis

Haiyan Zhang, Yue Zhang, Josep Garcia, Nicola Derbyshire, Simon White, Lei Song, Yuan Guo, Michael Webb, Peter Stockley and Dejian Zhou

Introduction

Nanoparticles have unique, size-dependent optical and electronic properties that are distinct and unavailable from the bulk, which in combination with the high target binding affinities and specificities of functional biomolecules (*e.g.* protein, DNA and antibody etc.), make them extremely well-suited for sensing and biomedical applications.

Results

Over the past few years, we have developed two types of nanoparticle-bioconjugates based sensors in an attempt to satisfy the different bioassay/biodetection needs. First, we have developed a simple gold nanoparticle (GNP)-aptamer based colorimetric sensor that exploits the unique, aggregation induced colour changes of GNPs (where isolated GNPs are red while aggregated ones are blue/purple) as well as the distinctly different adsorption behaviors of single-stranded (ss) DNAs/aptamers on citrate stabilised GNPs: unstructured, random coiled ssDNAs adsorb strongly onto GNPs to provide effective protection against salt-induced aggregation, whereas target-bound aptamer complexes cannot offer such protection. As a result, a ssDNA aptamer-GNP solution remains red after salt addition without target but turns into blue/purple with target (Figure 1A). Such colour changes are directly visible by the naked eye, making it well-suited for simple colorimetric sensing. We found that this simple sensor can detect specific low nM protein and ~100 nM small molecule targets in seconds by eye without using any instruments. Moreover, it can detect maximum residual limit (MRL) level of illegal additives and harmful residues (*e.g.* aminoglycosides antibiotics) in milk prescribed by EU law in seconds with the naked eye. Therefore, this simple sensor appears well-suited for rapid, on-site detection of relatively high abundant targets, such as illegal additives and harmful residues in food. It should be noted however that this sensor can only work in relatively clean solutions, the presence of large amount non-target proteins and other matrix materials can interfere with the specific target detection.

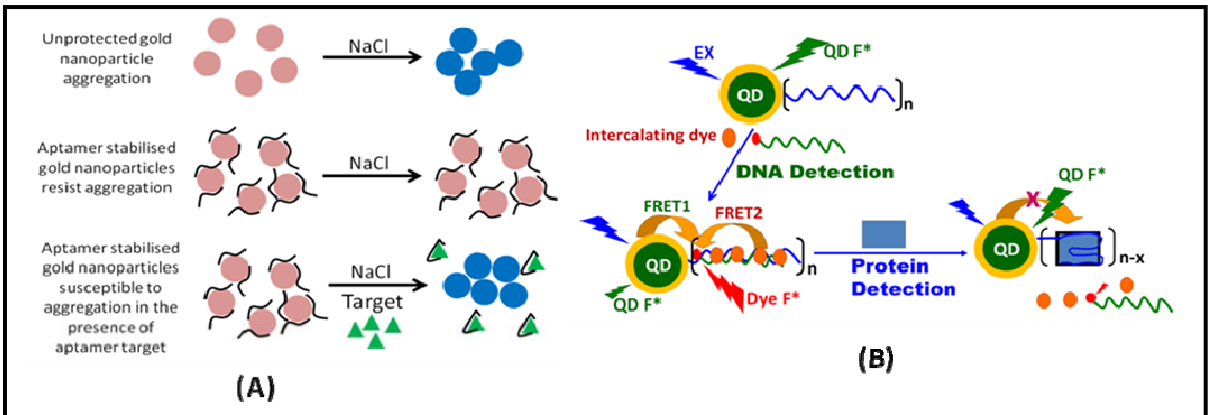

Figure 1: (**a**) Principle of the GNP-aptamer colorimetric sensor. (**b**) Schematic principle of the QD-intercalating dye dual-donor FRET sensor for detection of DNA and unlabelled protein targets.

Second, we have developed a novel intercalating dye (ethidinum bromide, EB)-quantum dot (QD) dual-donor FRET based sensor (Figure 1B). All previous QD-FRET based sensors have based on using the QD as the sole energy donor, whose sensitivity and specificity are limited by challenges associated with the ability of preparating functional QD-bioconjugates that are both copmpact (for high sensitivity) and effectively resisting non-specific adsorption (for high specificity and robustness) because these requirements are incompatible. The dual-donor

FRET system can overcome such limitations because of the enhanced FRET efficiency *via* both the QD and intercalated EBs donors. Moreover, the spatial closeness of the intercalated EBs to the acceptor in the dual-donor FRET system allows for efficient FRET even with relatively bulky QD-bioconjugates (and/or a QD-dye FRET system with relatively small spectral overlap), bypassing the strict requirement of compact QD-conjugates for high FRET in traditional single-donor FRET systems. The dual-donor FRET system has been used for sensitive detection of labelled DNA probes, where hybridization of the DNA probe to the QD-DNA conjugate leads to simultaneous intercalation of EBs, leading to significantly enhanced FRET for each target binding and hence improved sensitivity. This sensor can detect sub-nM level labelled DNA probes with high specificity: it can discriminate between perfect-match and single-base mismatch probes, which is equivalent to a SNP (single nucleotide polymorphysm) discrimination. Moreover, the sensor has been turned into a sensitive, label-free protein sensor *via* the incorporated anti-thrombin DNA aptamer sequence where target protein binding induced complementary DNA displacement and simultaneous removal of both QD and EB FRET signals. The dual-donor FRET sensor can quantitate thrombin down to 35 pM level, 2-4 orders of magnitude more sensitive than previously reported single-donor QD-FRET sensors, suggesting it has strong potential for disease diagnosis. Despite this, the current sensor however cannot work in complex media, *ca.* human serum, and therefore further optimizition of the QD surface and bioconjugation chemistries are still needed to make it suitable for real clinical detection and diagnostic applications.

Publications

Derbyshire, N., White, S., Bunka, D., Song, L., Stead, S., Tarbin, J., Sharman, M., Zhou, D. & Stockley, P. (2012) Toggled RNA aptamers against aminoglycosides allowing facile detection of antibiotics using gold nanoparticle assays. *Anal. Chem.* **84:** 6595-6602.

Zhang, H. & Zhou, D. (2012) A quantum dot-intercalating dye dual-donor fret based biosensor. *Chem. Commun. (Camb)* **48:** 5097-5099.

Zhang, S., Nelson, A. & Beales, P. (2012) Freezing or wrapping: the role of particle size in the mechanism of nanoparticle-biomembrane interaction. *Langmuir* **28:** 12831-12837.

Zhang, Y. & Zhou, D. (2012) Magnetic particle-based ultrasensitive biosensors for diagnostics. *Expert Rev. Mol. Diagn.* **12:** 565-571.

Funding

This work was supported by the University of Leeds, the Leeds Biomedical Health Research Centre and the Food and Environment Research Agency (FERA) laboratory.

Collaborators

External: M. Sharman (Food and Environment Research Agency).

ASTBURY SEMINARS 2012

11th January
Prof. James Hogle, Harvard Medical School
"Poliovirus entry: now that you've gotten in, what are you going to do?"

2nd February
Dr Justin Benesch, University of Oxford
"Untangling protein polydispersity and dynamics"

8th March
Prof Raymond E. Goldstein, University of Cambridge
"Stirring tails of evolution"

11th April
Prof. Dek Woolfson, University of Bristol
"Peptide and protein design in chemical and synthetic biology"

19th April
Dr Alessio Ciulli, University of Cambridge
"Structure-based design of chemical probes at protein surfaces that read posttranslational modifications"

25th April
Prof. Rob Liskamp, University of Utrecht
"Peptides and proteins as a continuing exciting source of inspiration for peptidomimetics and protein mimics"

2nd May
Prof. Ruedi Alleman, University of Cardiff
"Controlling cell fate with biophotonic nanoswitches"

3rd May
Dr Kevin Gaston, University of Bristol
"The papillomavirus E2 proteins and their interactions with p53"

7th June
Dr James Murray, Imperial College
"The light and the dark: structural basis of the repair and assembly of photosystem II and the regulation of carbon fixation."

3rd July
Annual Astbury Lecture
Prof. Roger Goody, Max Planck Institute of Molecular Physiology
"Combining structural biology, chemical biology and kinetics to understand Ras-family GTPases"

31st July
Prof. Tony Shing, The Chinese University of Hong Kong
"Entries to hydroxylated cyclohexa(e)nes via carbocyclization of carbohydrates"

16th October
Prof. Stephen Mann, FRS, University of Bristol
"New paradigms at the proto-life/synthetic biology interface"

1st November
Prof. Julea Butt, University of East Anglia
"Resolving the heart of the action - spectroelectrochemical studies of cytochromes"

6th December
Dr Edward Snell, Hauptman-Woodward Medical Research Institute, Buffalo, NY
"The structure of yeast glutaminyl-tRNA synthetase and modelling of its interaction with tRNA"

PUBLICATIONS BY ASTBURY CENTRE MEMBERS 2012

Ahire, J., Wang, Q., Coxon, P., Malhotra, G., Brydson, R., Chen, R. & Chao, Y. (2012) Highly luminescent and nontoxic amine-capped nanoparticles from porous silicon: synthesis and their use in biomedical imaging. *ACS Appl. Mater. Interfaces* **4:** 3285-3292.

Allan, P., de Willige, S., Abou-Saleh, R., Connell, S. & Ariens, R. (2012) Evidence that fibrinogen gamma ' directly interferes with protofibril growth: implications for fibrin structure and clot stiffness. *J. Thromb. Haemost.* **10:** 1072-1080.

Al-Lawati, Z., Alkhairalla, B., Bramble, J., Henderson, J., Bushby, R. & Evans, S. (2012) Alignment of discotic lyotropic liquid crystals at hydrophobic and hydrophilic self-assembled monolayers. *J. Phys. Chem. C Nanomater. Interfaces* **116:** 12627-12635.

Alster, J., Kabelac, M., Tuma, R., Psencik, J. & Burda, J. (2012) Computational study of short-range interactions in bacteriochlorophyll aggregates. *Comput. Theor. Chem.* **998:** 87-97.

Arscott, S., Descatoire, C., Buchaillot, L. & Ashcroft, A. (2012) A snapshot of electrified nanodroplets undergoing coulomb fission. *Appl. Phys. Lett.* **100:** 074103.

Auer, S., Ricchiuto, P. & Kashchiev, D. (2012) Two-step nucleation of amyloid fibrils: Omnipresent or not? *J. Mol. Biol.* **422:** 723-730.

Azzarito, V., Prabhakaran, P., Bartlett, A., Murphy, N., Hardie, M. J., Kilner, C., Edwards, T., Warriner, S. & Wilson, A. (2012) 2-o-alkylated para-benzamide alpha-helix mimetics: The role of scaffold curvature. *Org. Biomol. Chem.* **10:** 6469-6472.

Bakker, S., Ford, R., Barker, A., Robottom, J., Saunders, K., Pearson, A., Ranson, N. & Stockley, P. (2012) Isolation of an asymmetric RNA uncoating intermediate for a single-stranded RNA plant virus. *J. Mol. Biol.* **417:** 65-78.

Bao, L., Odell, A., Stephen, S., Wheatcroft, S., Walker, J. & Ponnambalam, S. (2012) The s100a6 calcium-binding protein regulates endothelial cell-cycle progression and senescence. *FEBS J.* **279:** 4576-4588.

Bao, P., Cheetham, M., Roth, J., Blakeston, A., Bushby, R. & Evans, S. (2012) On-chip alternating current electrophoresis in supported lipid bilayer membranes. *Anal. Chem.* **84:** 10702-10707.

Barrans, S., Crouch, S., Care, M., Worrillow, L., Smith, A., Patmore, R., Westhead, D., Tooze, R., Roman, E. & Jack, A. (2012) Whole genome expression profiling based on paraffin embedded tissue can be used to classify diffuse large b-cell lymphoma and predict clinical outcome. *Br. J. Haematol.* **159:** 441-453.

Bentham, M., Holmes, K., Forrest, S., Rowlands, D. & Stonehouse, N. (2012) Formation of higher-order foot-and-mouth disease virus 3d(pol) complexes is dependent on elongation activity. *J. Virol.* **86:** 2371-2374.

Billingsley, D., Bonass, W., Crampton, N., Kirkham, J. & Thomson, N. (2012) Single-molecule studies of DNA transcription using atomic force microscopy. *Phys. Biol.* **9:** 021001.

Billingsley, D., Crampton, N., Kirkham, J., Thomson, N. & Bonass, W. (2012) Single-stranded loops as end-label polarity markers for double-stranded linear DNA templates in atomic force microscopy. *Nucleic Acids Res.* **40:** e99.

Booth, M., Brown, A., Evans, S. & Critchley, K. (2012) Determining the concentration of cuins2 quantum dots from the size-dependent molar extinction coefficient. *Chem. Mater.* **24:** 2064-2070.

Borodavka, A., Tuma, R. & Stockley, P. (2012) Evidence that viral RNAs have evolved for efficient, two-stage packaging. *Proc. Natl. Acad. Sci. U.S.A.* **109:** 15769-15774.

Brukhno, A., Ricchiuto, P. & Auer, S. (2012) Tracking polypeptide folds on the free energy surface: effects of the chain length and sequence. *J. Phys. Chem. B* **116:** 8703-8713.

Bruns, A., Yuldasheva, N., Latham, A., Bao, L., Pellet-Many, C., Frankel, P., Stephen, S., Howell, G., Wheatcroft, S., Kearney, M., Zachary, I. & Ponnambalam, S. (2012) A heat-shock protein axis regulates VEGFR2 proteolysis, blood vessel development and repair. *PLoS ONE* **7:** e48539.

Cabriolu, R., Kashchiev, D. & Auer, S. (2012) Breakdown of nucleation theory for crystals with strongly anisotropic interactions between molecules. *J. Chem. Phys.* **137:** 204903.

Cao, J., Xu, Z., Wang, B. & Chen, R. (2012) Influence of injection air pressure on the microcapillary formation within extruded plastic films. *J. Mater. Sci.* **47:** 8188-8196.

Carter, S., Barr, J. & Edwards, T. (2012) Expression, purification and crystallization of the crimean-congo haemorrhagic fever virus nucleocapsid protein. *Acta Crystallogr. Sect. F Struct. Biol. Cryst. Commun.* **68:** 569-573.

Carter, S., Surtees, R., Walter, C., Ariza, A., Bergeron, E., Nichol, S., Hiscox, J., Edwards, T. & Barr, J. (2012) Structure, function, and evolution of the crimean-congo hemorrhagic fever virus nucleocapsid protein. *J. Virol.* **86:** 10914-10923.

Caryl, J., Cox, G., Trimble, S. & O'Neill, A. (2012) "Tet(u)" is not a tetracycline resistance determinant. *Antimicrob. Agents. Chemother.* **56:** 3378-3379.

Cheetham, M., Bramble, J., McMillan, D., Bushby, R., Olmsted, P., Jeuken, L. & Evans, S. (2012) Manipulation and sorting of membrane proteins using patterned diffusion-aided ratchets with ac fields in supported lipid bilayers. *Soft Matter* **8:** 5459-5465.

Cherukuri, A., Salama, A., Carter, C., Smalle, N., McCurtin, R., Hewitt, E., Hernandez-Fuentes, M., Clark, B. & Baker, R. (2012) An analysis of lymphocyte phenotype after steroid avoidance with either alemtuzumab or basiliximab induction in renal transplantation. *Am. J. Transplant.* **12:** 919-931.

Chiesa, M., Gadelrab, K., Stefancich, M., Armstrong, P., Li, G., Souier, T., Thomson, N., Barcons, V., Font, J., Verdaguer, A., Phillips, M. & Santos, S. (2012) Investigation of nanoscale interactions by means of subharmonic excitation. *J. Phys. Chem. Lett.* **3:** 2125-2129.

Chiesa, M., Gadelrab, K., Verdaguer, A., Segura, J., Barcons, V., Thomson, N., Phillips, M., Stefancich, M. & Santos, S. (2012) Energy dissipation in the presence of sub-harmonic excitation in dynamic atomic force microscopy. *EPL* **99:** 56002.

Cocco, M., Stephenson, S., Care, M., Newton, D., Barnes, N., Davison, A., Rawstron, A., Westhead, D., Doody, G. & Tooze, R. (2012) *In vitro* generation of long-lived human plasma cells. *J. Immunol.* **189:** 5773-5785.

Costello, C., Kreft, J.-U., Thomas, C., Hammes, D., Bao, P., Evans, S. & Mendes, P. (2012) Exploiting additive and subtractive patterning for spatially controlled and robust bacterial co-cultures. *Soft Matter* **8:** 9147-9155.

Cox, G., Thompson, G., Jenkins, H., Peske, F., Savelsbergh, A., Rodnina, M., Wintermeyer, W., Homans, S., Edwards, T. & O'Neill, A. (2012) Ribosome clearance by FusB-type proteins mediates resistance to the antibiotic fusidic acid. *Proc. Natl. Acad. Sci. U.S.A.* **109:** 2102-2107.

Czajlik, A., Thompson, G., Khan, G., Kalverda, A., Homans, S. & Trinick, J. (2012) H-1, N-15 and C-13 backbone chemical shift assignment of the titin A67-A68 domain tandem. *Biomol. NMR Assign.* **6:** 39-41.

Derbyshire, N., White, S., Bunka, D., Song, L., Stead, S., Tarbin, J., Sharman, M., Zhou, D. & Stockley, P. (2012) Toggled RNA aptamers against aminoglycosides allowing facile detection of antibiotics using gold nanoparticle assays. *Anal. Chem.* **84:** 6595-6602.

di Martino, E., Tomlinson, D. & Knowles, M. (2012) A decade of FGF receptor research in bladder cancer: past, present, and future challenges. *Adv Urol.* **2012:**429213.

Dove, B., Surtees, R., Bean, T., Munday, D., Wise, H., Digard, P., Carroll, M., Ajuh, P., Barr, J. & Hiscox, J. (2012) A quantitative proteomic analysis of lung epithelial (a549) cells infected with 2009 pandemic influenza a virus using stable isotope labelling with amino acids in cell culture. *Proteomics* **12:** 1431-1436.

Dow, M., Fisher, M., James, T., Marchetti, F. & Nelson, A. (2012) Towards the systematic exploration of chemical space. *Org. Biomol. Chem.* **10:** 17-28.

Dyson, O., Walker, L., Whitehouse, A., Cook, P. & Akula, S. (2012) Resveratrol inhibits KSHV reactivation by lowering the levels of cellular EGR-1. *PLoS ONE* **7:** e33364.

Fascione, M., Adshead, S., Mandal, P., Kilner, C., Leach, A. & Turnbull, W. (2012) Mechanistic studies on a sulfoxide transfer reaction mediated by diphenyl sulfoxide/triflic anhydride. *Chem. Eur. J.* **18:** 2987-2997.

Fascione, M., Kilner, C., Leach, A. & Turnbull, W. (2012) Do glycosyl sulfonium ions engage in neighbouring-group participation? A study of oxathiane glycosyl donors and the basis for their stereoselectivity. *Chem. Eur. J.* **18:** 321-333.

Fascione, M., Webb, N., Kilner, C., Warriner, S. & Turnbull, W. (2012) Stereoselective glycosylations using oxathiane spiroketal glycosyl donors. *Carbohydr. Res.* **348:** 6-13.

Fomovska, A., Huang, Q., El Bissati, K., Mui, E. , Witola, W., Cheng, G., Zhou, Y., Sommerville, C., Roberts, C., Bettis, S., Prigge, S., Afanador, G., Hickman, M., Lee, P., Leed, S., Auschwitz, J., Pieroni, M., Stec, J., Muench, S., Rice, D., Kozikowski, A. & McLeod, R. (2012) Novel n-benzoyl-2-hydroxybenzamide disrupts unique parasite secretory pathway. *Antimicrob. Agents. Chemother.* **56:** 2666-2682.

Font, J., Santos, S., Barcons, V., Thomson, N., Verdaguer, A. & Chiesa, M. (2012) Spatial horizons in amplitude and frequency modulation atomic force microscopy. *Nanoscale* **4:** 2463-2469.

Fuller, J., Jackson, R., Edwards, T., Wilson, A. & Shirts, M. (2012) Modeling of arylamide helix mimetics in the p53 peptide binding site of hdm2 suggests parallel and anti-parallel conformations are both stable. *PLoS ONE* **7:** e43253.

Galloway, J., Bramble, J., Rawlings, A., Burnell, G., Evans, S. & Staniland, S. (2012) Biotemplated magnetic nanoparticle arrays. *Small* **8:**204-208.

Galloway, J., Bramble, J., Rawlings, A., Burnell, G., Evans, S. & Staniland, S. (2012) Nanomagnetic arrays formed with the biomineralization protein mms6. *J. Nano Res.* **17:** 127-146.

Galloway, J. & Staniland, S. (2012) Protein and peptide biotemplated metal and metal oxide nanoparticles and their patterning onto surfaces. *J. Mater. Chem.* **22:** 12423-12434.

Gooch, A., Nedolisa, C., Houton, K., Lindsay, C., Saiani, A. & Wilson, A. (2012) Tunable self-assembled elastomers using triply hydrogen-bonded arrays. *Macromolecules* **45:** 4723-4729.

Grant, C., McKendry, J. & Evans, S. (2012) Temperature dependent stiffness and visco-elastic behaviour of lipid coated microbubbles using atomic force microscopy. *Soft Matter* **8:** 1321-1326.

Grant, C., Phillips, M. & Thomson, N. (2012) Dynamic mechanical analysis of collagen fibrils at the nanoscale. *J. Mech. Behav. Biomed. Mater.* **5:** 165-170.

Griffiths, H., Whitehouse, I. & Hooper, N. (2012) Regulation of amyloid-beta production by the prion protein. *Prion* **6:**1-6.

Griffiths, J. & O'Neill, A. (2012) Loss of function of the gdpp protein leads to joint beta-lactam/glycopeptide tolerance in *Staphylococcus aureus*. *Antimicrob. Agents. Chemother.* **56:** 579-581.

Henderson, P. & Baldwin, S. (2012) Structural biology bundles of insights into sugar transporters. *Nature* **490:** 348-350.

Hodkinson, J., Radford, S. & Ashcroft, A. (2012) The role of conformational flexibility in beta(2)-microglobulin amyloid fibril formation at neutral pH. *Rapid Commun. Mass Spectrom.* **26:** 1783-1792.

Hoffmann, T. & Dougan, L. (2012) Single molecule force spectroscopy using polyproteins. *Chem. Soc. Rev.* **41:** 4781-4796.

Huysmans, G., Chan, N., Baldwin, J., Postis, V., Tzokov, S., Deacon, S., Yao, S., Young, J., McPherson, M., Bullough, P. & Baldwin, S. (2012) A urea channel from *Bacillus cereus* reveals a novel hexameric structure. *Biochem. J.* **445:** 157-166.

Huysmans, G., Radford, S., Baldwin, S. & Brockwell, D. (2012) Malleability of the folding mechanism of the outer membrane protein pagp: Parallel pathways and the effect of membrane elasticity. *J. Mol. Biol.* **416:** 453-464.

Ikeda-Kobayashi, A., Taniguchi, Y., Brockwell, D., Paci, E. & Kawakami, M. (2012) Prying open single GroES ring complexes by force reveals co-operativity across domains. *Biophys. J.* **102:** 1961-1968.

Jackson, B., Noerenberg, M. & Whitehouse, A. (2012) The Kaposi's sarcoma-associated herpesvirus ORF57 protein and its multiple roles in mRNA biogenesis. *Front. Microbiol.* **3:** 59-59.

Joce, C., White, R., Stockley, P., Warriner, S., Turnbull, W. & Nelson, A. (2012) Design, synthesis and *in vitro* evaluation of novel bivalent s-adenosylmethionine analogues. *Bioorg. Med. Chem. Lett.* **22:** 278-284.

Kang, L., Moriarty, G., Woods, L., Ashcroft, A., Radford, S. & Baum, J. (2012) N-terminal acetylation of alpha-synuclein induces increased transient helical propensity and decreased aggregation rates in the intrinsically disordered monomer. *Protein Sci.* **21:** 911-917.

Kankanala, J., Latham, A., Johnson, A., Homer-Vanniasinkam, S., Fishwick, C. & Ponnambalam, S. (2012) A combinatorial *in silico* and cellular approach to identify a new class of compounds that target vegfr2 receptor tyrosine kinase activity and angiogenesis. *Br. J. Pharmacol.* **166:** 737-748.

Kennaway, C., Taylor, J., Song, C., Potrzebowski, W., Nicholson, W., White, J., Swiderska, A., Obarska-Kosinska, A., Callow, P., Cooper, L., Roberts, G., Artero, J.-B., Bujnicki, J., Trinick, J., Kneale, G. & Dryden, D. (2012) Structure and operation of the DNA-translocating type i DNA restriction enzymes. *Genes Dev.* **26:** 92-104.

Kinnell, A., Harman, T., Bingham, M., Berry, A. & Nelson, A. (2012) Development of an organo- and enzyme-catalysed one-pot, sequential three-component reaction. *Tetrahedron* **68:** 7719-7722.

Latham, A., Bruns, A., Kankanala, J., Johnson, A., Fishwick, C., Homer-Vanniasinkam, S. & Ponnambalam, S. (2012) Indolinones and anilinophthalazines differentially target vegf-a- and basic fibroblast growth factor-mediated responses in primary human endothelial cells. *Br. J. Pharmacol.* **165:** 245-259.

Latham, A., Odell, A., Mughal, N. A., Issitt, T., Ulyatt, C., Walker, J., Homer-Vanniasinkam, S. & Ponnambalam, S. (2012) A biphasic endothelial stress-survival mechanism regulates the cellular response to vascular endothelial growth factor a. *Exp. Cell Res.* **318:** 2297-2311.

Leney, A., McMorran, L., Radford, S. & Ashcroft, A. (2012) Amphipathic polymers enable the study of functional membrane proteins in the gas phase. *Anal. Chem.* **84:** 9841-9847.

Lewis, V., Whitehouse, I., Baybutt, H., Manson, J., Collins, S. & Hooper, N. (2012) Cellular prion protein expression is not regulated by the Alzheimer's amyloid precursor protein intracellular domain. *PLoS ONE* **7:** e31754.

Li, H., Atkins, E., Bruckner, J., McArdle, S., Qiu, W., Thomassen, L., Scott, J., Shuhart, M., Livingston, S., Townshend-Bulson, L., McMahon, B., Harris, M., Griffin, S. & Gretch, D. (2012) Genetic and functional heterogeneity of the hepatitis C virus p7 ion channel during natural chronic infection. *Virology* **423:** 30-37.

Lichtinger, M., Ingram, R., Hannah, R., Mueller, D., Clarke, D., Assi, S., Lie-A-Ling, M., Noailles, L., Vijayabaskar, M. S., Wu, M., Tenen, D., Westhead, D., Kouskoff, V., Lacaud, G., Goettgens, B. & Bonifer, C. (2012) Runx1 reshapes the epigenetic landscape at the onset of haematopoiesis. *EMBO J.* **31:** 4318-4333.

Mandal, P., Branson, T., Hayes, E., Ross, J., Gavin, J., Daranas, A. & Turnbull, W. (2012) Towards a structural basis for the relationship between blood group and the severity of el tor cholera. *Angew. Chem. Int. Ed. Engl.* **51:** 5143-5146.

Marritt, S., Lowe, T., Bye, J., McMillan, D., Shi, L., Fredrickson, J., Zachara, J., Richardson, D., Cheesman, M., Jeuken, L. & Butt, J. (2012) A functional description of cyma, an electron-transfer hub supporting anaerobic respiratory flexibility in shewanella. *Biochem. J.* **444:** 465-474.

Maude, S., Tai, L., Davies, R., Liu, B., Harris, S., Kocienski, P. & Aggeli, A. (2012) Peptide synthesis and self-assembly. *Top. Curr. Chem.* **310:** 27-69.

McAllister, T. & Webb, M. (2012) Triazole phosphohistidine analogues compatible with the fmoc-strategy. *Org. Biomol. Chem.* **10:** 4043-4049.

McMillan, D., Marritt, S., Butt, J. & Jeuken, L. (2012) Menaquinone-7 is specific cofactor in tetraheme quinol dehydrogenase cyma. *J. Biol. Chem.* **287:** 14215-14225.

Milanesi, L., Sheynis, T., Xue, W.-F., Orlova, E., Hellewell, A., Jelinek, R., Hewitt, E., Radford, S. & Saibil, H. (2012) Direct three-dimensional visualization of membrane disruption by amyloid fibrils. *Proc. Natl. Acad. Sci. U.S.A.* **109:** 20455-20460.

Mohl, B.-P., Tedbury, P., Griffin, S. & Harris, M. (2012) Hepatitis c virus-induced autophagy is independent of the unfolded protein response. *J. Virol.* **86:** 10724-10732.

Monteiro, D., Rugen, M., Shepherd, D., Nozaki, S., Niki, H. & Webb, M. (2012) Formation of a heterooctameric complex between aspartate alpha-decarboxylase and its cognate activating factor, panz, is coa-dependent. *Biochem. Biophys. Res. Commun.* **426:** 350-355.

Morra, R., Lee, B. , Shaw, H., Tuma, R. & Mancini, E. (2012) Concerted action of the PHD, chromo and motor domains regulates the human chromatin remodelling ATPase CHD4. *FEBS Lett.* **586:** 2513-2521.

Morrissey, B., Leney, A. , Toste Rego, A., Phan, G., Allen, W. , Verger, D., Waksman, G., Ashcroft, A. & Radford, S. (2012) The role of chaperone-subunit usher domain interactions in the mechanism of bacterial pilus biogenesis revealed by ESI-MS. *Mol. Cell Proteomics* **11:** M111.015289.

Mu, Q., Hondow, N., Krzeminski, L., Brown, A., Jeuken, L. & Routledge, M. (2012) Mechanism of cellular uptake of genotoxic silica nanoparticles. *Part. Fibre Toxicol.* **9:** 29.

Mughal, N., Russell, D., Ponnambalam, S. & Homer-Vanniasinkam, S. (2012) Gene therapy in the treatment of peripheral arterial disease. *Br. J. Surg.* **99:** 6-15.

Munday, D., Surtees, R., Emmott, E., Dove, B., Digard, P., Barr, J., Whitehouse, A., Matthews, D. & Hiscox, J. (2012) Using SILAC and quantitative proteomics to investigate the interactions between viral and host proteomes. *Proteomics* **12:** 666-672.

Murray, B., O'Sullivan, D., Atkinson, J. & Webb, M. (2012) Ice nucleation by particles immersed in supercooled cloud droplets. *Chem. Soc. Rev.* **41:** 6519-6554.

Nam, J., Vanderlick, T. & Beales, P. (2012) Formation and dissolution of phospholipid domains with varying textures in hybrid lipo-polymersomes. *Soft Matter* **8:** 7982-7988.

Ndlovu, H., Ashcroft, A., Radford, S. & Harris, S. (2012) Effect of sequence variation on the mechanical response of amyloid fibrils probed by steered molecular dynamics simulation. *Biophys. J.* **102:** 587-596.

Nozaki, S., Webb, M. & Niki, H. (2012) An activator for pyruvoyl-dependent L-aspartate alpha-decarboxylase is conserved in a small group of the gamma-proteobacteria including *Escherichia coli*. *MicrobiologyOpen* **1:**298-310.

Nyathi, Y., Zhang, X., Baldwin, J., Bernhardt, K., Johnson, B., Baldwin, S., Theodoulou, F. L. & Baker, A. (2012) Pseudo half-molecules of the ABC transporter, comatose, bind pex19 and target to peroxisomes independently but are both required for activity. *FEBS Lett.* **586:** 2280-2286.

Odell, A., Hollstein, M., Ponnambalam, S. & Walker, J. (2012) A VE-cadherin-PAR3-Alpha-catenin complex regulates the golgi localization and activity of cytosolic phospholipase a(2)alpha in endothelial cells. *Mol. Biol. Cell* **23:** 1783-1796.

O'Rorke, R., Wood, C., Waelti, C., Evans, S., Davies, A. & Cunningham, J. (2012) Acousto-microfluidics: transporting microbubble and microparticle arrays in acoustic traps using surface acoustic waves. *J. Appl. Phys.* **111:** 094911.

Owen, R., Yorke, B. & Pearson, A. (2012) X-ray-excited optical luminescence of protein crystals: a new tool for studying radiation damage during diffraction data collection. *Acta Crystallogr. D Biol. Crystallogr.* **68:** 505-510.

Paci, E. (2012) Using models to design new bio-inspired materials. *Biophys. J.* **103:** 1814-1815.

Pashley, C., Morgan, G., Kalverda, A., Thompson, G., Kleanthous, C. & Radford, S. (2012) Conformational properties of the unfolded state of Im7 in non-denaturing conditions. *J. Mol. Biol.* **416:** 300-318.

Pellizzaro, M., Barrett, S., Fisher, J. & Wilson, A. (2012) Design, synthesis and binding studies of a novel quadruple adda hydrogen-bond array. *Org. Biomol. Chem.* **10:** 4899-4906.

Peyman, S., Abou-Saleh, R., McLaughlan, J., Ingram, N., Johnson, B., Critchley, K., Freear, S., Evans, J., Markham, A., Coletta, P. & Evans, S. (2012) Expanding 3D geometry for enhanced on-chip microbubble production and single step formation of liposome modified microbubbles. *Lab Chip* **12:** 4544-4552.

Phillips, H., Chernikov, A., Fletcher, N., Ashcroft, A., Ault, J., Filby, M. & Wilson, A. (2012) The use of electrospray mass spectrometry to determine speciation in a dynamic combinatorial library for anion recognition. *Chem. Eur. J.* **18:** 13733-13742.

Prabhakaran, P., Azzarito, V., Jacobs, T., Hardie, M. J., Kilner, C., Edwards, T., Warriner, S. L. & Wilson, A. (2012) Conformational properties of O-alkylated benzamides. *Tetrahedron* **68:** 4485-4491.

Preston, G., Radford, S., Ashcroft, A. & Wilson, A. (2012) Covalent cross-linking within supramolecular peptide structures. *Anal. Chem.* **84:** 6790-6797.

Ptasinska, A., Assi, S., Mannari, D., James, S., Williamson, D., Dunne, J., Hoogenkamp, M., Wu, M., Care, M., McNeill, H., Cauchy, P., Cullen, M., Tooze, R., Tenen, D., Young, B., Cockerill, P., Westhead, D., Heidenreich, O. & Bonifer, C. (2012) Depletion of runx1/eto in t(8;21) aml cells leads to genome-wide changes in chromatin structure and transcription factor binding. *Leukemia* **26:** 1829-1841.

Radford, S. (2012) Molecular insights into aberrant protein self-assembly. *FEBS J.* **279:** 50-51.

Rawlings, A., Bramble, J. & Staniland, S. (2012) Innovation through imitation: biomimetic, bioinspired and biokleptic research. *Soft Matter* **8:** 6675-6679.

Rhys, N., Soper, A. & Dougan, L. (2012) The hydrogen-bonding ability of the amino acid glutamine revealed by neutron diffraction experiments. *J. Phys. Chem. B* **116:** 13308-13319.

Ricchiuto, P., Brukhno, A. & Auer, S. (2012) Protein aggregation: kinetics versus thermodynamics. *J. Phys. Chem. B* **116:** 5384-5390.

Roberts, A., Malkova, B., Walker, M., Sakakibara, H., Numata, N., Kon, T., Ohkura, R., Edwards, T., Knight, P., Sutoh, K., Oiwa, K. & Burgess, S. (2012) ATP-driven remodeling of the linker domain in the dynein motor. *Structure* **20:** 1670-1680.

Rosado, H., O'Neill, A., Blake, K., Walther, M., Long, P., Hinds, J. & Taylor, P. (2012) Rotating wall vessel exposure alters protein secretion and global gene expression in *Staphylococcus aureus*. *Int. J. Astrobiology* **11:** 71-81.

Russell, S., Casey, R., Hoang, D., Little, B., Olmsted, P., Rumschitzki, D., Wadghiri, Y. & Fisher, E. (2012) Quantification of the plasma clearance kinetics of a gadolinium-based contrast agent by photo-induced triplet harvesting. *Anal. Chem.* **84:** 8106-8109.

Ryder, V., Chopra, I. & O'Neill, A. (2012) Increased mutability of staphylococci in biofilms as a consequence of oxidative stress. *PLoS ONE* **7:** e47695.

Saha, K., Webb, M., Rigby, S., Leech, H., Warren, M. & Smith, A. (2012) Characterisation of the evolutionarily conserved iron sulphur cluster of sirohydrochlorin ferrochelatase from *Arabidopsis thaliana*. *Biochem. J.* **444:**227-237.

Santos, S., Guang, L., Souier, T., Gadelrab, K., Chiesa, M. & Thomson, N. (2012) A method to provide rapid in situ determination of tip radius in dynamic atomic force microscopy. *Rev. Sci. Instrum.* **83:** 043707.

Santos, S., Stefancich, M., Hernandez, H., Chiesa, M. & Thomson, N. (2012) Hydrophilicity of a single DNA molecule. *J. Phys. Chem. C Nanomater. Interfaces* **116:** 2807-2818.

Shalashilin, D., Beddard, G., Paci, E. & Glowacki, D. (2012) Peptide kinetics from picoseconds to microseconds using boxed molecular dynamics: power law rate coefficients in cyclisation reactions. *J. Chem. Phys.* **137:** 165102.

Simm, R., Voros, A., Ekman, J., Sodring, M., Nes, I., Kroeger, J., Saidijam, M., Bettaney, K. E., Henderson, P., Salkinoja-Salonen, M. & Kolsto, A.-B. (2012) BC4707 is a major facilitator superfamily multidrug resistance transport protein from *Bacillus cereus* implicated in fluoroquinolone tolerance. *PLoS ONE* **7:** e36720.

Skedelj, V., Arsovska, E., Tomasic, T., Kroflic, A., Hodnik, V., Hrast, M., Bester-Rogac, M., Anderluh, G., Gobec, S., Bostock, J., Chopra, I., O'Neill, A., Randall, C. & Zega, A. (2012) 6-arylpyrido 2,3-d pyrimidines as novel ATP-competitive inhibitors of bacterial d-alanine:D-alanine ligase. *PLoS ONE* **7:** e39922.

Tanaka, M., Brown, R., Hondow, N., Arakaki, A., Matsunaga, T. & Staniland, S. (2012) Highest levels of Cu, Mn and Co doped into nanomagnetic magnetosomes through optimized biomineralisation. *J. Mater. Chem.* **22:** 11919-11921.

Tanaka, M., Critchley, K., Matsunaga, T., Evans, S. Staniland, S. (2012) Fabrication of lipid tubules with embedded quantum dots by membrane tubulation protein. *Small* **8:** 1590-1595.

Tate, D., Anemian, R., Bushby, R., Nanan, S., Warriner, S. & Whitaker, B. (2012) Improved syntheses of high hole mobility phthalocyanines: a case of steric assistance in the cyclo-oligomerisation of phthalonitriles. *Beilstein J. Org. Chem.* **8:** 120-128.

Tomlinson, D., Baxter, E., Loadman, P., Hull, M. & Knowles M. (2012) FGFR1-induced epithelial to mesenchymal transition through MAPK/PLCγ/COX-2-mediated mechanisms. *PloS One.* **7:**e38972.

Tomlinson, D., Knowles, M. & Speirs, V. (2012) Mechanisms of FGFR3 actions in endocrine resistant breast cancer. *Int J Cancer*. **130:**2857-66.

Tosatti, P., Nelson, A. & Marsden, S. (2012) Recent advances and applications of iridium-catalysed asymmetric allylic substitution. *Org. Biomol. Chem.* **10:** 3147-3163.

Towey, J. & Dougan, L. (2012) Structural examination of the impact of glycerol on water structure. *J. Phys. Chem. B* **116:** 1633-1641.

Towey, J., Soper, A. & Dougan, L. (2012) Molecular insight into the hydrogen bonding and micro-segregation of a cryoprotectant molecule. *J. Phys. Chem. B* **116:** 13898-13904.

Tskhovrebova, L. & Trinick, J. (2012) Making muscle elastic: the structural basis of myomesin stretching. *PLoS Biol.* **10:** e1001264-e1001264.

Tskhovrebova, L. & Trinick, J. (2012) Molecular rulers? *Curr. Biol.* **22:** R317-R318.

Turnbull, W. & Stalford, S. (2012) Methylthioxylose - a jewel in the mycobacterial crown? *Org. Biomol. Chem.* **10:** 5698-5706.

Turrell, S., Filby, M., Whitehouse, A. & Wilson, A. (2012) Cellular uptake of highly-functionalized ruthenium(ii) tris-bipyridine protein-surface mimetics. *Bioorg. Med. Chem. Lett.* **22:** 985-988.

Turrell, S., Macnab, S., Rose, A., Melcher, A. & Whitehouse, A. (2012) A herpesvirus saimiri-based vector expressing trail induces cell death in human carcinoma cell lines and multicellular spheroid cultures. *Int. J. Oncol.* **40:** 2081-2089.

Twigg, M., Freestone, K., Homer-Vanniasinkam, S. & Ponnambalam, S. (2012) The LOX-1 scavenger receptor and its implications in the treatment of vascular disease. *Cardiol. Res. Pract.* **2012:** 632408-632408.

Valette, N., Radford, S., Harris, S. & Warriner, S. (2012) Phosphorylation as a tool to modulate aggregation propensity and to predict fibril architecture. *Chembiochem* **13:** 271-281.

Vardy, E., Kellett, K., Cocklin, S. & Hooper, N. (2012) Alkaline phosphatase is increased in both brain and plasma in Alzheimer's disease. *Neurodegener. Dis.* **9:** 31-37.

Wacker, S., Jurkowski, W., Simmons, K., Fishwick, C., Johnson, P., Madge, D., Lindahl, E., Rolland, J-F & de Groot, B. (2012) Identification of selective inhibitors of the potassium channel Kv1.1-1.2(3) by high-throughput virtual screening and automated patch clamp. *ChemMedChem* **7:** 1775-1783.

Watt, N., Taylor, D., Kerrigan, T., Griffiths, H., Rushworth, J., Whitehouse, I. & Hooper, N. (2012) Prion protein facilitates uptake of zinc into neuronal cells. *Nat. Commun.* **3:** 1134-1134.

Webb, M., Lobley, C., Soliman, F., Kilkenny, M., Smith, A., Blundell, T. & Abell, C. (2012) Structure of *Escherichia coli* aspartate alpha-decarboxylase Asn72Ala: probing the role of Asn72 in pyruvoyl cofactor formation. *Acta Crystallogr. Sect. F Struct. Biol. Cryst. Commun.* **68:** 414-417.

Wetherill, L., Holmes, K., Verow, M., Mueller, M., Howell, G., Harris, M., Fishwick, C., Stonehouse, N., Foster, R., Blair, G., Griffin, S. & Macdonald, A. (2012) High-risk human papillomavirus e5 oncoprotein displays channel-forming activity sensitive to small-molecule inhibitors. *J. Virol.* **86:** 5341-5351.

White, S., Johnson, S., Szymonik, M., Wardingley, R., Pye, D., Davies, A., Walti, C. & Stockley, P. (2012) Directed surface attachment of nanomaterials via coiled-coil-driven self-assembly. *Nanotechnology* **23:** 495304-495304.

White, S., Morton, D., Cheah, B., Bronowska, A., Davies, A., Stockley, P., Waelti, C. & Johnson, S. (2012) On-surface assembly of coiled-coil heterodimers. *Langmuir* **28:** 13877-13882.

Williamson, D., Fascione, M., Webb, M. & Turnbull, W. (2012) Efficient N-terminal labeling of proteins by use of sortase. *Angew. Chem. Int. Ed. Engl.* **51:** 9377-9380.

Wu, W., Macdonald, A., Hiscox, J. & Barr, J. (2012) Different NF-kappa B activation characteristics of human respiratory syncytial virus subgroups A and B. *Microb. Pathog.* **52:** 184-191.

Wu, W., Tran, K. , Teng, M., Heesom, K., Matthews, D., Barr, J. & Hiscox, J. (2012) The interactome of the human respiratory syncytial virus NS1 protein highlights multiple effects on host cell biology. *J. Virol.* **86:** 7777-7789.

Zhang, H. & Zhou, D. (2012) A quantum dot-intercalating dye dual-donor fret based biosensor. *Chem. Commun. (Camb)* **48:** 5097-5099.

Zhang, S., Nelson, A. & Beales, P. (2012) Freezing or wrapping: the role of particle size in the mechanism of nanoparticle-biomembrane interaction. *Langmuir* **28:** 12831-12837.

Zhang, Y. & Zhou, D. (2012) Magnetic particle-based ultrasensitive biosensors for diagnostics. *Expert Rev. Mol. Diagn.* **12:** 565-571.

Zhou, D. (2012) Quantum dot-nucleic acid/aptamer bioconjugate-based fluorimetric biosensors. *Biochem. Soc. Trans.* **40:** 635-639.

UNIVERSITY OF LEEDS

Leeds, United Kingdom
LS2 9JT
Tel. 0113 243 1751
www.leeds.ac.uk